

ATTEMPTED TOTAL SYNTHESSES OF A NOVEL LYCOPODINE-CLASS ALKALOID
AND (*R*)-MYRICANOL, COMPOUNDS FOR THE TREATMENT OF ALZHEIMER'S
DISEASE

A Dissertation
Submitted to the Graduate Faculty
of the
North Dakota State University
of Agriculture and Applied Science

By

Anthony John Ostlund

In Partial Fulfillment
for the Degree of
DOCTOR OF PHILOSOPHY

Major Department:
Chemistry and Biochemistry

March 2013

Fargo, North Dakota

North Dakota State University
Graduate School

Title

**ATTEMPTED TOTAL SYNTHESSES OF A NOVEL LYCOPODINE-CLASS
ALKALOID AND (R)-MYRICANOL, COMPOUNDS FOR THE
TREATMENT OF ALZHEIMER'S DISEASE**

By

Anthony John Ostlund

The Supervisory Committee certifies that this *disquisition* complies with North Dakota State University's regulations and meets the accepted standards for the degree of

DOCTOR OF PHILOSOPHY

SUPERVISORY COMMITTEE:

Dr. Gregory R. Cook

Chair

Dr. Mukund P. Sibi

Dr. Sivaguru Jayaraman

Dr. Dean Webster

Approved:

5-29-2013

Date

Dr. Gregory R. Cook

Department Chair

ABSTRACT

Alzheimer's Disease (AD) is a significant challenge to both the pharmaceutical world as well as the synthetic organic chemistry world. One of the most important problems in this field is the lack of a unified approach to the most biologically active class of natural products for the treatment of AD, the *lycopodine* alkaloids. Presented herein is an attempt at the total synthesis of a novel member of this family. The synthesis spans three complete generations of retrosynthesis and forward progress. In the ultimate effort, the carbon backbone of the entire *lycopodine* class was successfully synthesized using a 6 step process in 44% overall yield. Features of this synthesis are the formation of an intermediate aldehyde by tandem Horner-Wadsworth-Emmons olefination/Baylis-Hillman reaction, quantitative reduction resulting in a monoprotected diol, cationic Au(I) *O*-vinylation, and microwave assisted Claisen rearrangement. The final step towards the backbone was realized using a hydrozirconation/transmetalation sequence with addition to the aldehyde to make the penultimate allylic alcohol in 54% yield. Final studies on the elimination of the allylic alcohol to create the desired 1,3-diene functionality show limited access to this important precursor. Simultaneous model system studies have shown that an intramolecular, cationic Rh(I)-catalyzed ynamide Diels-Alder reaction is feasible to set the B and D rings of the final *lycopodine* core, although the reaction requires optimization. Model systems for the unique intramolecular allylation proposed in the retrosynthesis also show feasibility, however the intramolecular variant has not been fully explored. Additional studies towards the total synthesis (*R*)-myricanol are also presented as a continuance of efforts towards general approaches to AD combative compounds. Featured are straightforward methods to the two main segments of the natural product, including a three-step process to synthesize the southern half. Finally, a successful 2-step synthesis of (*R*)-convolutamydine E is used to showcase an In(0)-mediated allylation methodology.

ACKNOWLEDGEMENTS

I would like to thank firstly my committee, without whom I could not have realized this achievement. Special thanks is deserved of Dr. Gregory R. Cook, my advisor, who always allowed me to fully explore the potential in any project, and was always willing to give me an audience when I was hitting a wall, or when I succeeded. I would also like to thank my lab mates, in particular Dr. Narayanaganesh Balasubramanian (Ganesh) and Dr. Vesela Ugrinova, for being wonderful colleagues for a graduate student to have. In addition, I would like to acknowledge all of the graduate students and post-doctoral fellows I have interacted with during my time here at NDSU, particularly Messrs. Mulholland, Backous, McCausland, Evenson, Schwiderski, Larsen, and Wolfe, as well as Mr. and Mrs. Anderson and my undergraduate lab assistants, Ms. Weyer, Ms. Sun, and Mr. Nye. Everyone has made the experience a memorable one, and I go forward remembering all of the good times of the past.

In addition, I would like to thank my entire family, both my biological family, as well as my family through marriage. I have been inexplicably lucky in that I can count myself a member of such a wonderful group of people. Particular thanks go to my mother and mother-in-law, whom have always been exceedingly supportive and understanding.

Undoubtedly the single most important person in my time at NDSU has been my wonderful wife, Alisha. Without her consistent support and encouragement, there is absolutely no way I would be able to write this. She sacrificed a great deal to enable me to come to NDSU and I won't ever forget that. Hopefully now I can begin to repay the years of dedicated support she has shown me as we step into the future together.

DEDICATION

I would like to dedicate this dissertation to my late father.

PREFACE

My road to graduation began in a General Chemistry I lecture at 8:00 in the morning, my first day of freshman year at Hamline University. My professor was Dr. Olaf Rundquist, and from the first day, I was hooked. Upon my graduation from Hamline with my Bachelor's degree, Ole wrote something on an e-mail I will never forget.

“Always remember that as a philosopher, you can never prove, only disprove.

You can never find truth, only search for it.

If you cannot get pleasure from searching for truth, then quit now.

The philosopher finds the hunt for truth the exciting part.

When a problem is ‘solved’ the fun ends and you have to look for a new puzzle.”

Ole was right. Solving the puzzle is far more rewarding than reaching the endpoint. So here I am, years later, content with the fact that I never saw my project's completion. I enjoyed the fight, but it is time to explore the world through a new lens. It is time for a new puzzle.

This dissertation is a foray into the extremely complicated and often unsuccessful world of total synthesis.

TABLE OF CONTENTS

ABSTRACT.....	iii
ACKNOWLEDGMENTS	iv
DEDICATION	v
PREFACE	vi
LIST OF TABLES	xiii
LIST OF FIGURES	xiv
LIST OF SCHEMES	xvi
LIST OF ABBREVIATIONS/SYMBOLS	xx
CHAPTER 1. A REVIEW OF ALZHEIMER’S DISEASE AND THE ROLE OF ALKALOIDS FROM THE <i>LYCOPODIUM/HUPERZINE</i> FAMILY OF PHARMACOPHORES.....	1
1.1. Introduction.....	1
1.1.1. The Amyloid Cascade Hypothesis.....	2
1.1.2. The Tau Aggregation Hypothesis.....	4
1.1.3. The Acetylcholinesterase Hypothesis.....	4
1.2. Current Pharmaceutical Treatments for AD.....	5
1.3. Use of <i>Lycopodium</i> Alkaloids as Treatments of AD.....	10
1.3.1. Core Structure of <i>Lycopodium</i> Alkaloids and Their Relevant Activity.....	12
1.4. Conclusions and Implications.....	13

1.5. References.....	13
CHAPTER 2. ATTEMPTED TOTAL SYNTHESIS OF A NOVEL <i>HUPERZINE</i> ALKALOID.....	16
2.1. Introduction.....	16
2.2. Previous Syntheses of Lycopodine-Class <i>Lycopodium</i> Alkaloids.....	17
2.2.1. Previous Syntheses of Lycopodine.....	17
2.2.2. Novel Huperzine Alkaloid of the Lycopodine-Class.....	24
2.3. First-Generation Approach Towards the Total Synthesis of Huperzine X.....	24
2.3.1. Retrosynthetic Analysis.....	24
2.3.2. Forward Synthesis.....	34
2.3.3. First-Generation Synthesis Implications.....	38
2.4. Second-Generation Approach Towards the Total Synthesis of Huperzine X.....	38
2.4.1. Retrosynthetic Analysis.....	38
2.4.2. Forward Synthesis.....	40
2.4.3. Second-Generation Synthesis Implications.....	47
2.5. Third-Generation Approach Towards the Total Synthesis of Huperzine X.....	47
2.5.1. Retrosynthetic Analysis.....	47
2.5.2. Forward synthesis.....	48

2.5.3. Synthetic Approaches to Model Systems.....	52
2.5.3.1. Intramolecular Diels-Alder Model System.....	52
2.5.3.2. Intramolecular Allylation Model System.....	56
2.6. Conclusions and Implications of Model Systems.....	60
2.7. Experimental Section.....	61
2.7.1. General Reaction Considerations.....	61
2.7.2. Experimental Details.....	61
2.8. References.....	82
 CHAPTER 3. ATTEMPTED TOTAL SYNTHESIS OF (+)-(<i>R</i>)-MYCRICANOL.....	 85
3.1. Introduction.....	85
3.2. Tau Protein Aggregation Inhibitors.....	86
3.3. (+)- <i>R</i> -Myricanol.....	86
3.4. Previous Approaches Towards Myricanol-Like Molecules.....	87
3.5. Retrosynthetic Analysis.....	88

3.6. Forward Synthesis.....	90
3.7. Implications and Conclusions of the Synthesis.....	98
3.8. Experimental Section.....	98
3.8.1. General Reaction Considerations.....	98
3.8.2. Experimental Details.....	99
3.8. References.....	105
CHAPTER 4. TOTAL SYNTHESIS OF (+)-CONVOLUTAMYDINE E AND ATTEMPTED TOTAL SYNTHESIS OF RELATED 3-HYDROXYINDOLIN-2-ONE NATURAL PRODUCTS.....	107
4.1. Introduction.....	107
4.1.1. Allyl Groups as Functional Handles for Organic Synthesis.....	108
4.1.2. Allylation and the Cook Group Methodologies.....	111
4.1.3. Current Cook Group Allylation Methodologies.....	114
4.2. Selection of Natural Products for Total Synthesis.....	116
4.3. Previous Syntheses of (<i>R</i>)-Convolutamydines A and E.....	118
4.3.1. Previous Syntheses of (<i>R</i>)-Convolutamydine A.....	118
4.3.2. Previous syntheses of (<i>R</i>)-Convolutamydine E.....	122

4.4. Retrosynthetic Analysis for Convolutamydines A and E.....	124
4.5. Attempted Synthesis of (<i>R</i>)-Convolutamydine A.....	124
4.6. Synthesis of (<i>R</i>)-Convolutamydine E.....	129
4.7. Conclusions.....	131
4.8. Experimental Section.....	132
4.8.1. General Reaction Considerations.....	132
4.8.2. Experimental Details.....	133
4.9. References.....	138
CHAPTER 5. FINAL CONCLUSIONS AND FUTURE WORK.....	141
5.1. Attempted Total Synthesis of Huperzine X.....	141
5.1.1. The Main Synthesis.....	141
5.1.2. Diels-Alder Model System.....	144
5.1.3. Allylation Model System.....	146
5.1.4. Final Conclusions.....	147

5.2. Attempted Total Synthesis of (<i>R</i>)-Myricanol.....	148
5.2.1. Synthesis of the Northern Fragment.....	149
5.2.2. Synthesis of the Southern Fragment.....	149
5.2.3. Biaryl Formation and Completion Steps.....	150
5.3 Final Conclusions on the Synthesis of Convolutamydine E.....	152
5.4. References.....	153

LIST OF TABLES

<u>Table</u>	<u>Page</u>
2.1: <i>Attempted synthesis of vinyl triflate 2.40 using standard triflation methodologies</i>	42
2.2: <i>Hydrozirconation trials using 2.58 as an alkyne starting material</i>	49
2.3: <i>Attempts to add allyl trimethylsilane to 2.73 using various Lewis acids</i>	59
3.1: <i>Optimization of dimethylation reaction</i>	91
3.2: <i>Attempted [3.3]-sigmatropic rearrangement of 3.11</i>	93
4.1: <i>Trials for the reduction of 4.30 to 4.27</i>	126
4.2: <i>Cyclization of 4.31 to 4.26 – acid concentration and reaction time experiments</i>	127
4.3: <i>Attempts to oxidatively cleave 4.20</i>	130

LIST OF FIGURES

<u>Figure</u>	<u>Page</u>
1.1: <i>APP cleavage sites</i>	3
1.2: <i>Structure of cucumin</i>	7
1.3: <i>Structures of some anti-oxidant, metal chelating natural products</i>	7
1.4: <i>Structures of anti-oxidant, Fe²⁺ chelators based on 8-hydroxyquinoline</i>	8
1.5: <i>Three current pharmaceuticals for treatment of early-stage AD</i>	10
1.6: <i>Huperzine A</i>	10
1.7: <i>Three lycopodium alkaloids and their structural similarities</i>	11
1.8: <i>Structures of lycopodine and related alkaloids</i>	12
2.1: <i>Lycopodine with ring and stereochemical identification</i>	17
2.2: <i>Isolated lycopodine-class lycopodium alkaloid, total synthesis target</i>	24
2.3: <i>Model compound for ynamide Diels-Alder studies and optimization</i>	52
2.4: <i>Substrates for the study and optimization of the pyridone allylation model system</i>	57
3.1: <i>Structure of the diarylheptanoid (+)-aR,11S-myricanol</i>	87
4.1: <i>Vancomycin</i>	107
4.2: <i>Synthetic utility of the allyl group</i>	108
4.3: <i>Isatin</i>	114

4.4: Possible synthetic targets for total synthesis in support of the Cook group	
<i>allylation methodology</i>	117

LIST OF SCHEMES

<u>Scheme</u>	<u>Page</u>
2.1: <i>Synthesis of tetrahydroquinoline 2.03 as a lycopodine precursor</i>	18
2.2: <i>Heathcock synthesis of (±)-lycopodine</i>	19
2.3: <i>Kim synthesis of anhydrolycopodine</i>	20
2.4: <i>Grieco synthesis of lycopodine</i>	21
2.5: <i>Carter synthesis of lycopodine</i>	22
2.6: <i>Initial retrosynthetic disconnection to form the bridging ether linkage</i>	25
2.7: <i>Potential routes for the addition of Me⁻ to the bridged ketone 2.19</i>	27
2.8: <i>Retrosynthesis of 2.19, providing allylation intermediate 2.21</i>	28
2.9: <i>Application of the intramolecular allylation of the activated iminium of 2.21</i>	29
2.10: <i>Proposed synthesis of the A-ring</i>	30
2.11: <i>Literature report of Rh(I)⁺-catalyzed intramolecular ynamide Diels-Alder reaction</i>	30
2.12: <i>Retrosynthesis of 2.24 to provide carbamate 2.27 and bromoalkyne 2.26</i>	32
2.13: <i>Retrosynthesis of 2.27 resulting from olefination</i>	32
2.14: <i>Retrosynthesis of the allylic olefination partners</i>	33
2.15: <i>Synthesis of 1,4-skip diene 2.31</i>	34
2.16: <i>Synthesis of 2.32 and 2.33</i>	35

2.17: <i>Attempts at cross-metathesis of 2.32 with olefination partners</i>	36
2.18: <i>Attempts to incorporate the allylic bromide into 2.32</i>	37
2.19: <i>Retrosynthesis of 2.28 resulting from cross-coupling</i>	39
2.20: <i>Retrosynthesis of vinyl triflate 2.40</i>	39
2.21: <i>Synthesis of cross-coupling partners 2.41 and 2.42 from a common precursor</i>	40
2.22: <i>Synthesis of vinyl triflate precursor 2.43</i>	41
2.23: <i>Observed mechanistic implications in the synthesis of 2.40</i>	43
2.24: <i>Attempted hydroboration to install the vinyl boronate cross-coupling partner</i>	45
2.25: <i>Attempted synthesis of vinyl boronate 2.54 by cross-metathesis</i>	46
2.26: <i>Attempted synthesis of vinyl iodide 2.55</i>	47
2.27: <i>Third-generation retrosynthesis involving addition onto aldehyde 2.43</i>	48
2.28: <i>Hydrozirconation/transmetalation sequence for constructing 2.59</i>	50
2.29: <i>Attempted synthesis of Diels-Alder model compound 2.60</i>	54
2.30: <i>Ynamide formation using iodonium alkyne 2.68</i>	55
2.31: <i>Intramolecular Diels-Alder reaction of model compound 2.71</i>	56
2.32: <i>Retrosynthesis of the inter- and intra-molecular allylation model systems</i>	58
3.1: <i>Oxidative coupling of bisiodide 3.02 giving protected (\pm)-myricanol 3.03</i>	88

3.2: Retrosynthetic analysis of myricanol.....	90
3.3: Synthesis of allyl phenyl ether 3.11	92
3.4: Attempted DoM to install the C-6 allyl group.....	94
3.5: Attempted synthesis of the allyl group through metalation of 3.16	95
3.6: Synthesis of 3.20	96
3.7: Final synthesis of 3.21	97
4.1: Example of a [2,3]-Wittig rearrangement.....	109
4.2: Example of [3,3]-sigmatropic rearrangement (Claisen rearrangement) of an allyl vinyl ether.....	109
4.3: Example of an allyl group isomerization catalyzed by Rh.....	110
4.4: Example of allyl groups participating in RCM.....	110
4.5: Example of allylic C-H bond functionalization using Pd catalysis.....	111
4.6: Cook Group methodology for diastereoselective allylation of hydrazones.....	112
4.7: Cook group ligand control of enantioselective hydrazone allylation.....	113
4.8: Highly diastereoselective intramolecular allylation of hydrazones leading to aminochromanes.....	114
4.9: Allylation of isatin using Bi(0)/BiCl ₃ conditions.....	115
4.10: Allylation of isatin using In(0)-mediated conditions.....	116
4.11: General organocatalytic approach to the total synthesis of (R)-convolutamydine A.....	119

4.12: Previous total synthesis of (R)-convolutamydine A.....	120
4.13: Total synthesis of (R)-convolutamydine A without forming the isatin directly.....	121
4.14: Total synthesis of (R)-convolutamydine A using In-mediated diastereoselective allylation.....	122
4.15: Organocatalytic total synthesis of (R)-convolutamydine E.....	123
4.16: Vinylogous Mukaiyama Aldol reaction leading to (R)-convolutamydine E.....	123
4.17: Proposed retrosynthetic analysis of convolutamydines A and E.....	124
4.18: Synthesis of 3,5-dibromonitrobenzene (4.30).....	125
4.19: Synthesis of 4,6-dibromoisatin 4.26.....	127
4.20: In(0)-mediated allylation of 4.26.....	128
4.21: Attempted Wacker oxidation of 4.41 to give 4.23.....	129
4.22: Attempted oxidative cleavage of model system 4.20.....	129
4.23: Oxidative cleavage of 4.41 to yield 4.24.....	131
5.1: Attempted use of Ir-catalyzed nitrogenous coupling to produce viable transmetalation partner 5.02.....	142
5.2: Projected synthesis of the tricyclic core of Huperzine X.....	143
5.3: Alternative experiments to determine cause of low yield in ynamide formation.....	145
5.4: Projected synthesis of a more reactive intramolecular allylation model system.....	147

LIST OF ABBREVIATIONS/ SYMBOLS

$A\beta$	amyloid-beta
$A\beta_{1-42}$	amyloid-beta protein fragment 42 amino acids in length
Ac	acetate
AChE	acetylcholinesterase
AChEi	acetylcholinesterase inhibitor
AcOH	acetic acid
AD	Alzheimer's Disease
APP	amyloid precursor protein
Boc	<i>tert</i> -butyloxycarbonyl
<i>n</i> BuLi	<i>normal</i> -butyl lithium
CM	cross metathesis
DCM	dichloromethane (methylene chloride)
DIAD	Di- <i>iso</i> -propylazodicarboxylate
DMF	<i>N,N</i> -dimethylformamide
DMSO	dimethylsulfoxide
DMSO- d_6	hexadeuteriodimethylsulfoxide
<i>dr</i>	diastereomeric ratio
<i>ee</i>	enantiomeric excess
Et ₂ O	diethyl ether
EtOAc	ethyl acetate
FCC	flash column chromatography
GCMS	gas chromatography/mass spectrometry (coupled instrument)

Gly.....glycine
HMPA.....hexamethylphosphoramide
HPLC.....high pressure liquid chromatography
HRMS.....high resolution mass spectrometry
Me.....methyl
NMO.....*N*-methylnmorpholine *N*-oxide
¹H-NMR.....nuclear magnetic resonance (detecting protons)
¹³C-NMR.....nuclear magnetic resonance (detecting carbon isotope ¹³C)
Ns.....nosyl (*para*-nitrophenylsulfonyl)
*n*Oct.....*normal*-octyl
Ph.....phenyl
phen.....1,10-phenanthroline
(*S*)-PhPyBOX.....2,6-bis[(4*S*)-(-)-phenyl-2-oxazolin-2-yl]pyridine
*i*Pr.....*iso*-propyl
Pyr.....pyridine
RCM.....ring closing metathesis
TBAF.....tetra-*normal*-butylammonium fluoride
TBS.....*tert*-butyldimethylsilyl
Tf.....triflate (trifluoromethanesulfonate)
THF.....tetrahydrofuran
TIPS.....triisopropylsilyl
TLC.....thin-layer chromatography
TMS.....trimethylsilyl

Ts.....tosyl (*para*-toluene sulfonyl)

CHAPTER 1. A REVIEW OF ALZHEIMER'S DISEASE AND THE ROLE OF ALKALOIDS FROM THE *LYCOPodium/HUPERZINE* FAMILY OF PHARMACOPHORES

1.1. Introduction

Alzheimer's Disease (AD) is one of the most common forms of dementia¹. AD has been a ravaging neurological disorder in the public eye for over 100 years; ever since it was first identified and reported publicly at a convention of psychiatric professionals in 1906 by Dr. Alois Alzheimer. AD is characterized by a loss of memory and cognition leading to physical disability and death². These physiological changes are brought on by synaptic degradation and neuronal death. Traditionally, the extent of AD in dementia patients could only be determined posthumously via autopsy. Noticeable differences in brain appearance between healthy and AD patients appear in the frontal and temporal lobes, with a high concentration of deposited proteins around the neural clefts². This leads to a strangulation of the neurons and an overall shrinkage of the brain tissues as the neural networks atrophy.

AD is also characterized by high levels of oxidation (typically indicative of oxidative stress)³ as well as dyshomeostasis of several key metal ions, most notably calcium, copper, iron, and zinc⁴. Patient genetics also plays a role in AD progression⁵. There are many competing theories of AD initiation and disease progression and for the sake of context, only three main theories will be discussed here: the amyloid cascade hypothesis, the tau aggregation hypothesis, and the acetylcholinesterase hypothesis. While there are other theories, many of them do not yet possess clear therapeutic targets. It has also been shown that some of the factors which improve the likelihood that AD will develop are genetic and thus inheritable⁵.

1.1.1. The Amyloid Cascade Hypothesis

The amyloid cascade hypothesis is one which was developed through the autopsy-detected protein buildups around the neural networks. These proteins were found to be aggregates of proteins created through cleavage of the Amyloid Precursor Protein (APP), a transmembrane protein found in the primary membrane and mitochondrial membrane of neural cells². The plaques were dubbed amyloid- β ($A\beta$) proteins and the primary thought was that the buildup of the plaques was the direct cause of cognitive function. It was discovered later, however, that the plaques were non-toxic. Mice incapable of forming $A\beta$ plaques developed the disease while mice that formed plaques had no greater propensity for the disease⁶. It was found that the plaques were aggregating due to an imbalance in the clearance of the soluble $A\beta$ fragments, either by the ApoE clearance chaperones or the 20S proteasome⁷. Further elucidation showed that two fragments were primary constituents: $A\beta$ 1-40 and $A\beta$ 1-42⁸. Although structurally similar, $A\beta$ 1-42 is significantly more neurotoxic due to the additional hydrophobic residues⁹, which promote aggregation¹⁰ as well as favor protein-protein interactions with other cellular components¹¹. It was discovered that of the $A\beta$ 1-42 aggregates, the oligomeric fragments were the most cytotoxic¹², affecting synaptic transmission by altering the availability of synaptic vesicles¹³. Presumably this is due to the clogging of the vesicle fusion docking site (vesicle fusion is a synaptic trigger event).

Amyloid protein fragments are generated by a series of secretases located on the outer membrane, as well as the intracellular membrane wall. Initially, β -secretase cleaves APP between methionine 670 and aspartic acid 671, releasing a small fragment as well as a larger, mostly insoluble fragment (Figure 1.1).



Figure 1.1: *APP cleavage sites*

In an attempt to clear the formed insoluble mass, γ -secretase cleaves the mass into a 40 or 42 amino acid residue fragment, and a more soluble fragment which coils and is cleared by intracellular proteases. Since the action of γ -secretase is dependent on the initial cleavage by β -secretase, the process is regulated through the expression of the β -site APP-cleaving enzyme 1 gene (*BACE1*). Smith and co-workers have suggested that, due to an increase in *BACE1* expression in AD patients which corresponds to an increase in $A\beta_{1-42}$ concentration, *BACE1* is upregulated by $A\beta_{1-42}$ ¹⁴. This implies that once the soluble fragments of the APP are produced, a cascade effect is initiated whereby additional fragments are produced. After enough of these soluble protein fragments are generated, they begin to aggregate. The smaller oligomers are generally cytotoxic, while the larger oligomers tend to aggregate further and form fibrils¹⁵, which adhere to one another and become the inactive $A\beta$ plaque deposits commonly associated with AD. These plaques are not responsible for the symptoms of AD, but are rather used as repositories of soluble oligomers, which promote those symptoms. This occurs as the oligomers are removed from the system (either by bodily clearance or, more likely in AD, by complexation to neural proteins) and the plaques begin to release additional oligomers, reestablishing the equilibrium¹⁶.

1.1.2. The Tau Aggregation Hypothesis

In addition to the theory that the soluble fragments from APP are responsible for synaptic degradation, an alternative theory has been given, where the A β 1-42 fragment is indirectly responsible. Instead of interfering with synaptic processes, A β 1-42 is responsible for promoting oxidative stress and a marked increase in Ca²⁺ ion concentration in the intracellular matrix. It has been theorized that A β 1-42 initiates this increase in Ca²⁺ concentration by creating gateways in the cellular membrane (through intercalation of the membrane itself), or by activating Ca²⁺ pumps¹⁷. This sharp increase in internal Ca²⁺ concentration has been linked to a number of cellular mechanisms which are activated by the sudden dyshomeostasis of the Ca²⁺ concentration, including the hyperphosphorylation of the tau protein¹⁸.

The tau protein is the primary structural component of neural pathways inside of the neurons themselves. As synaptic activity is stimulated, tau is phosphorylated and dephosphorylated in a regulated fashion to allow for controlled microtubule formation, and synaptic information to be transmitted¹⁹. Hyperphosphorylation leads to destabilized microtubules, and thus inefficient and often disconnected transmissions²⁰.

Tau protein behavior and characteristics are regulated by specific genes which can be directly modulated to give rise to multiple neurological disorders, implying that these genes can be effective targets for AD therapies, or effective screening markers for AD susceptibility²¹.

1.1.3. The Acetylcholinesterase Hypothesis

Another predominant hypothesis in the field of AD preventative research is the acetylcholinesterase (AChE) hypothesis. In this pathway, AChE is responsible for maintaining synaptic cleft levels of choline and acetylcholine. Research has shown that AD patients over-

express AChE, and thus a buildup of choline occurs²². This affects a large number of neural processes downfield from AChE, and it has been implicated not only in AD, but also Parkinson's Disease and common dementia²³. Due to the large number of potential disease treatment options, acetylcholinesterase inhibitors (AChEi) have been the primary target of pharmaceutical companies interested in AD treatments.

One neural process downfield from AChE which has received a significant amount of attention is the evidence which links neurotransmitters in the choline pathway, namely choline and acetylcholine, appear to rapidly promote the cleavage and release of soluble *N*-terminal amyloid protein fragments²⁴. This connection between the acetylcholine pathway and the *Aβ* pathway not only provides additional possibilities towards a unified treatment of the disease but also showcases how extremely complex AD is, and how interconnected all of the neural pathways are.

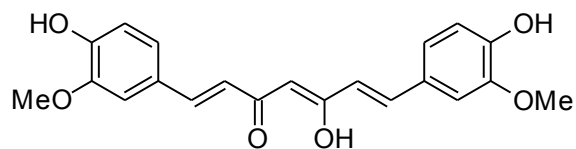
Due to this large interconnectivity, it is unfortunately realized that most compounds slated for AD treatment come with severe side-effects.

1.2. Current Pharmaceutical Treatments For AD

The current treatments for AD vary as much as the theories of action which drive their development. As such the compounds can fall into a variety of categories. For the purpose of comparison, these compounds will be classified as *β*-amyloid targeted, tau targeted, or acetylcholinesterase inhibitors. With the exception of the initial class, most of the compounds used to treat AD or show efficacy against AD in some way operate using different mechanisms. Since the brain is so complex, each pathway has multiple treatment options. As such, there is no definitive molecular scaffold on which pharmaceutical companies can build upon to increase

drug efficacy and stability. Due in part to this problem, more pharmaceutical companies have been examining the compounds which are derived from natural sources known to be beneficial to synaptic health and memory retention²⁵. Large classes of antibodies have also been developed, mostly to detect the toxic $A\beta_{1-42}$ fragment²⁶.

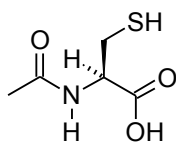
By identifying several of the contributing factors for each targeted pathway, researchers have developed novel ways to counteract the deleterious effects of AD's symptoms. While an outright cure for AD seems a long way off, a removal of the symptomatic suffering of AD patients is always a welcome goal. A corollary to all of the prevailing theories of AD development is that many AD patients experience high levels of reactive oxygen species (ROS), as well as the tell-tale signs of oxidative damage and high oxidative stress levels. A school of thought in this avenue is that AD creates a dyshomeostasis of various metal ions in the central nervous system (CNS), mainly Zn^{2+} , Cu^{2+} , $Fe^{2+/3+}$, and Ca^{2+} in the cytosol and extracellular medium²⁷. In this light, a wide range of metal chelating compounds have been screened against AD. The idea is that the chelating agents, in the right amounts and delivered to the correct locations, will help restore balance in the CNS, and the body's own mechanisms will help to restore the cognitive function. Initially, it was observed that the rate of AD was significantly lower in Indian populations of elderly patients²⁸. Correlations with consumption of curry led to the identification of cucumin (**1.01**) as a potent Cu^{2+} chelator, which may aid in destabilizing $A\beta$ plaque formation (Figure 1.2). It has been shown that Cu^{2+} can stabilize the aggregation of $A\beta_{1-42}$ ²⁹. Cu^{2+} has also been shown to favorably interact with the aggregate conformers, stabilizing specific geometries³⁰. Varying the concentration of NaCl also shifted the dyshomeostasis of specific ions, namely Cu^{2+} , suggesting that ionic strength of the neural media plays a critical role in the onset of AD-promoting conditions³¹.



1.01

Figure 1.2: Structure of cucumin

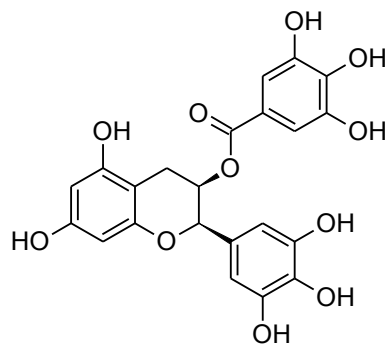
Based on the perceived notion that metal chelators could be used as effective AD therapies, many more chelating compounds were isolated (Figure 1.3). *N*-acetylcystine (**1.02**) is a membrane-penetrable chelating agent already used to treat cystic fibrosis³². Naturally occurring α -lipoic acid (**1.03**) is found in spinach, while epigallocatechin gallate (**1.04**) is found in green tea. Melatonin (**1.05**) is a hormone responsible for hippocampus memory formation³³ and galantamine (**1.06**) is a potent AChEi³⁴.



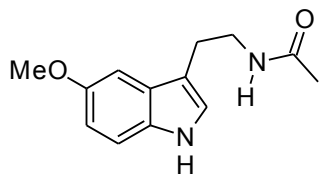
1.02



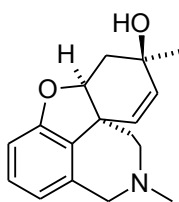
1.03



1.04



1.05



1.06

Figure 1.3: Structures of some anti-oxidant, metal-chelating natural products

A number of novel Fe^{2+} chelators have also been developed around the 8-hydroxyquinoline core structure, which have shown good potency as chelators as well as antioxidants (Figure 1.4)³⁵. These same structures have also been shown to be AChEi active³⁶.

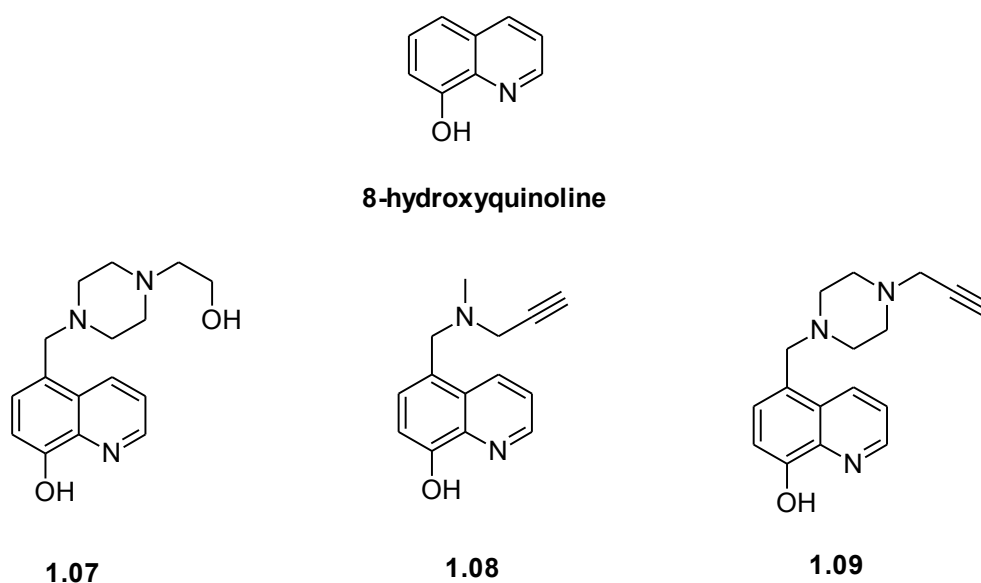
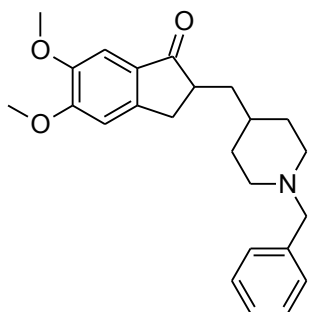


Figure 1.4: Structures of anti-oxidant, Fe^{2+} chelators based on 8-hydroxyquinoline

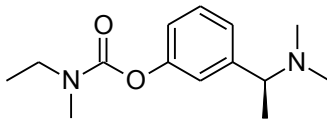
A number of peptides have been found to improve the cognitive function of AD-afflicted mice, most notably the discovery of an orally available peptide which improves clearance of $\text{A}\beta$ fragments³⁷. These operate by interacting with the soluble $\text{A}\beta$ fragments and preventing the aggregation that produces toxic, soluble oligomers³⁸. This prevention of aggregation is also a key target in pharmaceutical development. By inhibiting the aggregation, the soluble fragments exist in solution long enough as independent entities for the natural clearance apolipoproteins to chaperone them out of the cerebral media. In this light, Rangachari and co-workers have reported a bimetallic Rh-Pt complex which they have shown to bind to the *N*-terminus of $\text{A}\beta$ 1-42, thus preventing aggregation³⁹.

The prevention of acetylcholine breakdown by inhibition of AChE has widespread implications, and many compounds have been developed to reach this target. The choice of AChE over any of the secretases is partially due to lack of understanding of all of the roles secretases play in neurological health⁴⁰, as well as the ease with which AChE can be reached as a target system.

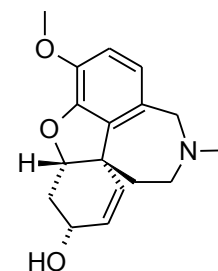
There are currently three main compounds available for the treatment of dementia associated with AD and Parkinson's disease (Figure 1.5). These compounds do not prevent dementia or restore cognitive ability, but they do prevent the onset of the more severe symptoms and are thus administered in early-stage AD and Parkinson's. Donepezil (**1.10**, trade name: *Aricept*, Pfizer), rivastigmine (**1.11**, trade name: *Exelon*, Novartis), and galantamine (**1.12**, trade name: *Razadyne*, Ortho-McNeil-Janssen Pharmaceuticals) are all AChEi which act by preventing the over-degradation of acetylcholine, and thus preventing choline-dependent interferences downstream⁴¹. All of these treatment options involve the transmission of the active compounds across the Blood-Brain Barrier (BBB), a feat which until recently was thought to be difficult for some of the compounds. Recent evidence has shown that there is a deterioration of the BBB which affects the efficacy of the administered pharmaceuticals⁴². Any new compound must be made with an eye towards this slightly different activity profile.



1.10



1.11

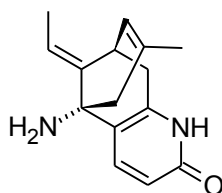


1.12

Figure 1.5: Three current pharmaceuticals for treatment of early-stage AD

1.3. Use of *Lycopodium* Alkaloids as Treatments of AD

Alkaloids from the *Lycopodium* family of club mosses have long been highly regarded in Chinese herbal medicine as promoters of memory and cognitive function⁴³. The most successful alkaloid isolated from these mosses and used in human patients is Huperzine A (1.13, Figure 1.6)⁴⁴.



1.13

Figure 1.6: *Huperzine A*

Huperzine A is a potent and reversible AChEi, with IC_{50} of 47 nM⁴⁵, currently in use as an AChEi in patients with mild AD symptoms. It is thought that the various alkaloids of the *lycopodium* family bind to AChE on the surface of the protein, rather than in the binding pocket⁴⁶. This causes a conformation change which disables the ability of the enzyme to perform

the hydrolysis of acetylcholine to choline. While monitoring the $^1\text{H-NMR}$ relaxation times for the binding of **1.13** to AChE, the authors found that other members of the *lycopodium* alkaloid family gave similar results when complexed with the enzyme. This suggests that all of these small molecules interact in similar ways with the surface of the protein. It is likely that a structural characteristic common to all three of the alkaloids is responsible for the binding affinities⁴⁷. Examining the three structures, a common feature is revealed: a bridging 2-methylpropene unit as well as a basic amine (ranging from 1° to 3°) in the same position (Figure 1.7). Kozikowski and co-workers suggested that the unsaturation point on the three-carbon bridge was critical for activity, and synthesized a number of analogs to prove this. It is likely, especially considering the activity of other members of the *lycopodium* alkaloid family which do not possess this unsaturation, that what is critical is the geometry around that area of the molecule.

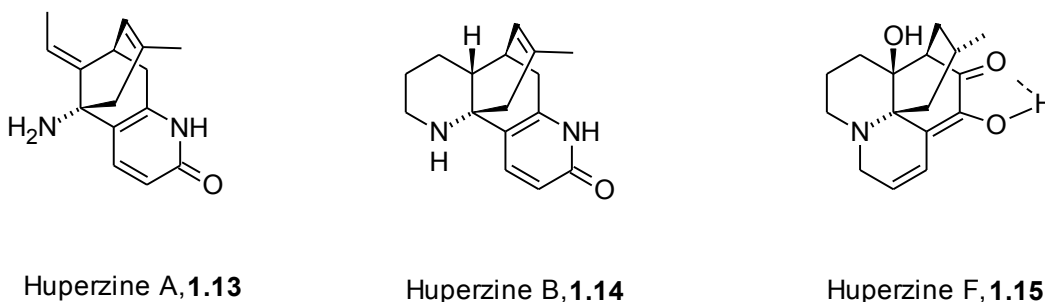


Figure 1.7: Three *lycopodium* alkaloids and their structural similarities

The same group reported later an X-ray crystal structure of **1.13** complexed with AChE, showing a blockage of the active site's channel opening by use of non-covalent interactions⁴⁸. The requirement of a basic amine and the sterically encumbered environment surrounding it may be to the advantage of complexation with an exposed acidic residue on the surface of the enzyme. Another possibility is that the 2-pyridone moiety in **1.13** and Huperzine B (**1.14**), as

well as the α -hydroxyketone in Huperzine F (**1.15**) could be used to chelate a metal ion, suggesting a connection between the Huperzine alkaloids and the metal-ion dyshomeostasis theory of AD pathology.

1.3.1. Core Structure of *Lycopodium* Alkaloids and Their Relevant Activity

While **1.13** and **1.14** reside in the lycodine class of *lycopodium* alkaloids, all of which possess the 2-ketopyridine functionality or similarly aromatic moieties, **1.15** is part of a structurally similar family known as the lycopodine class. This class is based off of lycopodine (**1.16**), a simplified variant of the Huperzine alkaloids which still possess the methylated 3-carbon bridge required for activity (Figure 1.8). Examples of this class include Huperzine G (**1.17**), Miyoshianine B (**1.18**), Selagoline (**1.19**), and Annotine (**1.20**).

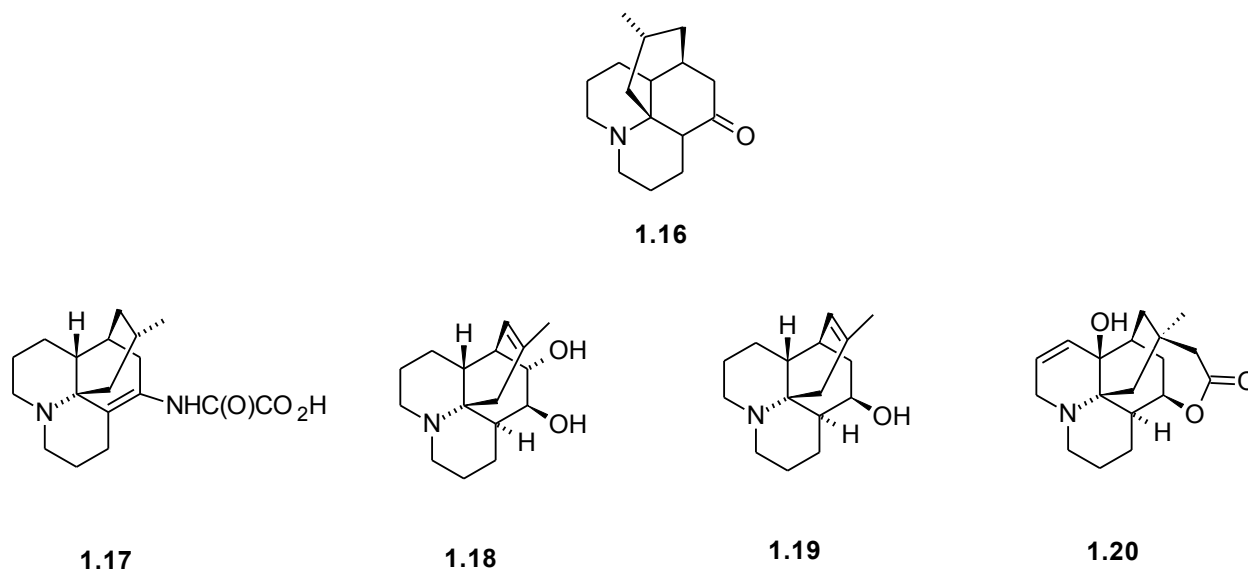


Figure 1.8: Structures of lycopodine and related alkaloids

While Huperzine A is an effective treatment for early AD, many main-stream pharmaceutical companies will not market it or its direct analogs due to its original isolation information/procedure being in the public domain⁴⁴. Thus, a strong desire for synthetic alternatives to the entire *lycopodium* family is present in the field of AD therapeutics.

1.4. Conclusions and Implications

With the need for new therapeutic compounds for the treatment of AD and the prevalence of the lycopodine skeleton in the *lycopodium* alkaloid family, synthetic efforts which will enhance our current ability to fight AD should focus on the synthetically challenging lycopodine core. Many different syntheses of the *lycopodium* alkaloids have been reported, but all of them provide industrially unsuitable processes, or focus mainly on a specific reaction that the research group wishes to showcase. In this light, it has been slow-moving towards a generalized approach to the entire family of natural products. A main goal of the projects to follow is to highlight synthetic routes towards this central core of the *lycopodium* alkaloid family during a total synthesis of a new *Huperzine* alkaloid discovered from the same club moss which has provided so much to the AD community already.

1.5. References

¹ Goedert, M., Spillantini, M. G.; *Science*, **2006**, *314*, 777-781.

² Mattson, M.; *Nature*, **2004**, *430*, 631-639.

³ Perry, G., Cash, A., Smith, M., *J. Biomol. and Biotech.*, **2002**, *2*, 120-123.

⁴ Mattson, M.; *Nature*, **2004**, *430*, 631-639; Mandel, S., Amit, T., Bar-Am, O., Youdim, M.; *Prog. Neurobiol.*, **2007**, *82*, 348-360; Frederickson, C., Koh, J., Bush, A.; *Nature Rev. Neurosci.*, **2005**, *6*, 449-462; Kepp, K.; *Chem Rev.*, **2012**, *112*, 5193-5239.

⁵ Hollingworth, P., Harold, D., Jones, L., Owen, M., Williams, J.; *Int. J. Geriatr. Psychiatry*, **2011**, *26*, 793-802.

- ⁶ Kaye, R., Head, E., Thompson, J., McIntire, T., Milton, S., Cotman, C., Glabe, C.; *Science*, **2003**, *300*, 486-489; Gandy, S., Simon, A., Steele, J., Lubin, A., Lah, J., Walker, L., Levey, A., Krafft, G., Levy, E., Checler, F., Glabe, C., Bilker, W., Abel, T., Schmeidler, J., Ehrlich, M.; *Annal. Neurol.*, **2010**, *68*, 220-230.
- ⁷ Zhao, X., Yang, J.; *ACS Chem. Neurosci.*, **2010**, *1*, 655-660.
- ⁸ Harigaya, Y., Saido, T., Eckman, C., Prada, C-M., Shoji, M., Younkin, S.; *Biochem. and Biophys. Res. Commun.*, **2000**, *276*, 422-427.
- ⁹ Yerbury, J., Favrin, G.; *ACS Chem. Biol.*, **2010**, *5*, 735-740.
- ¹⁰ Small, D.; "Research and Practice in Alzheimer's Disease", Vol. 3, pp 27-33, Springer Publishers, New York, NY.
- ¹¹ Kaye, R., Head, E., Thompson, J., McIntire, T., Milton, S., Cotman, C., Glabe, C.; *Science*, **2003**, *300*, 486-489.
- ¹² Naylor, R., Hill, A., Barnham, K.; *Eur. Biophys. J.*, **2008**, *37*, 265-268.
- ¹³ Moreno, H., Yu, E., Pigino, G., Hernandez, A., Kim, N., Moreira, J., Sugimori, M., Llinás, R.; *PNAS*; **2009**, *106*, 5901-5906.
- ¹⁴ Tabaton, M., Zhu, X., Perry, G., Smith, M., Giliberto, L.; *Exp. Neuro.*, **2010**, *221*, 18-25.
- ¹⁵ Bayro, M., Maly, T., Birkett, N., MacPhee, C., Dobson, C., Griffin, R.; *Biochemistry*, **2010**, *49*, 7474-7484.
- ¹⁶ Haass, C., Selkoe, D.; *Nature Reviews*, **2007**, *8*, 101-112.
- ¹⁷ Mattson, M.; *Nature*, **2004**, *430*, 631-639.
- ¹⁸ Blanchard, B., Hiniker, A., Lu, C., Margolin, Y., Yu, A., Ingram, V.; *J. Alzheimer's Disease*, **2000**, *2*, 137-149.
- ¹⁹ Johnson, G., Stoothoff, W.; *J. Cell. Sci.*, **2004**, *117*, 5721-5729.
- ²⁰ Stoothoff, W., Johnson, G.; *Biochem. Phys. Acta.*, **2005**, *1739*, 280-297.
- ²¹ Goedert, M., Spillantini, M.; *Science*, **2006**, *314*, 777-781.
- ²² Toiber, D., Berson, A., Greenberg, D., Melamed-Book, N., Diamant, S., Soreq, H.; *PLoS ONE*, **2008**, *3*, e3108.
- ²³ Greenfield, S., Vaux, D.; *Neuroscience*, **2002**, *113*, 485-492.
- ²⁴ Nitsch, R., Slack, B., Wurtman, R., Growdon, J.; *Science*, **1992**, *258*, 304-307.
- ²⁵ Haefner, B.; *Drug Discovery Today*, **2003**, *8*, 536-544.
- ²⁶ Shimizu, T., Irie, K.; *ACS Chem. Neurosci.*, **2010**, *1*, 747-756.
- ²⁷ Kepp, K.; *Chem Rev.*, **2012**, *112*, 5193-5239.
- ²⁸ Ganguli, M., Chandra, V., Kamboh, I., Johnston, J., Dodge, H., Thelma, B., Juyal, R., Pandav, R., Belle, S., DeKosky, S.; *Arch. Neurol.*, **2000**, *57*, 824-830.
- ²⁹ Epa, V., Streltsov, V., Varghese, J.; *Aust. J. Chem.*, **2010**, *63*, 345-349.
- ³⁰ Miller, Y., Ma, B., Nussinov, R.; *J. Am. Chem. Soc.*, **2011**, *133*, 2742-2748.
- ³¹ Jain, S., Udganokar, J.; *Biochemistry*, **2010**, *49*, 7615-7624.
- ³² Henke, M., Ratjen, F.; *Paediatr Respir. Rev.*, **2007**, *8*, 24-29.; Garrett, C., Prasad, K.; *Adv. Synth. Cat.*, **2004**, *346*, 889-900.
- ³³ Larson, J., Jessen, R., Uz, T., Arslan, A., Kurtuncu, M., Imbesi, M., Manev, H.; *Neurosci. Lett.*, **2006**, *393*, 26-26.
- ³⁴ Woodruff-Pak, D., Lander, C., Geerts, H.; *CNS Drug Rev.*, **2002**, *8*, 405-426.
- ³⁵ Mandel, S., Amit, T., Bar-Am, O., Youdim, M.; *Progress in Neurobiol.*, **2007**, *82*, 348-360.
- ³⁶ Zheng, H., Youdim, M., Fridkin, M.; *ACS Chem Neurosci.*, **2010**, *1*, 737-746.

- ³⁷ Funke, S., van Groen, T., Kadish, I., Bartnik, D., Nagel-Steger, L., Brener, O., Sehl, T., Batra-Safferling, R., Moriscot, C., Schoehn, G., Horn, A., Muller-Schiffmann, A., Korth, C., Sticht, H., Willbold, D.; *ACS Chem. Neurosci.*, **2010**, *1*, 639-648.
- ³⁸ Bett, C., Ngunjiri, J., Serem, W., Fontenot, K., Hammer, R., McCarley, R., Garno, J.; *ACS Chem Neurosci.*, **2010**, *1*, 608-626.
- ³⁹ Kumar, A., Moody, L., Olaivar, J., Lewis, N., Khade, R., Holder, A., Zhang, Y., Rangachari, V.; *ACS Chem. Neurosci.*, **2010**, *1*, 691-701.
- ⁴⁰ Eli Lilly developed *Semagacetstat* as a gamma-secretase inhibitor, which failed in Phase III clinical trials by being worse than the placebo. It is to date one of the more advanced (in terms of developmental progress) forms of secretase inhibitor. See: Yi, P., Hadden, C., Kulanthaivel, P., Calvert, N., Annes, W., Brown, T., Barbuch, R., Chaudhary, A., Ayan-Oshodi, M., Ring, B.; *Drug Metabolism and Disposition*, **2010**, *38*, 554-565.
- ⁴¹ Emilien, G., Beyreuther, K., Masters, C., Maloteaux, J-M.; *Arch. Neurol.*, **2000**, *57*, 454-459.
- ⁴² Desai, B., Monahan, A., Carvey, P., Hendey, B.; *Cell Transplantation*, **2007**, *16*, 285-299.
- ⁴³ Ma, X., Gang, D.; *Nat. Prod. Rep.*, **2004**, *21*, 752-772.
- ⁴⁴ Kozikowski, A., Tüchmantel, W.; *Acct. Chem. Res.*, **1999**, *32*, 641-650.
- ⁴⁵ Luo, W., Yu, Q.-S., Kulkarni, S., Parrish, D., Holloway, H., Tweedie, D., Shafferman, A., Lahiri, D., Brossi, A., Greig, N.; *J. Med. Chem.*, **2006**, *49*, 2174-2185.
- ⁴⁶ Li, Y., Yin, G., Wei, W., Wang, H., Jiang, S., Zhu, D., Du, W.; *Biophys. Chem.*, **2007**, *129*, 212-217.
- ⁴⁷ Kozikowski, A., Miller, C., Yamada, F., Pang, Y., Miller, J., McKinney, M., Ball, R.; *J. Med. Chem.*, **1991**, *34*, 3399-3402.
- ⁴⁸ Raves, M., Harel, M., Pang, Y-P., Silman, I., Kozikowski, A., Sussman, J.; *Nat. Struct. Biol.*, **1997**, *4*, 57-63.

2.1. Introduction

As discussed in the previous chapter, the total synthesis of *lycopodium* alkaloids is a key feature in the fight against AD. The vast majority of the reported syntheses focus on Huperzine A, which is the most studied clinically. Many structural analogs have been reported based around the Huperzine A nucleus, but many of them are merely modifying peripheral groups to make the compound more potent and selective¹. Due to Huperzine A's classification as a lycodine-class alkaloid, those structures have the most well-developed synthetic strategies. The alternative Fawcettimine-class also has a number of well-established protocols for their synthesis. Lycopodine-class alkaloids, however, have not found such a niche in the synthetic community.

Generally speaking, the lycopodine-class of *lycopodium* alkaloids are not as metabolically stable, or occasionally do not possess the desired activity¹. Many of the Huperzine alkaloids are oxidative products of the parent lycopodine (**2.01**). As such, their synthesis becomes more difficult, as many of the oxidations occur on carbons which bench chemists cannot selectively oxidize. As such, the oxygen-containing functionalities have to be incorporated into the synthesis in alternative ways.

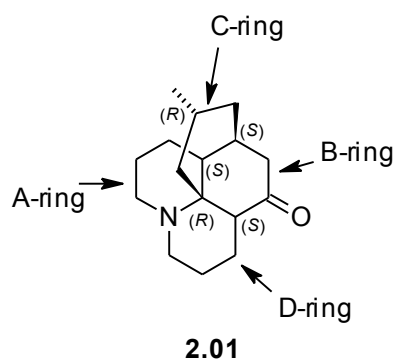


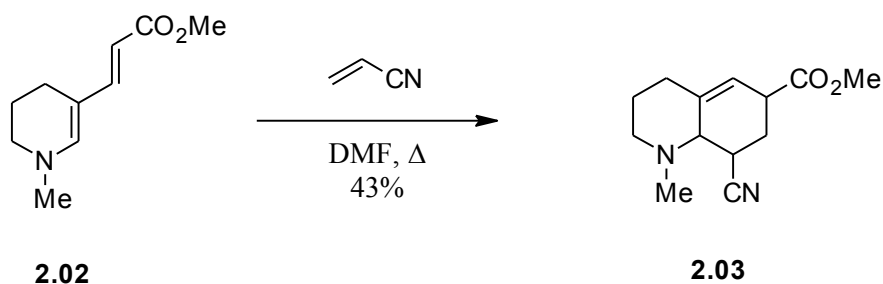
Figure 2.1: *Lycopodine with ring and stereochemical identification*

There have been a number of syntheses focused on this class of alkaloids, and they all bring something different to the challenging problem of synthesizing the core quinolizidine moiety.

2.2. Previous Syntheses of Lycopodine-Class *Lycopodium* Alkaloids

2.2.1. Previous Syntheses of Lycopodine

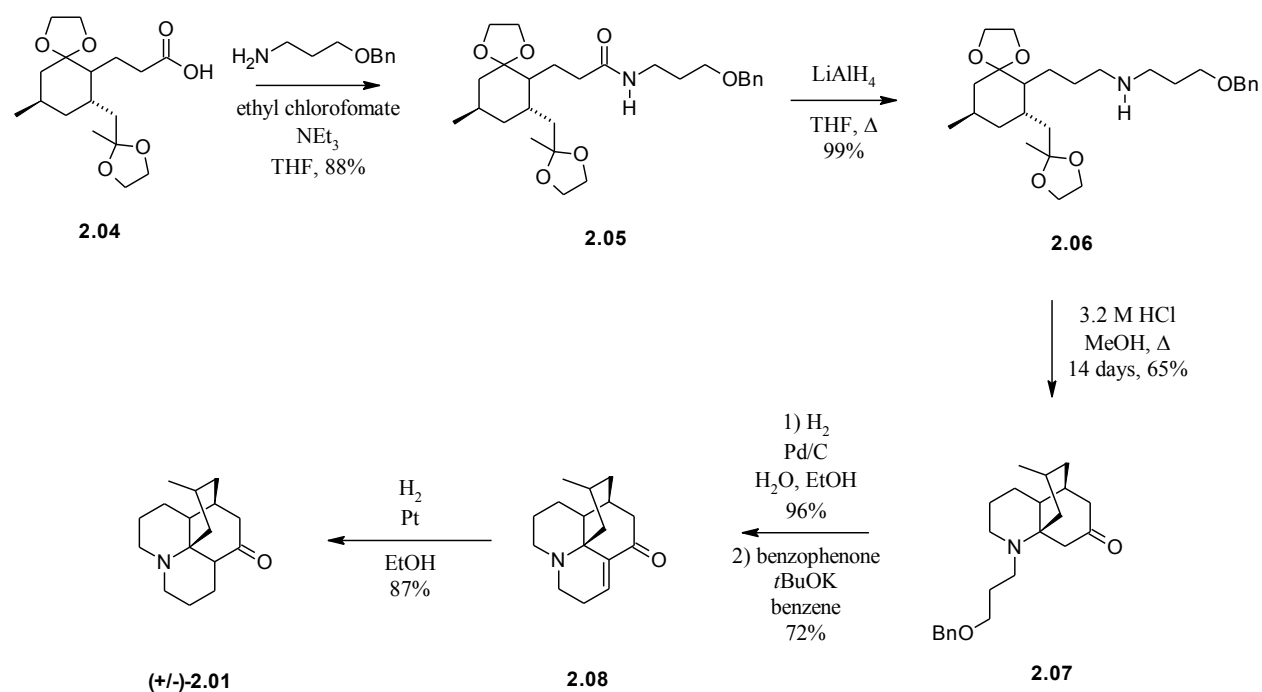
One of the major problems faced by synthetic chemists who undertake total synthesis projects of these alkaloids is how to incorporate and preserve the 3° amine functionality while constructing the rest of the molecule. Apart from being highly basic, the electronics of many of the intermediates suggest an affinity of the nitrogen's lone pair towards metal chelation. This complicates the ability to form the desired quinolizidine structure. A method of attenuating this electronic hazard is to utilize it directly to drive the reaction progress. Husson and co-workers did just that by using the nitrogen as enamine-enone **2.02** and performing a Diels-Alder reaction with acrylonitrile (Scheme 2.1)². The *N*-methyl group is present as an artifact from a previous reduction of a pyridinium salt.



Scheme 2.1: *Synthesis of tetrahydroquinoline 2.03 as a lycopodine precursor*

Locking the problematic amine away as an enamine is highly useful, and helps to prevent many of the unwanted side-effects of having a basic nitrogen group present during a synthesis. Enamines however, are not stable to a number of synthetic transformations, and a majority of the syntheses utilize conventional amide or carbamate protecting groups to mask the amine's functionality. In the context of a Diels-Alder reaction, this makes the corresponding diene or dienophile (whichever the amine is incorporated therewithin) more electronically neutral, and thus mismatches the electronics of the cyclization. This is the reasoning behind leaving the amine exposed as part of an enamine or similar motif – to drive electronically favorable cyclizations to produce the desired 6-membered ring systems.

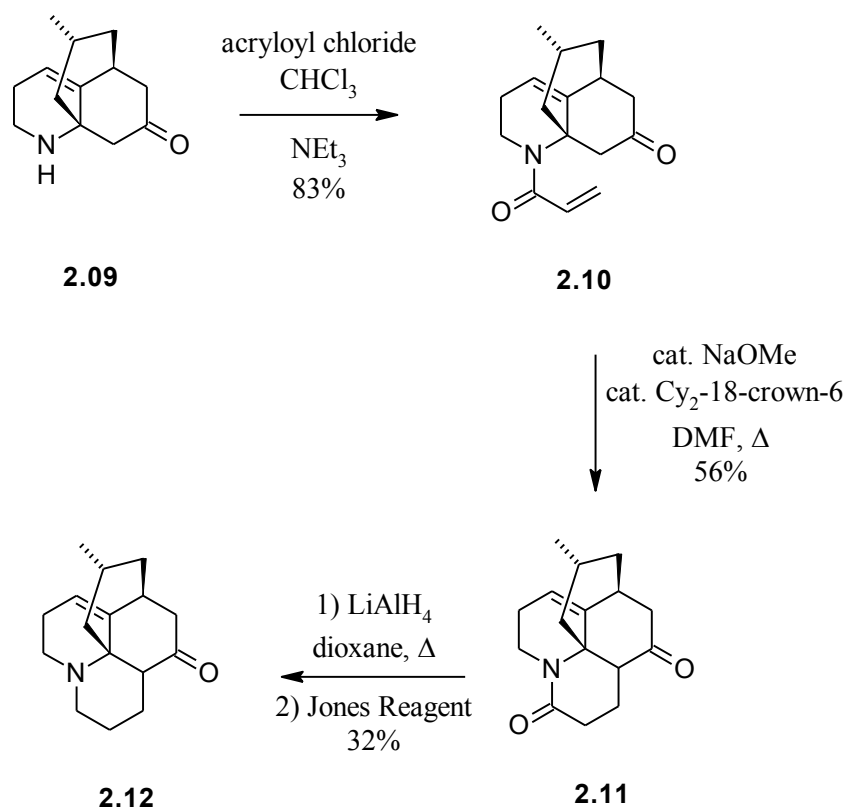
Heathcock and co-workers utilized an intramolecular Mannich reaction to form three of the four quinolizidine rings in one step, but the reaction is racemic. Beginning from diketal acid **2.04**, they first installed the amine through amidation (**2.05**), followed by reduction of the amide to produce the 2° amine **2.06**, with a pendant protected alcohol. Acid-mediated deprotection of the two ketal units gave the quinolizidine ring system minus the D ring. (**2.07**). Deprotection of the alcohol, oxidation under Oppenauer conditions, and aldolization with the cyclic ketone provided the dehydrolycopodine **2.08**. Catalytic hydrogenation gave the racemate of **2.01** in 18% overall yield from their chosen starting material (Scheme 2.2)³.



Scheme 2.2: Heathcock synthesis of (\pm)-lycopodine

While the Heathcock synthesis is quite nice for the construction of the quinolizidine core, it is racemic, and the deprotection/Mannich reaction is extremely slow, providing only 65% yield after a full fortnight. The **2.04** starting material is also semi-tedious to synthesize, involving a conjugate addition from which epimerization of the α position is unavoidable. In this light, the Heathcock synthesis lacks the ability to form the central quinolizidine core of the *lycopodine*-class in an enantioselective fashion. The inability of the starting material (**2.04**) to be produced in even a diastomerically pure fashion highlights the limitations faced by researchers who attempt to synthesize the ring systems with any stereocontrol. It is also possible to optimize the final hydrogenation to include much of the robust homogeneous hydrogenation catalysts which could impart stereoselectivity. In this particular case, however, it could only be beneficial if the initial ring formations were performed with stereocontrol.

An alternative to closing the D ring was introduced by Kim and co-workers using acryloyl chloride to acylate the 2° amine (**2.09**), already contained in the ABC-ring system (**2.10**). Catalytic enolization of the B-ring ketone using NaOMe and a dicyclohexyl-18-crown-6 furnished the Michael adduct **2.11** in 56% yield. LAH reduction of the amide gave the anhydrolycopodine derivative **2.12** (Scheme 2.3)⁴.

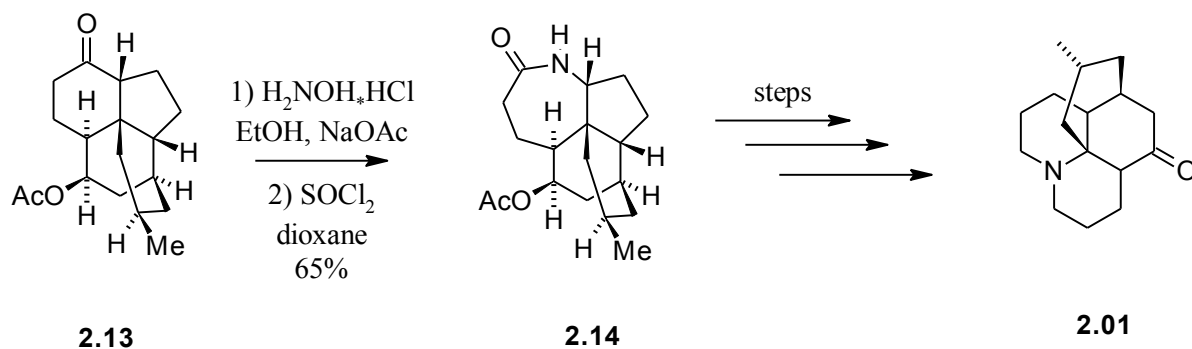


Scheme 2.3: Kim synthesis of anhydrolycopodine

The acylamide Michael addition is an attractive methodology, but the yields are unimpressive and the subsequent Jones oxidation after LAH over-reduction diminish the yield even further. Nonetheless, it showcases that the D ring is typically the final ring to be synthesized in order to make the quinolizidine core structure. While the Kim synthesis is

racemic, it would be difficult to form the D-ring closure stereoselectively without the initial material being enantiopure. If the C-ring is closed enantioselectively, the adjacent carbon center's chirality can directly influence the approach of the enolate to the β position of the acrylamide. In addition to the implications of the C-ring's stereochemistry, this synthesis is of dehydrolycopodine, which possesses a unit of unsaturation higher than the parent lycopodine. One of the stereocenters is locked into an sp^2 C=C bond. Even the more active Pt hydrogenation catalyst could not hydrogenate such a sterically encumbered double bond.

Due to the amine's natural reactivity, the choice to incorporate it in the final steps of the synthesis is a natural one. Grieco and co-workers installed the nitrogenous functionality into the all-carbon backbone of their lycopodine skeleton (**2.13**) through a Beckmann rearrangement, followed by a series of reactions culminating in a ring-contracting Stieglitz rearrangement (Scheme 2.4)⁵.

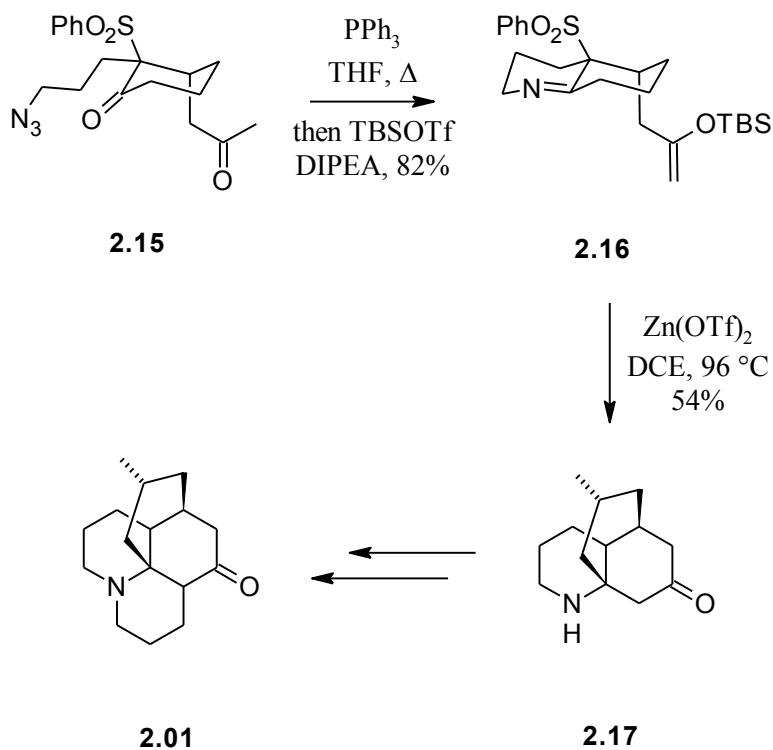


Scheme 2.4: Grieco synthesis of lycopodine

The Grieco synthesis of lycopodine illustrates the problems with installing the amine group. By using a Beckmann rearrangement, they obtain a 7-membered lactam, which must be converted through a series of oxidations and reductions (including an *N*-chlorination) to a

suitable precursor for the Stieglitz rearrangement. This lengthens the synthesis and makes it less appealing as a general approach towards the synthesis of the quinolizidine core of the *lycopodium* alkaloid's lycopodine-class of natural products. It is also apparent that a reasonable amount of structural complexity must be lost to make the desired lycopodine.

Alternatively, Carter and co-workers developed a novel strategy utilizing the imine-enamine tautomerization to drive a sulfone rearrangement with a tandem Mannich reaction, forming the B and D rings (Scheme 2.5)⁶. Thus, the advanced azide/sulfone intermediate **2.15** was reduced with subsequent imine formation using PPh₃ to form the A ring in **2.16**. This was subjected to their developed methodology using a Lewis acid to mediate the formation of the B ring, providing **2.17** in moderate yields. Alkylation, followed by the previously described Oppenauer oxidation/aldolization reaction provided, after conjugate reduction, **2.01**.



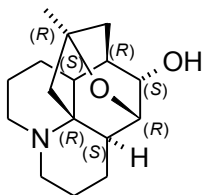
Scheme 2.5: Carter synthesis of lycopodine

Again, the Carter synthesis utilizes the Oppenauer oxidation/aldolization reaction to form the D ring, while their interesting methodology closes the C ring. They begin the synthesis of **2.15** with forming the B ring first, which is relatively unique to their synthetic strategy. Using a single ring's established stereochemistry is an effective way of establishing the stereochemistry of the other rings. Unfortunately, even if the stereochemistry was controlled (here it is racemic), the final Knoevenagel condensation and hydrogenation provides a racemic center at the C-11 position. While the Carter synthesis is very enlightening and their Lewis acid chemistry takes advantage of an important enamine-imine tautomerization, the Lewis acid must be added in stoichiometric amounts. This severely minimizes the utility of the reaction for larger-scale syntheses, as well as increases the potential cost of the reaction.

While all of these syntheses are excellent examples of total synthesis, all of them suffer from the same few problems. Firstly, the amine functionality typically hinders the application of many reactions in this particular system. Circumventing this issue by incorporating the nitrogen in the final few steps poses alternative challenges such as control of when and where to insert it into the typically complex carbon-skeletal intermediate. It has also been shown that installing the nitrogen earlier and using its unique reactivity to assist in reactions is also possible, but the yields are somewhat diminished. Ideally, it would be attractive to install the amine early, to avoid the late-stage issues involved with its installation and selectivity, but to mask the amine (i.e. protection) until the late stages. While focusing on these issues, we have decided to embark on a total synthesis of a new Huperzine-type alkaloid isolated from the same club moss that has spawned so much interest in the lycopodine-class of *lycopodium* alkaloids.

2.2.2. Novel Huperzine Alkaloid of the Lycopodine-Class

In 2010, a group of researchers led by Tan isolated a natural product which displayed very similar NMR correlations to other known lycopodine-class *lycopodium* alkaloids. Isolated from the same *lycopodium* club moss species as many of the same class of alkaloids, this new alkaloid possesses some key differences (Figure 2.2)⁷.



2.18

Figure 2.2: *Isolated lycopodine-class lycopodium alkaloid, total synthesis target*

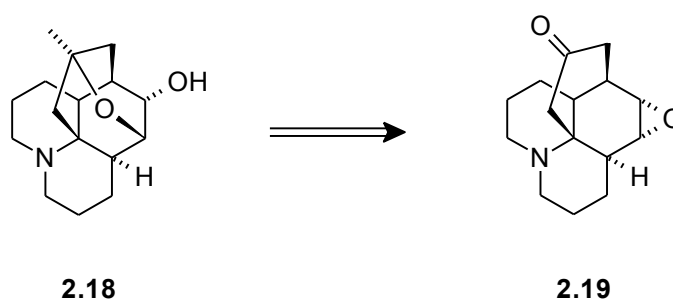
In addition to the standard quinolizidine ring system, there is a fifth ring, created by a bridging ether linkage from the already bridging C-ring onto the B-ring at the location of the ketone moiety in lycopodine. The second oxygen functionality is also on the B-ring as a hydroxyl group. This bridging ether linkage creates a “cage”-like structural motif, which makes this member of the lycopodine-class a standout. Officially named, it is 6 α -hydroxy-5,15-oxide-lycopodane, but for simplicity, it will be referred to from here on as Huperzine X.

2.3. First-Generation Approach Towards the Total Synthesis of Huperzine X

2.3.1. Retrosynthetic Analysis

To begin with, we desired a method to make the quinolizidine core in an efficient manner. If we utilized the B and D-ring’s carbon backbone as a built-in tether for further

reactivity, we could potentially form the A-ring through a similar Michael addition-type of reaction. This Michael addition should be more facile, as nitrogenous nucleophiles are more efficient as Michael addition partners. One of the major hurdles, however, was the construction of the bridging ether linkage. We envisioned first that the action of an oxanion derived from a ketone on the C-ring by the addition of a methyl nucleophile could be seen to favor the opening of a pendant epoxide on the B-ring (Scheme 2.6).

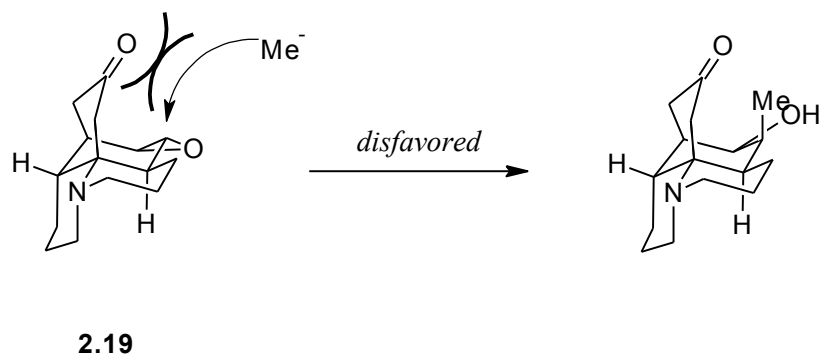
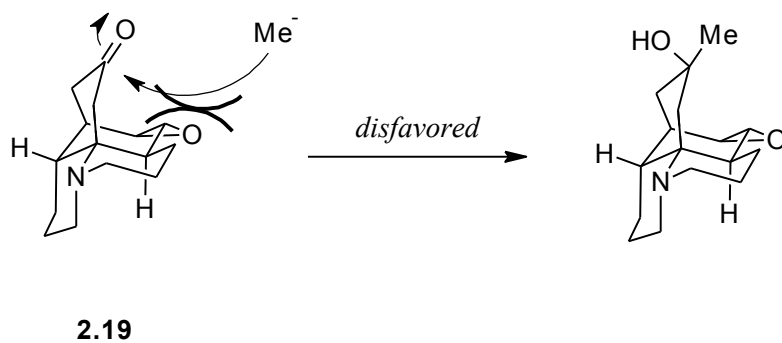
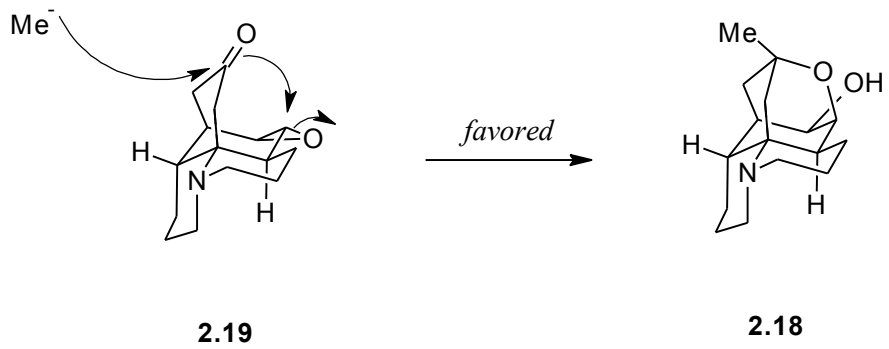


Scheme 2.6: *Initial retrosynthetic disconnection to form the bridging ether linkage*

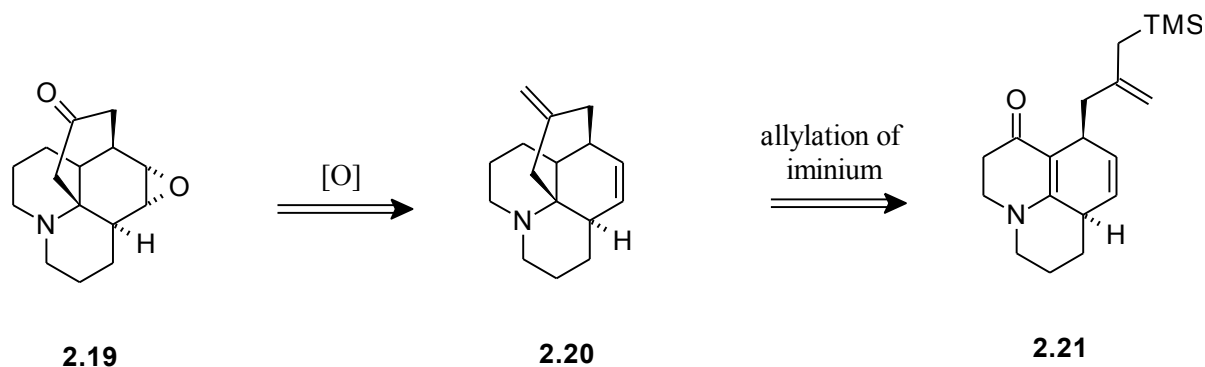
Closer inspection of the steric placement of the bridging ketone in relation to both the incoming nucleophile and the reactive epoxide shows that not only is the positioning favorable for a nucleophile to approach from the desired face of the ketone, but that the ketone itself is blocking the reactive face of the epoxide (Scheme 2.7). While it is only shown for the ketone-containing ring (C-ring) to be in the thermodynamically favorable chair conformation, it is also possible for it to be in the boat conformation. If it adopts the boat conformation, the ketone's opposing face will be exposed to nucleophilic attack (i.e. opposite stereoselectivity), as will be the electropositive carbons of the epoxide. It is envisioned that while in the boat conformation, the carbonyl will experience unfavorable interactions with the lone pair orbital of the nearby nitrogen. In the shown chair conformation, the orbital of the nitrogen's lone pair is presumed

(due to the chair conformations on all of the rings being lowest in energy and thus adjacent atoms are staggered from one another) to be gauche to the α -methylene's hydrogen atoms of the C-ring. In the boat conformation of the C-ring, the nitrogen's lone pair orbital could potentially encounter the lone pair orbitals of the carbonyl oxygen. Thus the electron-electron repulsion dynamic would increase the energy of the C-ring boat conformation even further, allowing for a more favorable chair conformation. In this light, the proposed mechanistic implications are shown for the chair conformation only.

The oxygenated functionality of **2.19** can be thought of as coming from the parent alkenes through oxidative cleavage and epoxidation, respectively, giving **2.20**. Due to the C-ring's C=C bond being terminal, it should undergo oxidative cleavage at a much faster rate than the internal C=C bond of the B-ring. This leaves the B-ring's olefin as the only one left in the structure, and being that the molecule possesses a rigid structure due to the bridging nature of the C-ring, simple epoxidation agents such as *meta*-Chloroperoxybenzoic acid (*m*CPBA) should be sufficient in producing the epoxide with the desired stereochemistry. The bridging methylene structure is homoallylic to the nitrogen, suggesting that an allylation of some oxidized form of the nitrogen could produce the bridging structure, giving rise to **2.21** as a viable intermediate (Scheme 2.8).

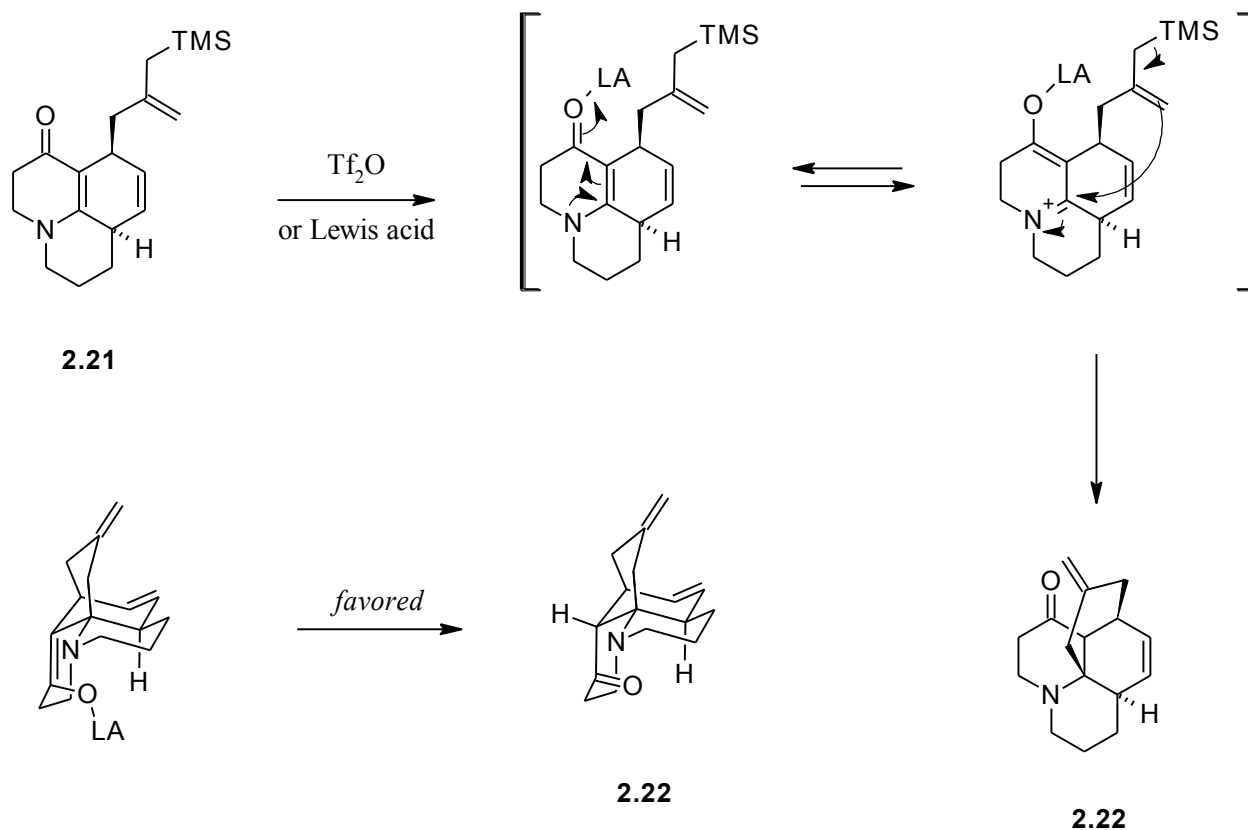


Scheme 2.7: Potential routes for the addition of Me^- to the bridged ketone **2.19**



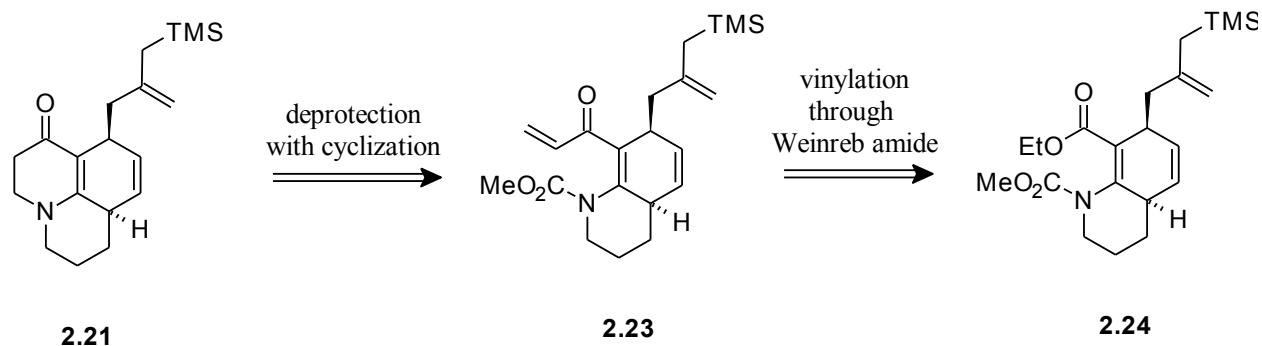
Scheme 2.8: Retrosynthesis of **2.19**, providing allylation intermediate **2.21**

We envisioned that the allylation could result from the activation of the 2,3-dihydropyridone carbonyl via triflic anhydride (producing the enol triflate) or a general Lewis acid (Scheme 2.9). Activation of the carbonyl would promote electron migration from the nitrogen's lone pair into the imine form of the imine-enamine tautomer, generating an enolate-Lewis acid pair (or enol triflate), which could be quenched *in situ* by the reactive allyl trimethylsilane unit. The re-protonation of the enolate can only occur from one direction due to the rigid structure of the now completely formed quinolizidine ring system, giving **2.22**. Removal of the ketone is expected to be straightforward due to its non-proximity to other reactive functional groups.



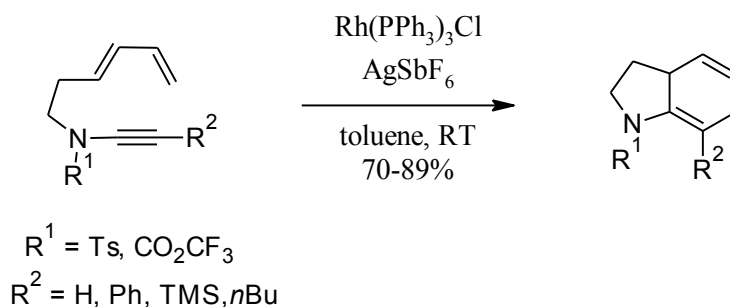
Scheme 2.9: Application of the intramolecular allylation of the activated iminium of **2.21**

Beginning from the 1,4-cyclohexadiene substructure of **2.21**, we foresaw the use of a Diels-Alder to set the desired stereochemistry of the allyl unit as well as the junction onto the D-ring (*syn*). In order to preserve the olefin in the pyridone, it was required that we use a ynamide precursor. This did not allow us to have the A ring formed during the Diels-Alder, and we decided to form the ring through a series of transformations which greatly resembled the previous syntheses applied to the D-ring (Scheme 2.10).



Scheme 2.10: *Proposed synthesis of the A-ring*

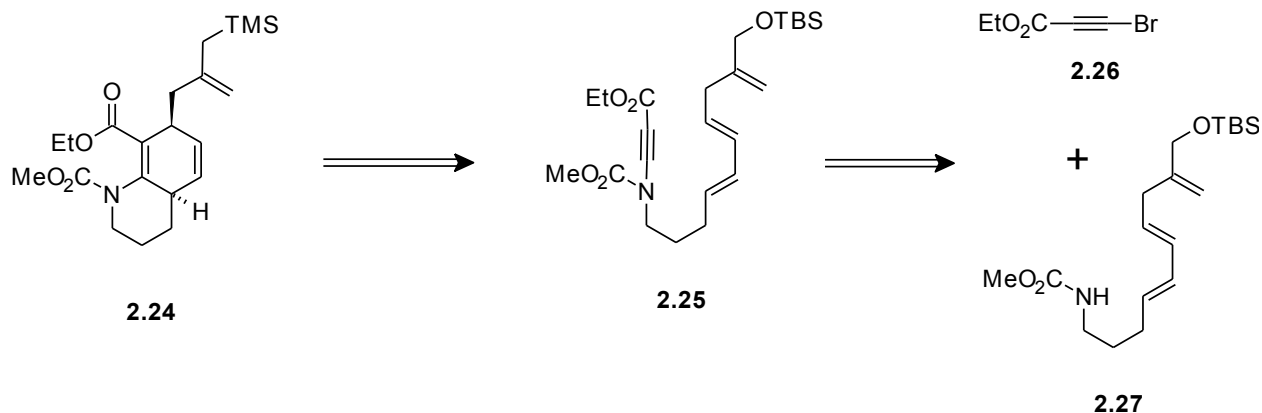
The Diels-Alder between the parent diene and ynamide is intramolecular, which should be a favorable process when considering thermal requirements. However, literature suggests that the three reaction sites (diene olefins and ynamide alkyne) can be made to template to a transition metal, which brings them into the appropriate orientation. Rh appears to be uniquely poised to accomplish this task, although the only report of this occurring does not control the stereoselectivity (Scheme 2.11)⁸.



Scheme 2.11: *Literature report of Rh(I)⁺-catalyzed intramolecular ynamide Diels-Alder reaction*

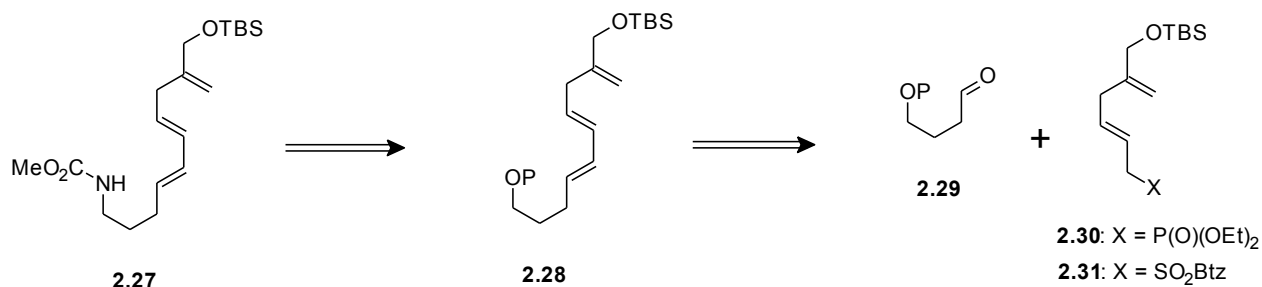
Although the literature report uses only ynamides without electron withdrawing groups, they were able to perform the reaction using thermal conditions (80°C, benzene, approx. 50%), but obtained much better yields with a templating catalyst. Rh(I) was unable to perform the

reaction, but removing the Cl⁻ ligand by using AgSbF₆ created a cationic species which performed the reaction at RT. While the thermal reaction gave aromatization as a side product, the cationic Rh(I) catalyst did not give any major side products. The authors suggest that, since Rh(I) has been used in previous studies to cyclotrimerize ynamides with other alkynes (both intra- as well as intermolecular) by templation, that this reaction behaved much in the same way⁹. The authors also suggest that the reaction occurs because the ynamide nitrogen is electron withdrawing due to the tosyl or trifluoroacetate substituent, and thus the ynamide alkyne is electron deficient. In our system the ynamide nitrogen is part of a carbamate, so the alkyne is not as electron deficient, but this is offset by the presence of an ester directly conjugated to the alkyne. In theory, our system should work equally as well, since the electronics are similar and the templation should be the same. Thus, **2.24** can come from ynamide **2.25** which in turn can be synthesized from diene-carbamate **2.27** (Scheme 2.12). The diene was chosen to not include the trimethylsilyl functionality for fear that during the ynamide coupling, it would be removed. It was decided to use a protected alcohol, which can be transformed into a TMS group through displacement of the acetate with hexamethyldisilane and Rh(I)¹⁰, or displacement of the methyl ether with NaTMS¹¹. The ynamide coupling can be done in a number of interesting ways, many of which involve Cu catalysis, the most notable and successfully applied being the Danheiser method¹² and the Hsung method¹³. Unfortunately, we were unable to get the procedure of Stahl, *et al.* to provide any material¹⁴. Due to the electron withdrawing nature of the bromoalkyne, the Cu-catalysis often promotes dual Michael-type additions of the amide-cuprate to the bromoalkyne, and so simple deprotonation (NaH, DMF) can provide a less-reactive, more amenable procedure for our purposes¹⁵.



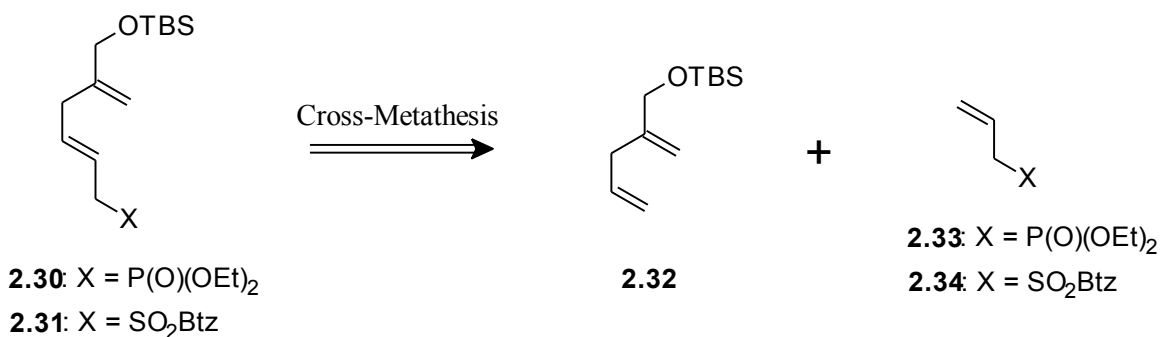
Scheme 2.12: Retrosynthesis of **2.24** to provide carbamate **2.27** and bromoalkyne **2.26**

Carbamate **2.27** was thought to come from the parent alcohol **2.28** through either a Mitsunobu reaction with the primary carbamate or a mesylation/displacement with azide/reduction/acylation sequence. We recognized that the 1,3-diene was the logical position to break apart for the next stage of the retrosynthesis and we decided that olefination would be an acceptable method, since we required both olefins of the diene to possess the *trans*-geometry. Thusly, we envisioned the cleavage occurring between the C7-C8 olefin (numbering from the TBS-protected alcohol), giving aldehyde **2.29** and the olefination partner with either a phosphonate ester (**2.30**) or a 2-sulfonylbenzothiazole (**2.31**). These would allow for Horner-Wadsworth-Emmons olefination or Julia olefination, respectively (Scheme 2.13).



Scheme 2.13: Retrosynthesis of **2.27** resulting from olefination

The aldehyde **2.29** is easily synthesized by monoprotection of the diol followed by routine oxidation. The allylic olefination partner was a more problematic piece to synthesize, and we saw it arising from the 1,4-skip diene **2.32** and the simple allylic partner, either **2.33** (X = P(O)(OEt)₂) or **2.34** (X = SO₂Btz). The two materials could be combined in a cross-metathesis reaction, since the skip diene (Type I) and the allylic olefination partner (Type II) are a good match for cross-metathesis (Scheme 2.14)¹⁶.

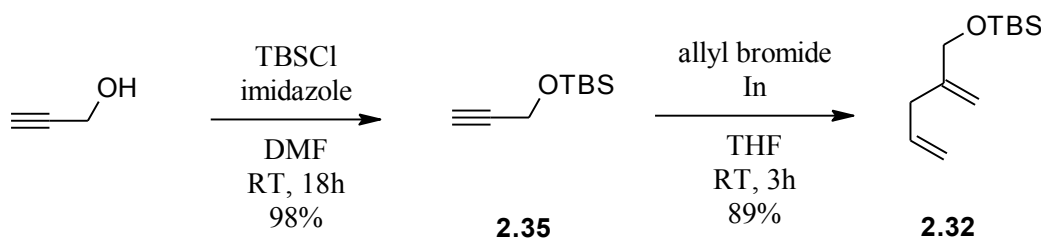


Scheme 2.14: Retrosynthesis of the allylic olefination partners

Using the Cook Group's expertise in the field of organoindium chemistry, we envisioned an analogous reaction to allylzincation¹⁷ using allyl indium¹⁸. Thus, we decided **2.31** could be synthesized from commercially available allyl bromide and TBS-protected propargyl alcohol **2.35**. The allylic olefination precursors are easily synthesized by Arbuzov reaction of P(OEt)₃ and allyl bromide (**2.33**) or by the sodium salt of 2-mercaptobenzothiazole and allyl bromide, followed by oxidation of the sulfide to the sulfone (**2.34**).

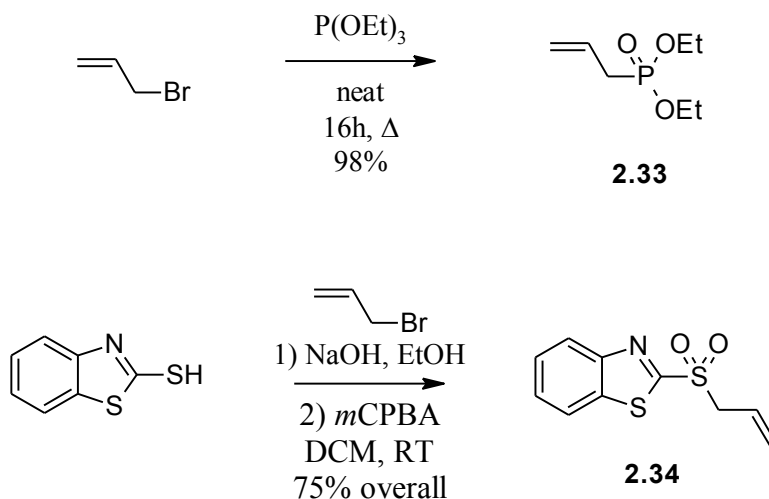
2.3.2. Forward Synthesis

Our forward synthesis began with the allylindation of **2.35**. Allylzincation was unsuccessful in this case due to excessive heat build-up causing minor explosions during the ultrasound-required reaction. The zinc powder must also be activated by TMSCl and I₂, which the indium reaction does not require. The indium reaction also does not require ultrasound, and the room temperature reaction provided **2.32** in high yields (Scheme 2.15).



Scheme 2.15: Synthesis of 1,4-skip diene **2.32**

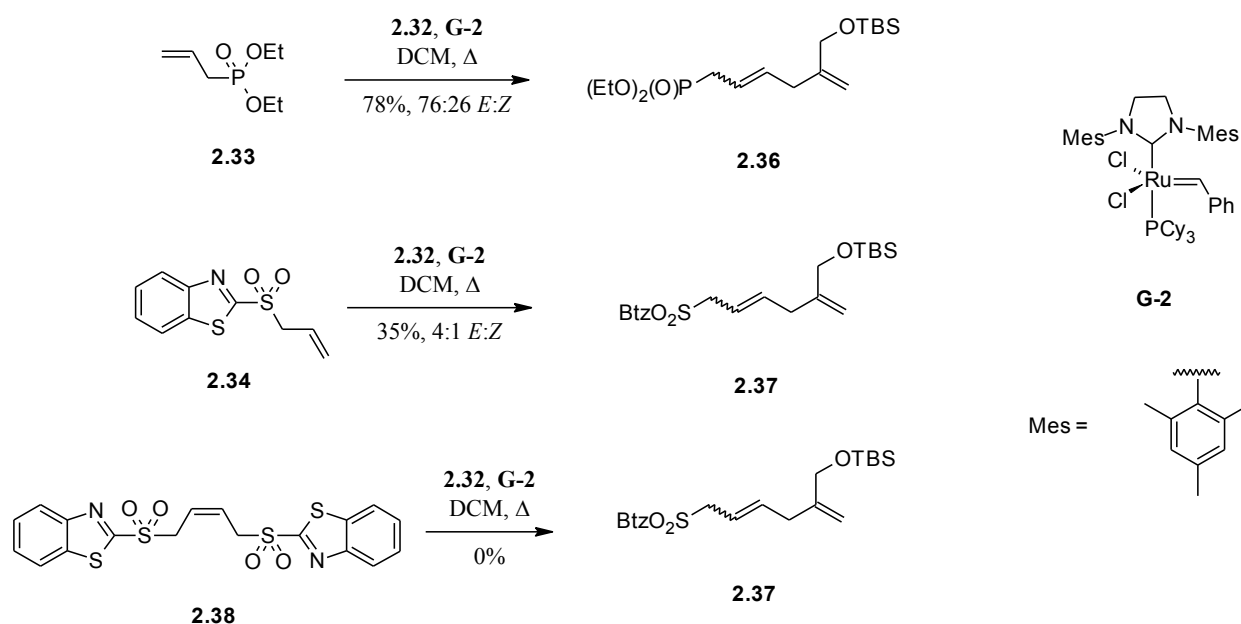
With **2.32** in hand, we attempted to synthesize **2.33** and **2.34** using standard methods. The Arbuzov reaction was an obvious choice for the installation of the phosphonate. Using neat conditions with triethylphosphite and allyl bromide, we obtained the desired allylic phosphonate in near quantitative yield¹⁹. The allylic sulfone was synthesized by alkylation of 2-mercaptobenzothiazole with allyl bromide in EtOH, followed by *m*CPBA oxidation to the sulfone gave **2.34** in good yield (Scheme 2.16)²⁰.



Scheme 2.16: *Synthesis of 2.33 and 2.34.*

Encouraged by such excellent preliminary results, we turned our attention to the cross-metathesis of the respective olefination precursors and **2.32**. Allylic phosphonate **2.33** was efficiently metathesized onto **2.32** in good yields²¹, but the large amount of Ru impurities decomposed the product (**2.36**) rapidly, even at freezing temperatures. Integrations of the newly formed olefin protons showed a 74:26 *E:Z* ratio, suggesting the reaction favors our desired stereoisomer. The Ru impurities are generally Ru-H species, created by the *in situ* decomposition of the metathesis catalysts during the reaction. These Ru-H species have been recently shown to isomerize dienes under general metathesis conditions²². Yields were calculated immediately after column purification, but the material was unuseable in further reactions. This is presumably due to the isomerization (conjugation) of the 1,4-skip diene, which moves the internal olefin further away from the electron withdrawing group (phosphonate or 2-mercaptobenzothiazole), thus making the α position no longer allylic, increasing its pKa. This increase must be sufficient to either render the proton inert to the tested bases, or lowers the *trans* selectivity of the reaction. We then attempted to utilize the same protocol by combining **2.34**

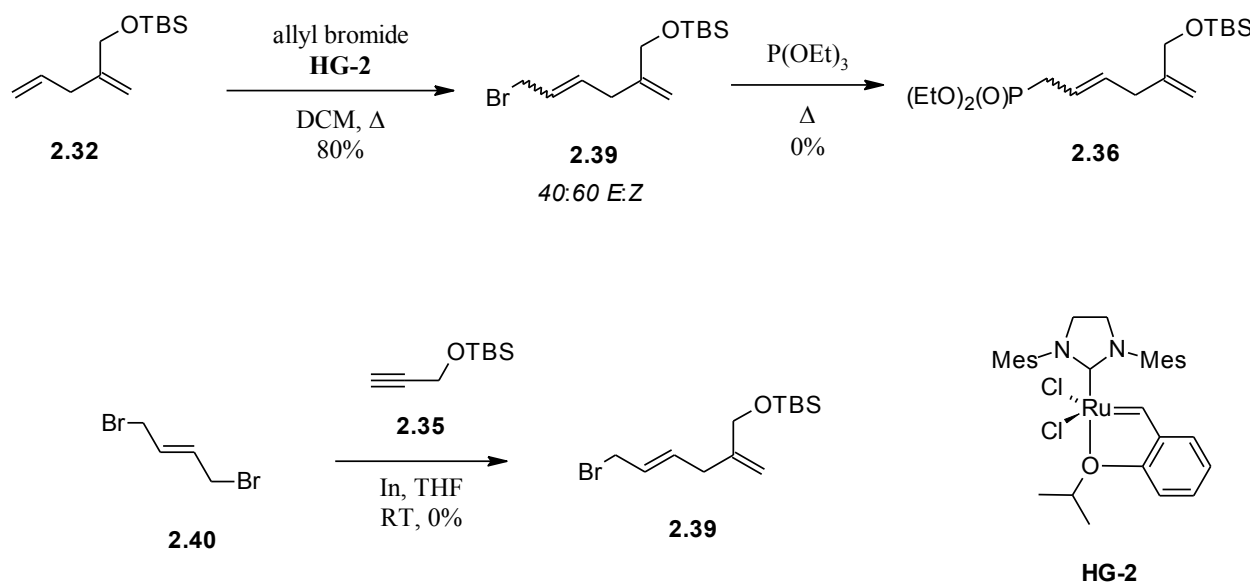
and **2.32**. The yield was significantly lower, but the *E:Z* ratio remained relatively unchanged. Ru impurities also decomposed the product (**2.37**) rapidly. We also attempted to cross-metathesize bis-sulfone **2.38**²³ onto **2.32**, harnessing what has been observed for the bis-acetate species²⁴, but found the reaction to be unsuccessful (Scheme 2.17). This is presumably due to the highly electron poor nature of **2.38**. The use of alternative metathesis catalysts (i.e. Hoveyda-Grubbs 2nd generation) did not improve the performance. All attempts to remove Ru impurities by published methods²⁵ were successful at removing most color, but whatever residual metal impurities remained quickly decomposed even the treated material.



Scheme 2.17: Attempts at cross-metathesis of **2.32** with olefination partners

It became apparent that the direct cross-metathesis of the allylic olefination partners was not feasible for a lengthy total synthesis. We therefore attempted to incorporate the starting allylic bromide into **2.32** (Scheme 2.18). Directly via cross-metathesis required the use of a

more robust catalyst due to the electron withdrawing nature of the bromomethyl unit on the alkene. The Hoveyda-Grubbs 2nd generation metathesis catalyst (**HG-2**) performs well in these cases²⁶. While the yield of allyl bromide **2.39** was very good, the *E:Z* ratio was not, and we obtained it as an inseparable 2:3 mixture, favoring the *Z* isomer (undesired). Regardless, the Arbuzov conditions resulted in decomposition of the starting material, presumably due to the Ru residues which very clearly darkened the reagent. We also attempted to incorporate the allylic bromide during the allylindation reaction we had been using. In this light, we subjected **2.35** to the allylindation reaction using bis-allyl bromide **2.40**. Unfortunately we observed no conversion, owing likely to the formation of 1,3-butadiene *in situ*, even with the typically stable allyl indium species.



Scheme 2.18: Attempts to incorporate the allylic bromide into **2.32**

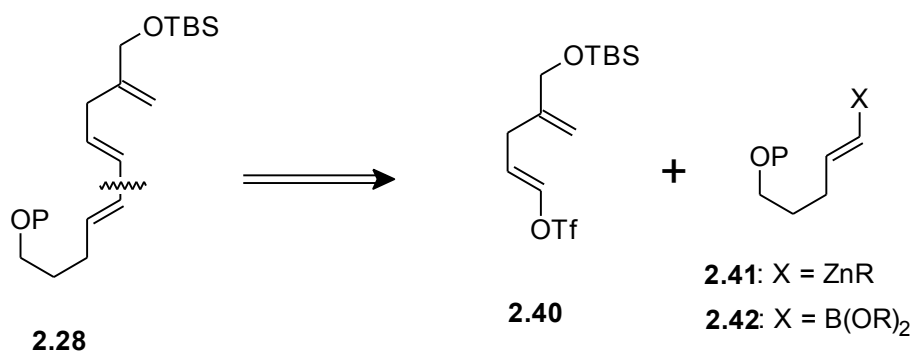
2.3.3. First-Generation Synthesis Implications

While we were unsuccessful at efficiently constructing the backbone of the quinolizidine core of Huperzine X, we did develop a significant allylindation procedure which is operationally simple and reproducible. The cross-metatheses were successful, but the products were not stable to direct storage. An attempt was made to perform the olefination using **2.36** immediately after it was synthesized, but no reaction was found. This is presumably due to the impurities in the reagent interfering with deprotonation or nucleophilic attack onto the aldehyde.

2.4. Second-Generation Approach Towards the Total Synthesis of Huperzine X

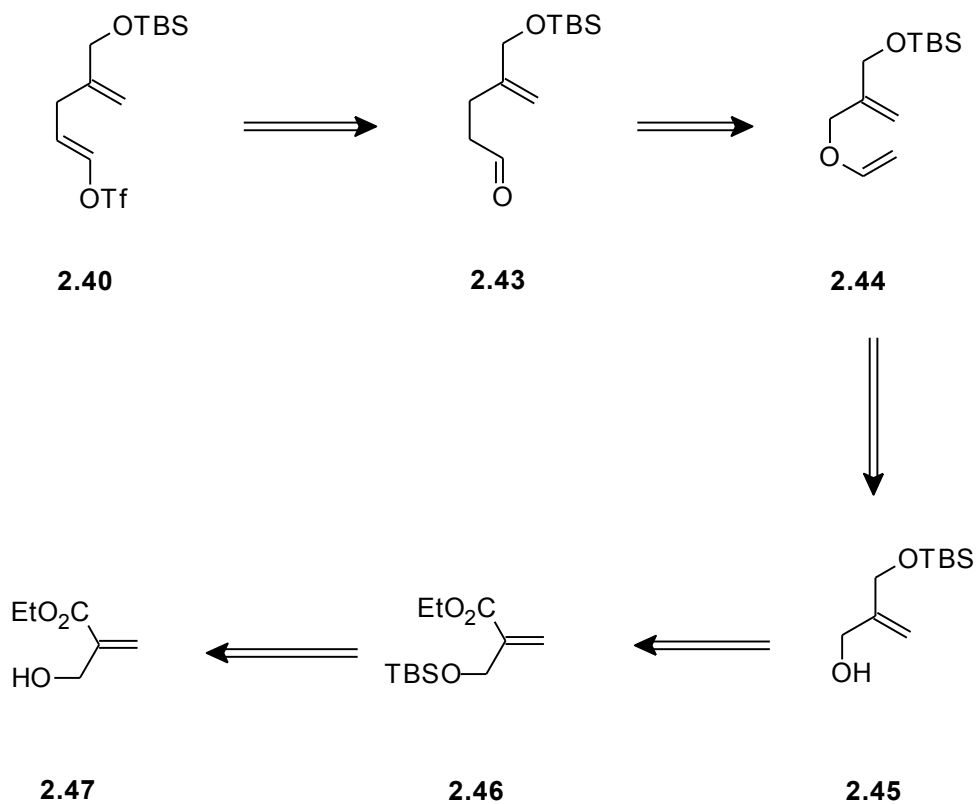
2.4.1. Retrosynthetic Analysis

After our failed attempts at creating the 1,3-diene motif by synthesizing one of the olefins, we decided to embark on a route centered around creating the σ -bond linkage of the 1,3-diene. Due to the two partners being sp^2 -hybridized, we quickly realized that Pd-mediated cross-coupling could provide us with such a system. We envisioned thusly, an identical retrosynthetic analysis, but with the key step of forming the carbon skeleton of **2.28** replaced from olefination to cross-coupling of vinyl triflate **2.40** with either vinyl zincate **2.41** or vinyl boronate **2.42** (Scheme 2.19).



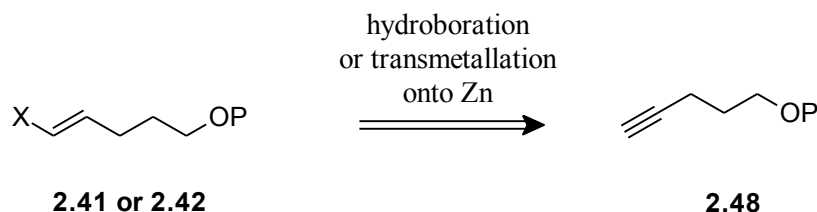
Scheme 2.19: Retrosynthesis of **2.28** resulting from cross-coupling

We anticipated that **2.40** could come from the parent aldehyde (**2.43**) through simple enolization/trapping. The aldehyde was envisioned to come from the mono-protected diol **2.45**, through the *O*-vinylated **2.44** intermediate via Claisen rearrangement. The diol could then be seen as coming from the hydroxymethylacrylate **2.47** (Scheme 2.20).



Scheme 2.20: Retrosynthesis of vinyl triflate **2.40**

The vinyl nucleophile for the cross-coupling was thought to arise from the terminal alkyne **2.48**, with the heteroatom being attached through transmetalation onto zinc, or by direct hydroboration. The alkyne could thus allow for the early incorporation of the nitrogen, as it does not conflict with these reactions (Scheme 2.21).

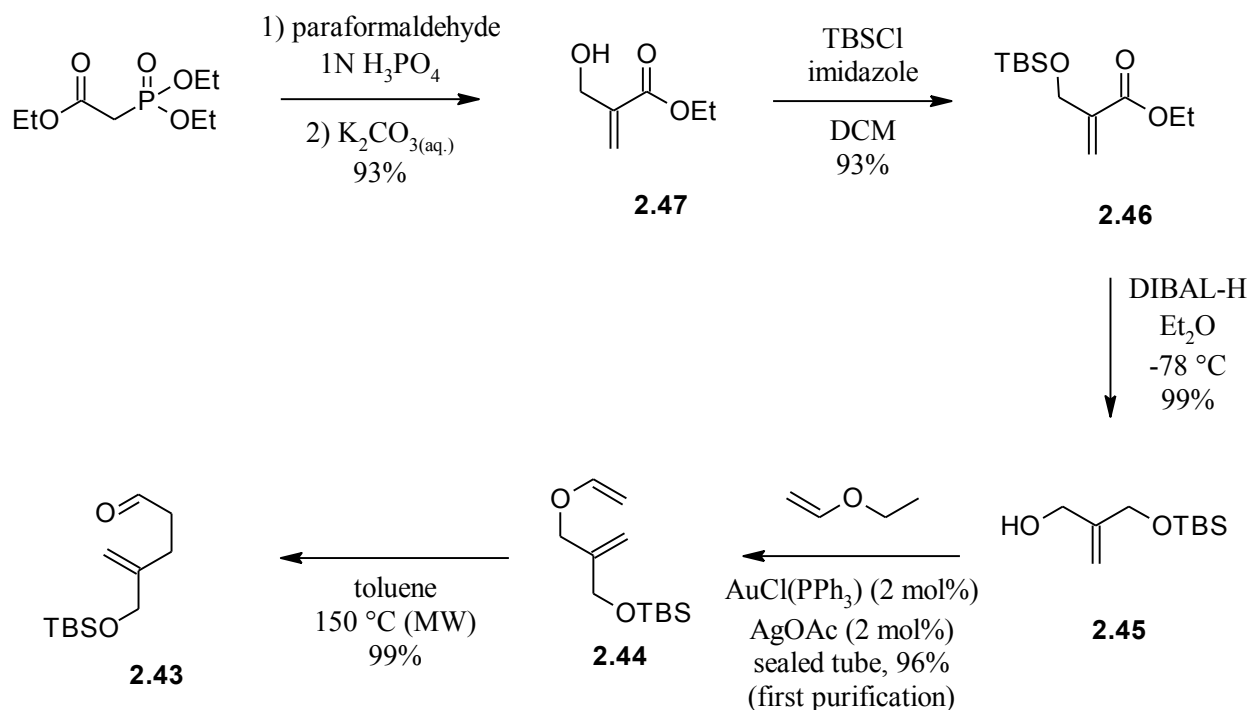


Scheme 2.21: *Synthesis of cross-coupling partners 2.41 and 2.42 from a common precursor*

2.4.2. Forward Synthesis

Our synthesis first began with an attempt to synthesize the vinyl triflate **2.40**. Treatment of triethylphosphonoacetate with aqueous formaldehyde allowed for a very smooth synthesis of **2.47** through tandem Horner-Wadsworth-Emmons olefination and a Baylis-Hillman reaction (Scheme 3.22). Interestingly enough, if ethyl acrylate (the intermediate product) was directly subjected to standard Baylis-Hillman protocol (cat. DABCO, DMF, RT)²⁷, only small amounts of the desired product were formed. This is presumably due to the propensity of **2.47** to polymerize upon standing, and is likely accelerated by the Baylis-Hillman conditions. TBS protection using standard conditions provided **2.46**, which is much more stable to storage. Subsequent DIBAL-H reduction provided the mono-protected diol (**2.45**), which was subjected to an *O*-vinylation protocol using a cationic Au(I) system to effect vinyl transfer from ethyl vinyl ether²⁸. Finally, Claisen rearrangement was effected using microwaves to accelerate the reaction. Thermal reaction conditions (toluene, 150°C, sealed tube) provided only approx. 50%

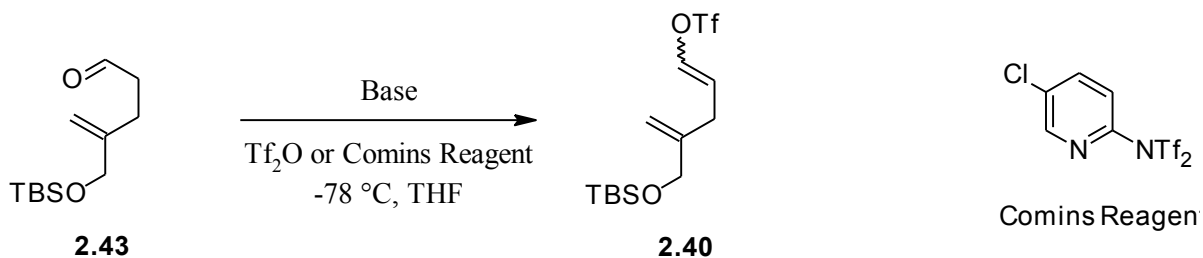
yield after 6 days of reaction. Microwave conditions allowed for nearly quantitative yield in only 15 hours. This supports the known ability of microwaves to accelerate rearrangement reactions²⁹. Previous syntheses have utilized Claisen rearrangements to effect this same homologation³⁰. The reaction pathway is very efficient, with the precursor aldehyde being synthesized in 5 steps with 81% yield and only two required silica-gel plugs for purification.



Scheme 2.22: *Synthesis of vinyl triflate precursor 2.43*

In our attempt to transform **2.43** into the required *E*-vinyl triflate, we utilized a number of protocols (Table 2.1). Although there is much literature evidence to suggest that vinyl triflate formation can occur using sterically hindered bases and Comins Reagent [3-chloro-6-(1,1-bis(trifluoromethylsulfonyl)aminopyridine)], we saw no success in applying these procedures³¹.

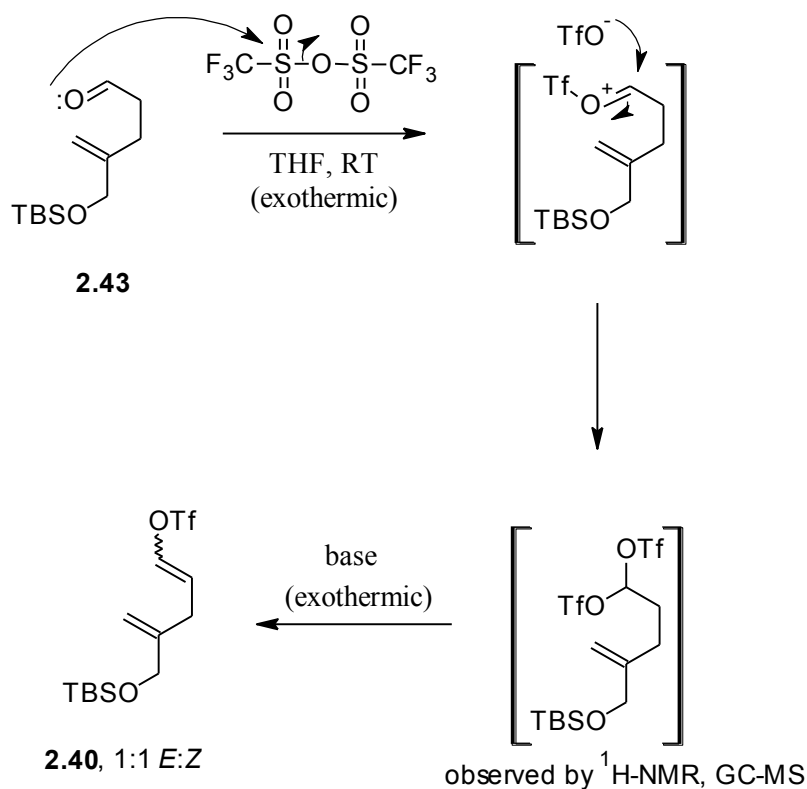
Table 2.1: Attempted synthesis of vinyl triflate **2.40** using standard triflation methodologies



Entry	Base	Triflating Agent	Yield (%) ^a
1	Pyridine	Comins Reagent or Tf_2O	0
2	2,6-lutidine	Comins Reagent or Tf_2O	0
3	2,4,6-collidine	Comins Reagent or Tf_2O	0
4	KHDMS	Comins Reagent or Tf_2O	0
5	$\text{KO}t\text{Bu}$	Comins Reagent or Tf_2O	0

^a: Refers to yield of desired product as detected by GC-MS

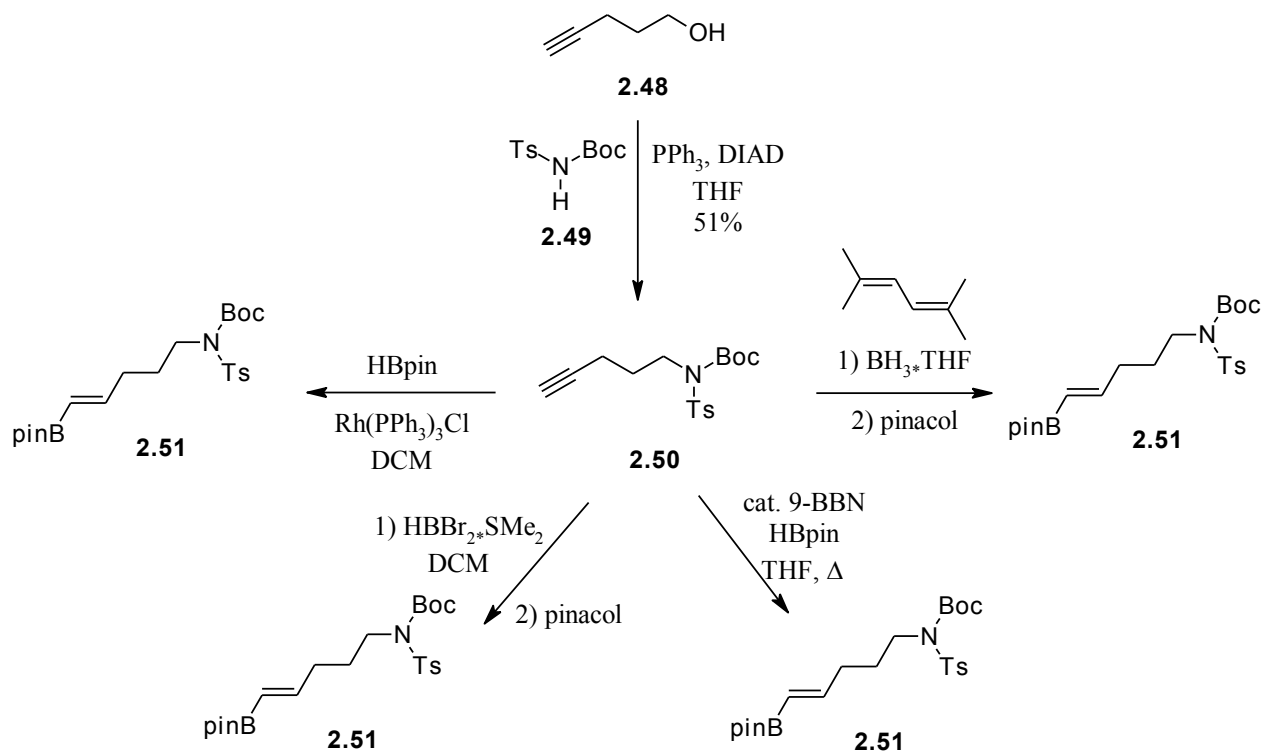
We were unable to achieve success with the established protocols, so we attempted to divine some of our own. Literature shows that terminal carbonyl compounds tend to be more reactive to simple triflic anhydride in the absence of base. This is due to the initial activation of the carbonyl by a triflyl unit, followed by nucleophilic addition of the triflate counteranion, generating a bis-triflate species. This is then acted upon by an added base to provide *cis* and *trans* isomers of the resultant vinyl triflate (Scheme 2.23)³².



Scheme 2.23: Observed mechanistic implications in the synthesis of **2.40**

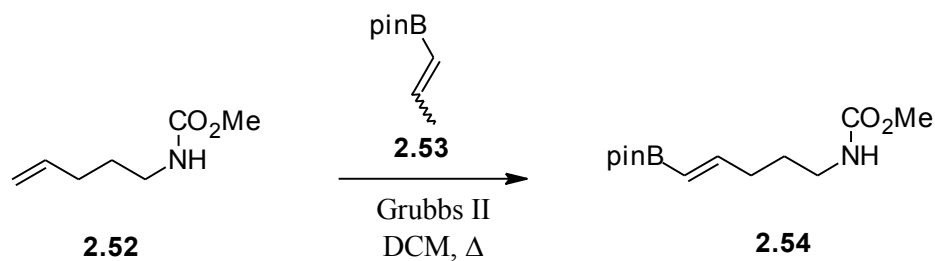
By first adding Tf_2O to the THF solution of **2.43**, a dark solution was obtained after 5 minutes, that GC-MS showed was the bis-triflate, formed in 100% conversion. Addition of any base (NEt_3 , DMAP, KHMDS, pyridine, 2,6-lutidine, KOtBu) gave exactly 1:1 mixtures of *cis:trans* vinyl triflate, also formed in 100% conversion from the bis-triflate. However, we did not desire the *cis* isomer, and it was not possible to separate the isomers from each other. We also investigated the possibility of using a larger base (DBU or similar) to effect the elimination with *trans*-favorability. We were unsuccessful at all attempts to do so. It was decided that we might be able to separate the currently unseparable *cis:trans* mixture after Suzuki cross-coupling to the expected vinyl boronate or Negishi coupling to the vinyl zincate.

In preparation for this coupling, we investigated the synthesis of vinyl boronate **2.42** from 4-butyn-1-ol via a series of hydroboration experiments. Thusly, we subjected **2.48** to standard Mitsunobu conditions to install the nitrogen as the bis-protected tosylamide, and subjected the produced **2.50** to a large variety of hydroboration experiments (Scheme 2.24). Direct hydroboration using HBpin (Bpin represents the pinacolate ester of the boron species shown) was unsuccessful, as were the two main catalytic versions, using Rh(I) and using a catalytic B-H species to effect transborylation³³. Additional experiments using the Me₂S adduct of dibromoborane and subsequent trapping of the vinyl dibromoboron species with pinacol were also unsuccessful³⁴. Finally, we attempted direct hydroboration using a novel new method reported by Snieckus, *et al.* involving the pre-generation of a dialkylborane and trapping of the product with pinacol³⁵. Unfortunately, no products were ever isolated from these reactions. All starting material was consumed, but it is presumably a decomposition pathway that is undergone by the unstable terminal vinyl boronate during these reactions. This is supported by the disappearance of the starting alkyne by TLC, NMR, and FTIR. Although the starting material is being consumed, the isolated products do not show many of the desired characteristic peaks in their NMR spectra, mostly notably the tosyl peaks as well as the pinacol's methyl group peak(s).



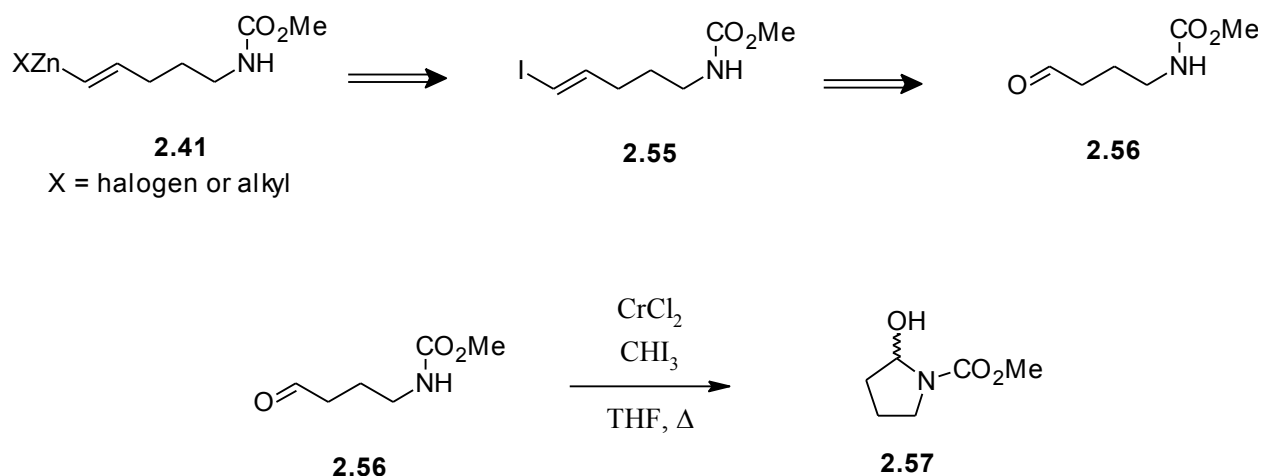
Scheme 2.24: Attempted hydroboration to install the vinyl boronate cross-coupling partner

In a last-ditch effort to synthesize the required *trans*-vinyl boronate, we utilized a protocol established by Grubbs *et al.*, involving the cross-metathesis of a propenyl boronate onto a terminal alkene³⁶. Unfortunately, the analogous amino-alkene **2.52** did not provide the desired compound, but rather a large amount of homocoupled material (Scheme 2.25). Changing the concentration, which typically has a large impact on these reactions, did not alter the singularly disappointing product distribution. Undoubtedly this arises from the terminal olefin being Type I and highly reactive to olefin metathesis, while **2.53** is Type II and is thus less reactive. Type I olefins tend to homometathesize under cross-metathesis conditions, and are typically not used for this reason.



Scheme 2.25: Attempted synthesis of vinyl boronate **2.54** by cross-metathesis

Our attempts to synthesize the vinyl zinc reagent **2.41** began with an attempt to synthesize vinyl iodide **2.55** (Scheme 2.26). We envisioned that by lithiating the iodide, we could effectively transmetallate onto zinc and be provided with a reactive cross-coupling partner in one pot. Unfortunately, all attempts to synthesize the vinyl iodide failed. The most promising pathway required the aldehyde **2.56** to be converted to the vinyl iodide by a Takai olefination³⁷. The cyclic aminal **2.57** was isolated in all cases, a result of the cyclization/acetalization of **2.56** *in situ*. This cyclic aminal was subjected to several iterations of olefination protocols, but remained unchanged. It is not known why **2.57** is so stable to olefination conditions. It is possible that the hydroxyl group directly interacts (most likely through hydrogen-bonding) with the carbamate protecting group. This may increase the stability of the cyclic form, preventing the aldehyde functionality from being exposed to participate in the desired reactions.



Scheme 2.26: Attempted synthesis of vinyl iodide **2.55**

2.4.3. Second-Generation Synthesis Implications

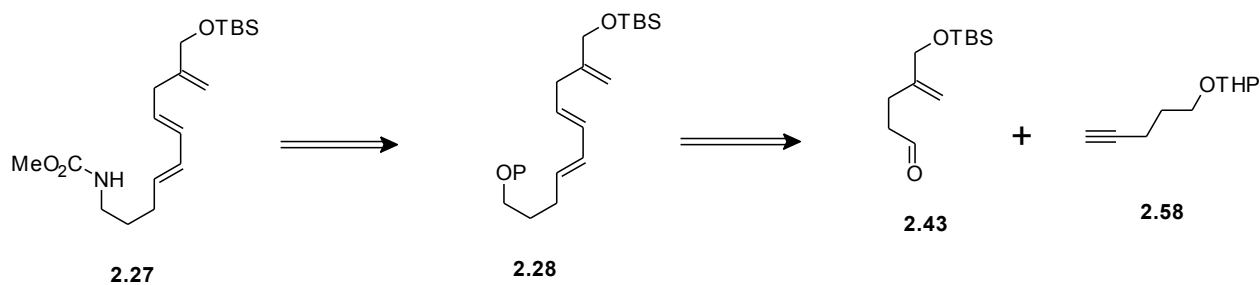
It became apparent that our approach towards the cross-coupling was fruitless. We were able to synthesize aldehyde **2.43** in excellent yields, with minimal purification steps. We therefore wanted to move forward being able to incorporate this molecule into our new synthetic strategy. We also learned that the terminal nucleophile was highly problematic, and that many of the precursors (boronates and halides) were highly unstable. The presence of the nitrogen also seemed to make things much more complicated and difficult. However, performing the reactions on a THP-protected alcohol analog did not change the outcomes, suggesting that the product moieties are the truly unstable portions.

2.5. Third-Generation Approach Towards the Total Synthesis of Huperzine X

2.5.1. Retrosynthetic Analysis

Similarly to the second-generation synthesis, we maintained focus on the identical steps to completion of the natural product. Since we had invested a significant amount of time and effort to synthesize **2.43**, we decided the best pathway would be to add a vinyl nucleophile

directly to the aldehyde. As described in the previous section, we had experience difficulties in creating a vinyl nucleophile such as a vinyl zinc reagent from direct transmetalation onto the vinyl lithiate. However, we decided that we might be able to make the vinyl zinc compound if we transmetalated from a more stable transition metal. If we could accomplish this, we could still utilize our aldehyde synthesis as well as our terminal alkyne starting material (Scheme 2.27).



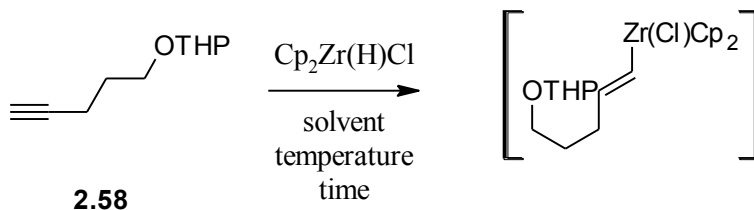
Scheme 2.27: *Third-generation retrosynthesis involving addition onto aldehyde 2.43*

2.5.2. Forward Synthesis

Our synthesis of the vinyl zinc reagent **2.41** began with firstly protecting 4-pentyn-1-ol as its tetrahydropyranyl acetal. Using Amberlyst-15 ion exchange resin as a source of catalytic protons, we were able to isolate the protected alcohol **2.58** in quantitative yield. We next turned to the literature to provide us with alternatives to lithiation of a vinyl iodide, so that we could transmetalate directly from a metallated vinylic species created from the terminal alkyne. There are many reports in the literature to accomplish this task. Most notably among them are hydroalumination and hydrozirconation. In both cases it has been reported that amides containing acidic protons or tosyl groups are generally incompatible with these reactions types. We therefore attempted to synthesize the hydroaluminated material as well as the hydrozirconated material, and found the hydrozirconation to be successful.

Hydrozirconation studies were conducted using the numerous reported literature protocols (Table 2.2), and it was found that 1.1 equivalent of Schwartz Reagent in DCM was an applicable method for providing the hydrozirconated intermediate.

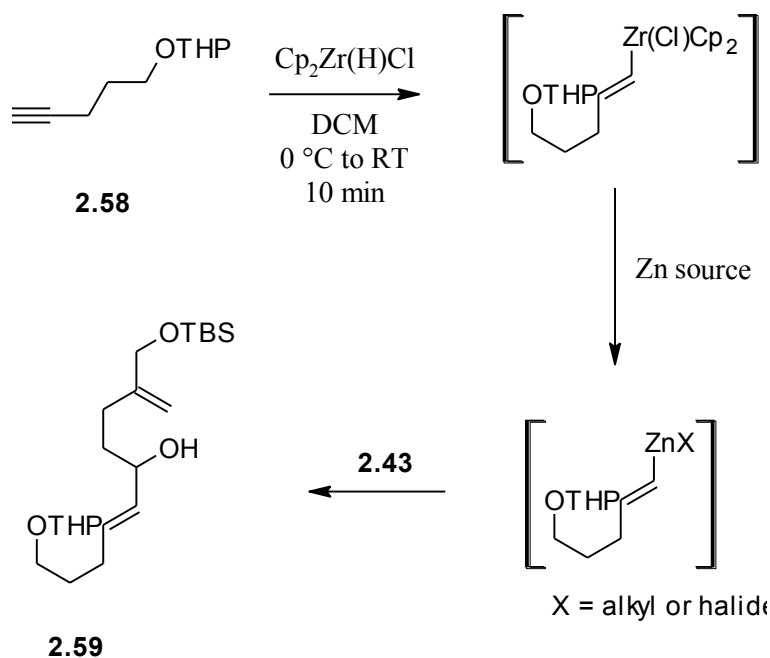
Table 2.2: Hydrozirconation trials using **2.58** as an alkyne starting material



Entry	Schwartz Reagent (eq.)	Solvent	Temperature (°C)	Time	conversion ^a
1	2.2	toluene	reflux	5 hrs	decomp. ^b
2	2.2	THF	RT → reflux	16 hrs	none
3	1.5	DCM	0°C → RT	25 min	complete
4	1.1	DCM	0°C → RT	10 min	complete

^a: conversion monitored by TLC using *p*-anisaldehyde as a stain. Hydrozirconated product appears as red while starting alkyne is blue.
^b: Decomposition confirmed by crude ¹H-NMR analysis

Thus, using the optimized protocol, we subjected alkyne **2.58** to hydrozirconation in DCM and followed with transmetalation (Scheme 2.28). Of note is the lack of formation of any *cis* isomers during the hydrozirconation. This is typical of hydrometalations (hydrozirconation, hydrostannation, and hydroaluminum being most common), as the metal-hydride is added to the alkyne in a *syn* addition, resulting in the alkyl group and the metal being *trans* to one another in the resultant product. Regioselectivity is also not a problem for this particular reaction due to the alkyne being terminal, and thus the steric bulk of the zirconium species favors the least hindered carbon of the alkyne, giving rise to the only observed regioisomer.



Scheme 2.28: *Hydrozirconation/transmetalation sequence for constructing 2.59*

Initially ZnCl_2 was used as a solution in THF for the reaction, but it resulted in no conversion to product. The main products were the reduced alkyne (reduced to alkene, result of protonation of the C-Zr bond) and the recovered aldehyde (**2.43**). This is presumably due to our inability to exclude all water from the ZnCl_2 solution. As an alternative, we attempted to use ZnMe_2 (as a commercially available solution in toluene) and found that the reaction was successful, giving 54% yield of the allylic alcohol. We also attempted a reported protocol where, using a silver salt (AgClO_4 or AgOTf), the vinyl zirconium reagent would be ionized to the cation and act as a vinyl transfer agent to the aldehyde³⁸. While the mechanistic details located in the original paper are convincing, we did not obtain any product even after 24 hours under their reported conditions. The use of a dialkyl zinc reagent is required because the initial stage of the transmetalation process is the methylation of the zirconium, forming a transient, hypervalent

zirconium complex. This is much more reactive to transmetalation, and reacts with the present ZnMe_2 . The released $\text{Cp}_2\text{Zr}(\text{Cl})\text{Me}$ is a proficient Lewis acid, and actually accelerates the addition of the vinyl zinc reagent to the aldehyde. When using chiral ligands to effect a stereoselective addition to aldehydes, it is common to have to use a larger excess of ligand in order for the zinc Lewis acid to effectively compete with the *in situ* generated zirconocene Lewis acid³⁹.

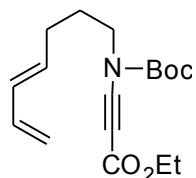
With the structurally significant carbon backbone **2.59** in hand, we turned our attention to the required elimination of the allylic alcohol to make the desired 1,3-diene motif. Using standard conditions (MsCl , NEt_3 , DCM , then DBU , THF , reflux) resulted in a 1:1 mixture of *cis:trans* isomers for the newly formed olefin. An alternative procedure using Hünig's base and HMPA ⁴⁰ at 160°C resulted also in 1:1 isomeric ratios, but with the added issue of significant decomposition of the starting mesylate due to the high temperatures. The generation of the HCl salt of Hünig's base also promotes the deprotection of the THP ether, which is not found in the crude mixture NMR analysis. It was also explored to initially oxidize the allylic alcohol (MnO_2 , DCM , RT, 24 hrs, 95%), then subject the enone to enolization and trapping with Tf_2O . Reduction of this 1,3-diene-2-triflate with $\text{Pd}(0)$ catalysis proved ineffective at producing the deoxygenated compound. Although we worked diligently to produce the desired 1,3-diene structure, we were unable to achieve the transformation. Due to this limitation, the synthesis was halted due to lack of forward progress. We turned our attention to a proof-of-concept set of model system experiments designed to illustrate our vision of the future key reactions in this synthesis.

2.5.3. Synthetic Approaches to Model Systems

With many of our synthetic options exhausted, we turned our attention to creating model systems in order to illustrate the potential that the incomplete synthetic steps possess. Our initial approach was to create two distinct models, one dealing with the intramolecular ynamide Diels-Alder reaction and another dealing with the intramolecular allylation reaction. Since these two reactions are crucial for the success of our entire synthetic strategy, it was imperative that the model systems be as similar as possible, while still allowing us access to readily available materials for synthetic optimization.

2.5.3.1. Intramolecular Diels-Alder Model System

In preparing our ynamide Diels-Alder model system, we realized that although the two appendages to the resultant cyclohexadiene ring would be *syn* to one another, control of such a sterically encumbered system may be detrimental to our optimization of the reaction conditions. In this light, we designed a potential system (**2.60**) which could facilitate our understanding of the reaction, its conditions, and the potential for chiral ligand introduction (Figure 2.3).

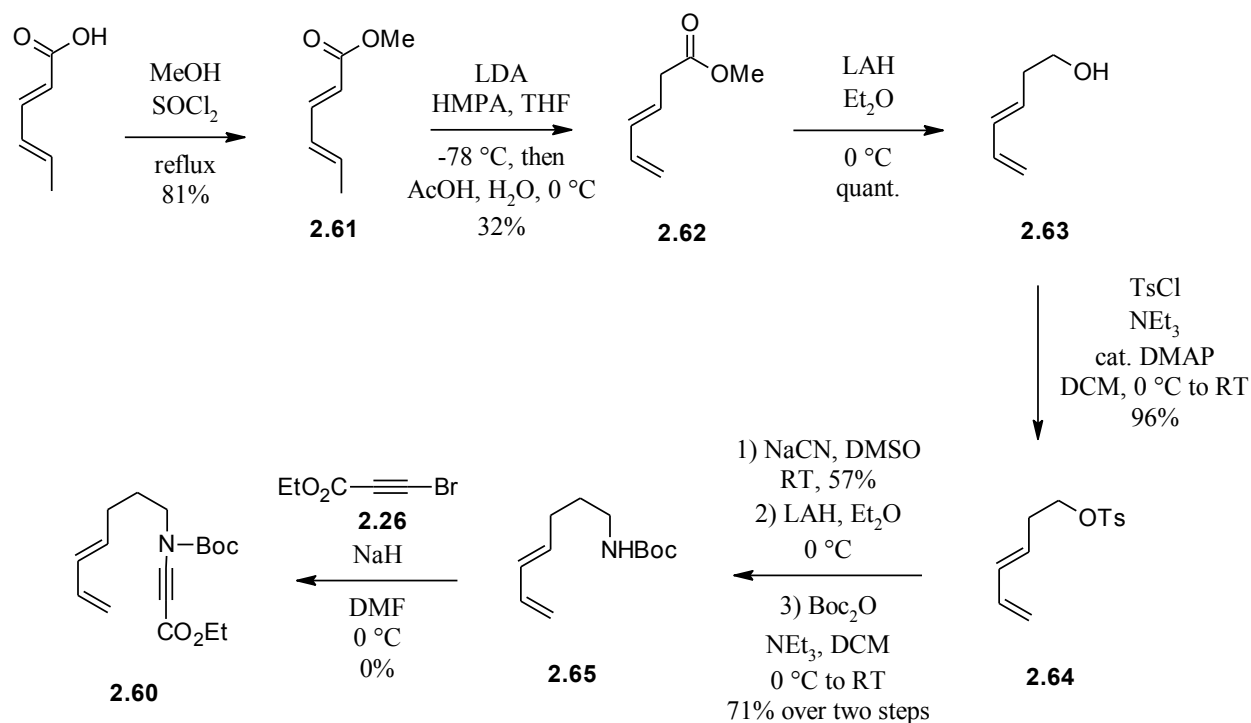


2.60

Figure 2.3: Model compound for ynamide Diels-Alder studies and optimization

Our attempts to synthesize this compound were mainly unsuccessful, due in large part to the inability of previously described procedures to provide usable product. This is mainly due to

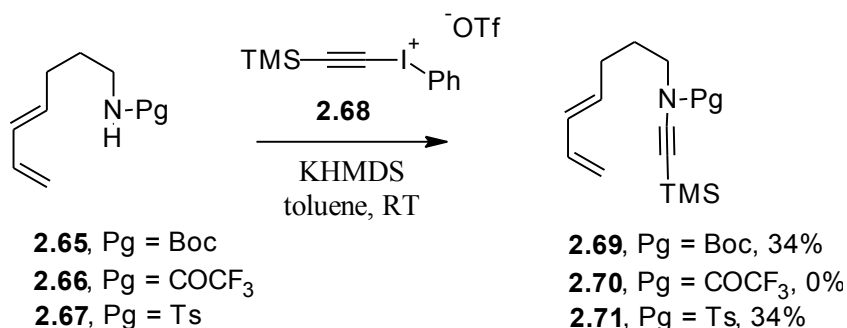
the instability of the resultant ynamide-ester as well as the high reactivity of the standard Cu-amide reaction intermediates with bromoalkyne **2.26**. Unfortunately, the C₇ backbone, due almost certainly to the odd number of carbons, is not commercially available, so the terminal carbon must be included with the nitrogen as a cyanide addition. Thusly, simple esterification of sorbic acid gave methyl sorbate (**2.61**)⁴¹, which was subjected to base-induced olefin isomerization⁴², giving the 1,3-diene as a terminal moiety in **2.62**. Reduction with LAH gave the alcohol **2.63**, which was tosylated to give **2.64**. Cyanide displacement and subsequent LAH reduction gave the free amine⁴³, which was directly protected as the Boc carbamate **2.65** in 71% yield over two steps. With the amine in hand, we attempted the previously described ynamide formation procedure using the “push-pull” bromoalkyne¹⁴. Unfortunately, the product was not stable to chromatography and it was unable to be isolated. The starting carbamate was recovered in a 10% yield. The corresponding amount of bromoalkyne was also recovered (Scheme 2.29). These results point to the electron withdrawing nature of the ester group being a primary culprit in the instability of the resultant ynamide. It is possible that the desired Diels-Alder cycloaddition is occurring due to the high electronic instability of the ynamide-ester, however there was no indication of this material passing through the column used to purify the ynamide.



Scheme 2.29: Attempted synthesis of Diels-Alder model compound **2.60**

Due to the unstable nature of the ynamide product, we sought an alternative ynamide formation procedure which would give us a stable precursor to test the Diels-Alder reaction upon. In this light, we identified the ynamide synthesis described by Witulski and co-workers^{7,8}. Using the hypervalent iodine TMS-alkyne, we subjected **2.65-2.67** to the KHMDS-mediated coupling of hypervalent iodine reagent **2.68** (Scheme 2.30). This reaction functions by the initial anionic amide nitrogen attacking the β carbon of the iodonium alkyne, forming an intermediate iodoylide, which decomposes to iodobenzene and a vinylidene carbene⁴⁴. This carbene can undergo the desired 1,2-migration of the TMS group to provide the ynamide in low yields. The carbene can also undergo rapid 1,5-insertion to form a 2,3-dihydropyrrole-type of product, which may undergo further reactions. Lastly, the carbene can be envisioned to participate in [2+1] cycloadditions with the pendant olefins present in the model system. One way to remove this

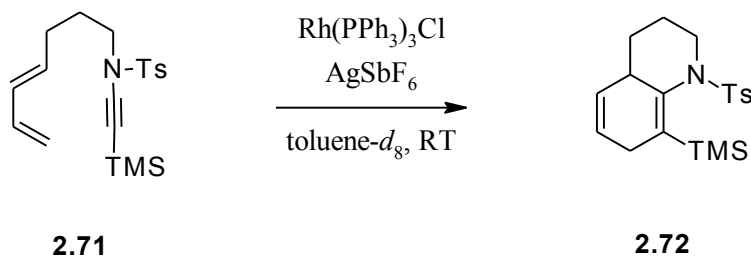
reactivity is to conjugate the vinylidene carbene to a phenyl group, which removes the electron density around the carbene center and allows for more time to facilitate the 1,2-migration⁴⁵. In the case of **2.71**, the ultimate goal is to functionalize the position onto which the TMS group migrates. If the TMS group is maintained, it becomes vinylic, which allows for the *ipso* substitution by a reactive acid chloride; something a larger, potentially more stable group cannot do. In this light, the possible permutations of replacement groups for TMS is severely limited to 1,2-migratory aptitude.



Scheme 2.30: Ynamide formation using iodonium alkyne **2.68**

All protecting groups gave acceptable yields for our model system studies with the exception of **2.66**, which did not allow us to purify either the starting amide or the resultant ynamide, as the trifluoroacetyl group was too unstable to chromatographic separations, which are required after the aforementioned reaction. The Boc and Tosyl protected compounds (**2.65** and **2.67**, respectively) gave acceptable yields with pure products after chromatography. Due to limitations in the scale of these reactions and the length of time to synthesize additional material, we elected to perform the studies on the Diels-Alder cyclizations *in situ* using NMR studies.

Thus we subjected **2.71** as a model compound to the reaction conditions described in Witulski *et al* (Scheme 2.31)⁷.



Scheme 2.31: *Intramolecular Diels-Alder reaction of model compound 2.71*

Our results were promising: we obtained **2.72** after column chromatography (neutral Al₂O₃) in a 20% yield (isolated, ¹H-NMR indicated only a 75% purity of the isolated material even after chromatography). These results indicate that the intramolecular ynamide Diels-Alder system does indeed work for our system. While the yield discrepancies with the original paper are unfortunate, it does indicate that there is promise in the Diels-Alder system. The reason for the difference is most likely due to the reported protocol providing 5,6-fused ring systems, whereas the approach towards **2.72** produces 6,6-fused ring systems, which are kinetically less stable, and the reaction is under kinetic control.

2.5.3.2. Intramolecular Allylation Model System

The intramolecular allylation is made more complicated by the presence of the D-ring in the backbone of the molecule. While the stereochemistry of the allyl appendage would direct the stereochemistry of the allylation, our inability to synthesize the backbone makes it essential that we establish the correct set of conditions in order to not waste precious material. We therefore

set out to create a model system which would mimic the electronic complexity of the 2,3-hydro-4-pyridone structural motif without the aliphatic side chain. This resulted in our decision to attempt the intermolecular allylation using allyltrimethylsilane on 2,3-dihydro-4-pyridone **2.73** as well as the intramolecular variant using the tethered pyridone-allyl silane **2.74** (Figure 2.4).

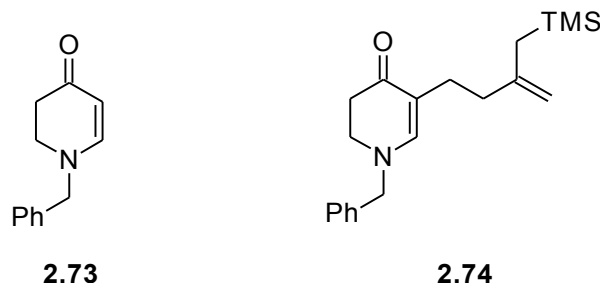
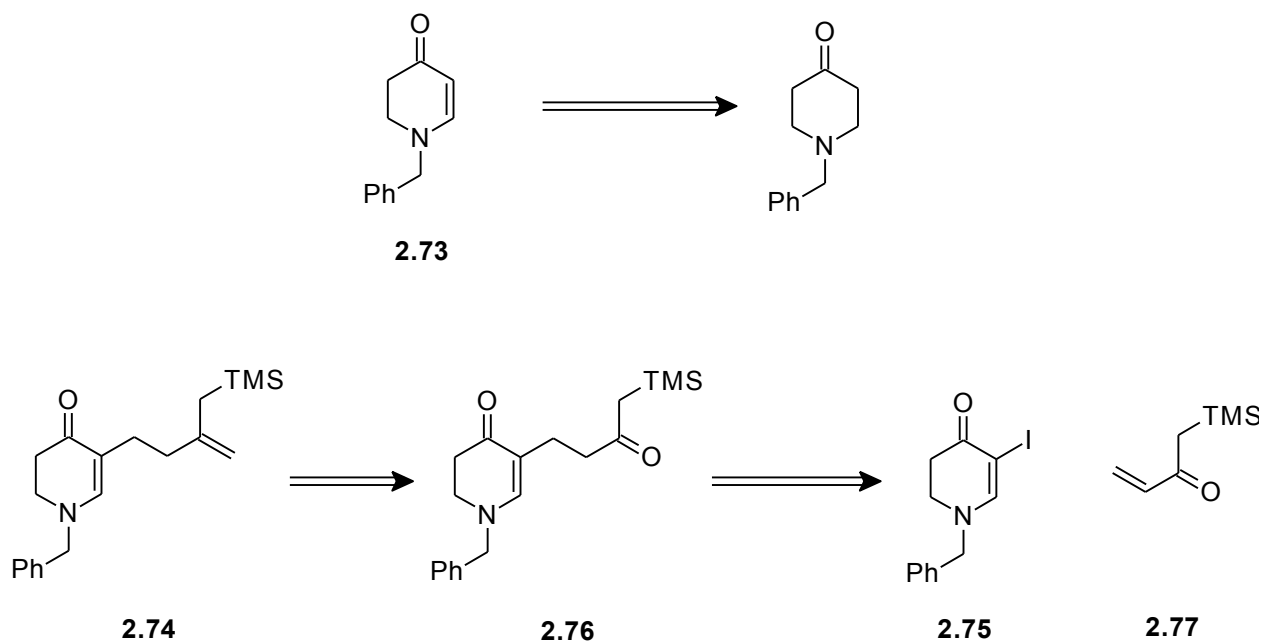


Figure 2.4: *Substrates for the study and optimization of the pyridone allylation model system*

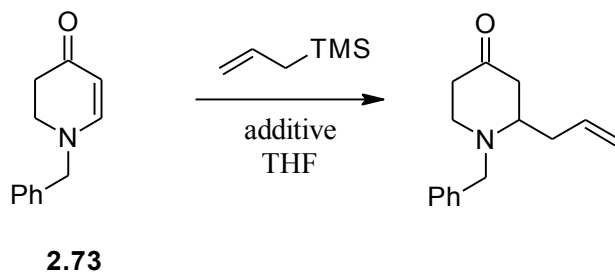
The 2,3-dihydro-4-pyridone **2.73** is synthesized by $\text{Hg}(\text{OAc})_2$ -mediated dehydrogenation from the readily available 4-piperidone⁴⁶, while **2.74** can be envisioned as coming from the α -iodo analog of **2.73** (**2.75**) by way of a Cu-catalyzed conjugate addition of the metallated Grignard followed by a Wittig olefination from **2.76** (Scheme 2.32).



Scheme 2.32: Retrosynthesis of the inter- and intra-molecular allylation model systems

We initially synthesized **2.73** from the saturated piperidone using the $\text{Hg}(\text{OAc})_2$ -catalyzed reaction. While the original publication reports high yields, the transformation was only able to reproducibly give average yields of 50%. Nonetheless, **2.73** was taken forward to install the iodine at the α position using standard DMAP-catalyzed halogenation⁴⁷, providing **2.75** in high yield (Scheme 2.33). Using **2.73**, it was attempted to utilize a number of different Lewis acids, as well as triflic anhydride to promote the addition of allyl trimethylsilane (Table 2.3). Unfortunately, none of our efforts were successful. Even the use of TBAF to force the silicon-carbon bond cleavage resulted in no yield (Table 2.3, Entry 7).

Table 2.3: Attempts to add allyl trimethylsilane to **2.73** using various Lewis acids



Entry	Activating Agent (mol %)	Result ^a
1	InCl ₃ (10%)	NR
2	InBr ₃ (10%)	NR
3	BiCl ₃ (10%)	NR
4	BiBr ₃ (10%)	NR
5	In(OTf) ₃ (10%)	NR
6	Tf ₂ O (110%)	NR
7	TBAF (110%)	NR

^a: NR = No Reaction (no **2.73** consumption);
AllylTMS reagent consumed in all cases.

It occurred to us that the β position of the enone/enamine **2.73** was too electron rich, since the nitrogen's lone pair is in direct conjugation with the system. This would prevent additional electron density from being introduced by the nucleophile. A compensation to this would be to replace the benzyl protecting group with a more electron withdrawing group, such as a tosyl. Doing this would also make the model system more analogous to our Diels-Alder model system.

In preparation for the synthesis of the intramolecular allylation model system, the α -iodoenaminone **2.75** was metalated using *iso*-propylmagnesium chloride in the manner described by Luzung and co-workers for aryl iodides⁴⁸. After transmetalating onto CuI (-30°C), the

prepared reagent was combined with methyl vinyl ketone to produce the desilylated analog of **2.76** (35% yield). It was attempted to take this material to **2.76** through many different transformations, including direct α -silylation, α -hydroxylation (to be converted to the TMS compound), and enolization/triflation followed by Kumada coupling with $\text{TMSCH}_2\text{MgCl}$. None of these procedures were successful. The current hypothesis is that the electron rich nitrogen is interfering with the reactions, particularly the triflation and Kumada coupling route.

2.6. Conclusions and Implications of Model Systems

Our experiments into the generation of model systems for our *lycopodine*-class alkaloid synthesis have shown us a great deal about our synthetic strategy and our future directions with this project. While our main synthesis does not seem overly feasible from its current standpoint, we have been able to demonstrate that the intramolecular Diels-Alder reaction is a feasible forward step. Something to note is that the DA reaction in question does not result in aromatization of the final compound, and thus we are able to obtain the 1,4-cyclohexadiene core required for our future endeavors. With the allylation system, we have shown that the nitrogen requires a highly electron withdrawing protecting group in order to activate the β position for nucleophilic attack from an allyl silane. Reports of this kind are already known⁴⁹, and thus our choice of a tosylate is a good decision, as it will make the nitrogen electron poor enough to undergo the Diels-Alder while also being effective for the allylation step.

2.7. Experimental Section

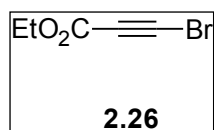
2.7.1. General Reaction Considerations

All reactions were conducted in oven-dried (100°C) glassware, and were run under an atmosphere of argon, unless otherwise stated. DCM and THF were dried by passing the degassed solvent through a column of activated Cu/alumina under N₂ immediately before use. Toluene was dried over activated 3Å molecular sieves. EtOH used as absolute. Acetone was used as HPLC-grade. NBS was recrystallized from hot H₂O and dried in a dessicator. Allyl bromide was purified by washing with sat. aq. NaHCO₃ followed by distilled H₂O, drying over CaCl₂, and distilling under reduced pressure. Chromatography was performed on EMD silica gel (40-60 microns) using air pressure, unless otherwise specified. All other solvents and reagents were purchased at the highest level of purity and were used as received.

NMR spectra were obtained on a Varian INOVA NMR instrument, at the indicated field strength in the indicated deuterated solvent. NMR spectra are referenced to internal tetramethylsilane. HRMS were collected on a Bruker BIOTOF III instrument with a positive ESI mode and are referenced to appropriate PEG or NaTFA standards. FTIR spectra were collected on a Bruker Dalton FTIR instrument. Melting points were collected on a Fisher-Johns apparatus and are uncorrected.

2.7.2. Experimental Details

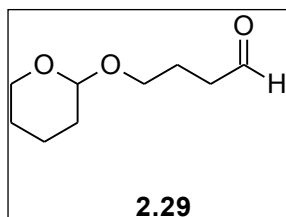
Ethyl 3-bromopropiolate (2.26)⁵⁰



A 25-mL round bottom flask equipped with a magnetic stir bar was charged with ethyl propiolate (0.78 mL, 7.66 mmol) and acetone (16 mL). AgNO₃ (0.13 g, 0.77 mmol) was added in one portion and the reaction was wrapped in foil to protect it

against light. After stirring at RT for 10 min., freshly recrystallized and dried *N*-bromosuccinimide (NBS, 1.50 g, 8.43 mmol) was added in one portion and the reaction was stirred at RT for 2 hrs. The reaction mixture was filtered through Celite, with the filter cake being washed with acetone (50 mL), and the filtrate was concentrated. The residue was purified by FCC (15% Et₂O in pentane) to give **2.26** as a slightly yellow oil which solidifies into a colorless solid upon standing (1.19 g, 88%). CAUTION: The compound is a severe lachrymator! ¹H-NMR (400 MHz, CDCl₃) δ 4.24 (q, *J*=6.8 Hz, 2H), 1.32 (t, *J*=6 Hz, 3H); ¹³C-NMR (100 MHz, CDCl₃) δ 152.7, 77.0, 62.7, 52.5, 14.2; FTIR (thin film) $\bar{\nu}$ (max) 3001, 2983, 2191, 1688, 1271 cm⁻¹.

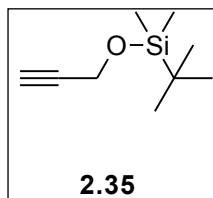
4-(Tetrahydropyranyl)oxobutylaldehyde (**2.29**)⁵¹



A 500-mL round bottom flask equipped with a magnetic stir bar was charged with 1,4-butanediol (22.6 mL, 255 mmol) and DCM (250 mL). (+)-camphorsulfonic acid (CSA, 5.92 g, 25.5 mmol) was added in one portion to the RT, stirred solution, and the reaction was charged with 3,4-dihydro-2*H*-pyran (23.3 mL, 255 mmol). After stirring for 4 hrs at RT, the reaction mixture was washed with sat. aq. NaHCO₃ (3 x 150 mL) and H₂O (3 x 150 mL). The organic phase was dried over MgSO₄, filtered, and concentrated to give 4-(tetrahydropyranyl)oxo-1-butanol as a colorless oil (32.6 g, 74%). ¹H-NMR (400 MHz, CDCl₃) δ 4.46 (m, 1H), 3.72 (m, 1H), 3.62 (m, 1H), 3.51 (m, 1H), 3.37 (m, 1H), 3.31 (m, 1H), 2.85 (bs, 1H), 1.68 (m, 1H), 1.59 (m, 4H), 1.40 (m, 5H); ¹³C-NMR (100 MHz, CDCl₃) δ 98.9, 67.6, 53.8, 30.8, 30.0, 26.7, 25.6, 19.7

A 50-mL round bottom flask equipped with a stir bar was charged with the alcohol from the previous step (2.00 g, 11.48 mmol) and DCM (16.4 mL). The reaction was stirred at RT and TEMPO (0.18 g, 1.15 mmol) was added, followed by a portion-wise addition of $\text{PhI}(\text{OAc})_2$ (4.07 g, 12.63 mmol). The reaction stirred at RT overnight, then was quenched by addition of 1:1 sat. aq. $\text{Na}_2\text{S}_2\text{O}_3$:sat. aq. NaHCO_3 (20 mL). The phases were separated and the organic phase was washed with brine (10 mL), dried over MgSO_4 , filtered, and concentrated. FCC of the residue (1:1 pet. ether: Et_2O) gave **2.29** as a slightly yellow oil (1.05 g, 50%). $^1\text{H-NMR}$ (400 MHz, CDCl_3) δ 9.74 (t, $J=1.6$ Hz, 1H), 4.54 (dt, $J=8.4$ Hz, 4 Hz, 1H), 3.74 (m, 2H), 3.35 (m, 2H), 2.50 (tt, $J=2$ Hz, 6.8 Hz, 1H), 2.43 (td, $J=2$ Hz, 7.6 Hz, 1H), 1.76-1.45 (m, 9H); $^{13}\text{C-NMR}$ (100 MHz, CDCl_3) δ 202.6, 98.9, 62.4, 41.2, 30.9, 26.7, 25.7, 22.8, 19.7; FTIR (thin film) $\bar{\nu}$ (max) 2946, 2874, 1723 cm^{-1} .

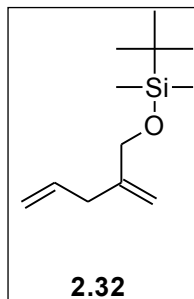
1-(*tert*-Butyldimethylsilyl)propargyl alcohol (**2.35**)⁵²



A 250-mL round bottom flask equipped with a magnetic stir bar was charged with *tert*-butyldimethylsilyl chloride (TBSCl, 7.12 g, 47.27 mmol) and DMF (75 mL). Imidazole (3.22 g, 47.27 mmol) was added to this solution at RT. Propargyl alcohol (2.59 mL, 44.59 mmol) was added dropwise at RT, with a slight exotherm being observed upon addition. After addition was complete, the reaction ran at RT overnight, then was poured into a separatory funnel containing 125 mL H_2O . The product was extracted with Et_2O (2 x 100 mL) and the combined organic phases were washed with H_2O (200 mL), brine (150 mL), dried over MgSO_4 , filtered, and concentrated. The crude product was purified by passage through a plug of silica gel using 20% EtOAc in hexanes as eluent, providing **2.35** as a colorless oil (7.59 g, quant.). $^1\text{H-NMR}$ (400 MHz, CDCl_3) δ 4.31 (d, $J=2.4$ Hz, 2H), 2.39 (t,

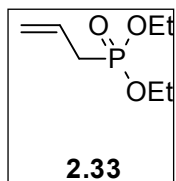
$J=2.4$ Hz, 1H), 0.91 (s, 9H), 0.13 (s, 6H); $^{13}\text{C-NMR}$ (100 MHz, CDCl_3) δ 73.0, 51.7, 25.8, 25.7, 18.5, -5.0.

2-(*tert*-Butyldimethylsilyloxy)methyl-1,4-pentadiene (**2.32**)⁵³



A 10-mL reaction vial equipped with a magnetic stir bar was charged with **2.35** (0.341 g, 2.00 mmol) and THF (2.00 mL). Freshly distilled allyl bromide (1.38 mL, 16.00 mmol) was added and the reaction stirred at RT as In powder (0.344 g, 3.00 mmol) was added. The reaction was capped without concern for air or moisture and left to stir overnight. The reaction mixture was concentrated and the residue was suspended in 3:2 EtOAc:hexane and passed through a plug of silica gel, using the same eluent. The filtrate was concentrated and the residue was purified by FCC (2% EtOAc in hexane) to give **2.32** as a colorless oil (0.425 g, quant.). $^1\text{H-NMR}$ (400 MHz, CDCl_3) δ 5.82 (m, 1H), 5.06 (m, 3H), 4.84 (m, 1H), 4.07 (s, 2H), 2.76 (dd, $J=0.8$ Hz, 6.8 Hz, 2H), 0.92 (s, 9H), 0.07 (s, 6H); $^{13}\text{C-NMR}$ (100 MHz, CDCl_3) δ 147.1, 136.2, 116.4, 109.8, 65.8, 37.5, 26.1, 18.6, -5.2; FTIR (thin film) $\bar{\nu}$ (max) 2956, 2928, 2856, 1472, 1463, 1257 cm^{-1} .

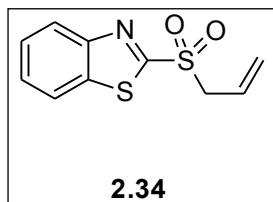
Diethyl allylphosphonate (**2.33**)⁵⁴



A 100-mL round bottom flask equipped with a magnetic stir bar was charged with triethylphosphite (20.0 mL, 116.6 mmol) and freshly distilled allyl bromide (11.0 mL, 127.1 mmol). The reaction mixture was heated to reflux (ca. 125°C) for 4 hrs then cooled to RT. The excess allyl bromide was removed *in vacuo* and the resultant yellow oil was purified by FCC (100% EtOAc) giving **2.33** as a colorless, odiferous liquid with a minor (<5%) presence of triethylphosphite (20.4 g, 98%). Material is sufficiently pure for all desired

uses. Continued chromatography (40% EtOAc in hexane) provides analytically pure material. $^1\text{H-NMR}$ (400 MHz, CDCl_3) δ 5.64 (m, 1H), 5.04 (m, 2H), 3.95 (m, 4H), 2.46 (dd, $J=7.2$ Hz, 22Hz), 1.18 (m, 6H); $^{13}\text{C-NMR}$ (100 MHz, CDCl_3) δ 127.7, 119.8, 61.9, 60.3, 16.4; FTIR (thin film) $\bar{\nu}$ (max) 2984, 2939, 2907, 2240, 1733, 1249, 1030 cm^{-1} .

2-Allylsulfonyl-benzothiazole (2.34)⁵⁵

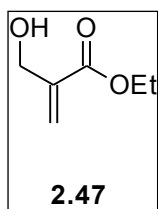


A 50-mL round bottom flask equipped with a magnetic stir bar was charged with 2-mercaptobenzothiazole (0.836 g, 5.00 mmol), NaOH (0.31 g, 7.75 mmol), and EtOH (25 mL). With stirring at RT, freshly distilled allyl bromide (0.498 mL, 5.75 mmol) was added dropwise, and the reaction mixture was stirred at RT for 20 hrs. The slurried reaction was then diluted with EtOAc (50 mL) and quenched with H_2O (25 mL). The phases were separated and the aq. phase was extracted with EtOAc (25 mL). The combined organic phases were washed with H_2O (25 mL), brine (25 mL), dried over MgSO_4 , filtered, and concentrated. The crude allyl sulfide was used directly in the next step (1.04 g, quant.)

A 50-mL round bottom flask equipped with a magnetic stir bar was charged with the crude allyl sulfide (0.34 g, 1.64 mmol) and DCM (20 mL). The reaction mixture was cooled to 0°C and stirred as *m*CPBA (77%, 0.742 g, 3.31 mmol) was added in portions over 5 min. After 10 additional min. the reaction was allowed to warm to RT and stirred there for 18 hrs. The reaction was concentrated and the residue was suspended in EtOAc (20 mL) and washed with sat. aq. NaHCO_3 (20 mL). The aq. phase was re-extracted with EtOAc (20 mL), and the combined organic phases were washed with sat. aq. NaHCO_3 (25 mL), H_2O (25 mL), brine (25

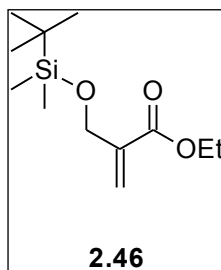
mL), dried over MgSO₄, filtered and concentrated. FCC of the residue (15% Et₂O in pentane) gave **2.34** as a white solid (0.294 g, 75%). mp 59-60°C; ¹H-NMR (400 MHz, CDCl₃) δ 8.23 (dd, *J*=0.8 Hz, 7.2 Hz, 1H), 8.01 (dd, *J*=0.8 Hz, 7.2 Hz, 1H), 7.62 (m, 2H), 5.89 (m, 1H), 5.37 (dd, *J*=10.4 Hz, 11.6 Hz, 2H), 4.25 (d, *J*=7.2 Hz); ¹³C-NMR (100 MHz, CDCl₃) δ 128.3, 127.9, 126.4, 125.7, 123.3, 122.5, 59.3; FTIR (thin film) $\bar{\nu}$ (max) 2919, 1471, 1328, 1144 cm⁻¹.

α -Hydroxymethylethyl acrylate (2.47**)**⁵⁶



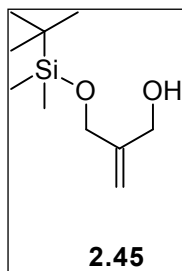
A 50-mL round bottom flask equipped with a magnetic stir bar was charged with paraformaldehyde (6.05 g, 201.4 mmol) and H₂O (15 mL). The slurry was then charged with 1 N H₃PO₄ (0.575 mL) and set to stir at reflux until the reaction became a clear, homogeneous solution (approx. 30 min. – 1 hour). The reaction was then cooled to RT and triethylphosphonoacetate (10.00 mL, 50.40 mmol) was added in one portion. The reaction was warmed to 40°C and stirred while a solution of K₂CO₃ (7.66 g, 55.44 mmol) in H₂O (8.15 mL) was added dropwise. The reaction ran at 40°C for 10 min., then was placed directly in an ice bath and quickly diluted with Et₂O and brine (15 mL each). The phases were separated and the aq. phase was extracted with Et₂O (3 x 15 mL). The combined organic phases were washed with brine (15 mL), dried over Na₂SO₄, filtered, and concentrated to give **2.47** (6.54 g, 99%) as a colorless oil. ¹H-NMR (400 MHz, CDCl₃) δ 6.26 (d, *J*=1.2 Hz, 1H), 5.85 (d, *J*=1.2 Hz, 1H), 4.33 (s, 2H), 4.24, (q, *J*=7.2 Hz, 2H), 2.12 (bs, 1H), 1.32 (t, *J*=7.2 Hz, 3H); ¹³C-NMR (100 MHz, CDCl₃) δ 166.6, 139.8, 125.6, 62.4, 61.0, 14.3; FTIR (thin film) $\bar{\nu}$ (max) 3447, 2926, 1716, 1456 cm⁻¹; HRMS: material polymerizes rapidly upon exposure to ESI.

α -(*tert*-Butyldimethylsilyl)hydroxymethylethyl acrylate (**2.46**)⁵⁶



A 250-mL round bottom flask equipped with a magnetic stir bar was charged with **2.47** (6.00 g, 46.10 mmol) and DCM (150 mL). With stirring, imidazole (7.85 g, 115.26 mmol) was added in one portion, followed by TBSCl (8.69 g, 57.63) in portions over 5 min. The cloudy solution was stirred at RT for 2.5hrs, then was quenched by the addition of sat. aq. NH₄Cl, and the phases were separated. The aq. phase was extracted with DCM (3 x 50 mL), and the combined organic phases were dried over Na₂SO₄, filtered, and concentrated to give a light yellow oil. Further reactions did not require additional purification, however, analytically pure material was obtained by FCC (Si gel, 100% hexane → 5% EtOAc in hexane), providing **2.46** (11.16 g, 99%) as a colorless oil. ¹H-NMR (400 MHz, CDCl₃) δ 6.23 (apparent q, $J=1.6$ Hz, 2.0 Hz, 1H), 5.88 (apparent q, $J=2.0$ Hz, 2.4 Hz, 1H), 4.35 (apparent t, $J=2.4$ Hz, 2H), 4.18 (q, $J=7.2$ Hz, 2H), 1.27 (t, $J=7.2$ Hz, 3H), 0.91 (s, 9H), 0.07 (s, 6H); ¹³C-NMR (100 MHz, CDCl₃) δ 166.0, 140.1, 123.6, 61.6, 60.6, 25.9, 14.2, -3.5, -5.4; FTIR (thin film) $\bar{\nu}$ (max) 2956, 2858, 1716, 1472 cm⁻¹; HRMS (ESI), m/z : 267.1394 (M+Na⁺), calc. for C₁₂H₂₄O₃SiNa: 267.1387.

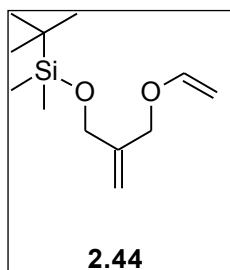
2-Methylidene-3-(*tert*-butyldimethylsiloxy)-1-propanol (**2.45**)⁵⁶



A 1-L round bottom flask equipped with a magnetic stir bar and an addition funnel was charged with **2.46** (9.65 g, 39.48 mmol) and Et₂O (340 mL). The reaction was cooled to -78°C and the addition funnel was charged via cannula with DIBAL-H (1.0 M solution in hexane, 118.45 mL). The DIBAL-H solution was added dropwise over 2 hrs., and the reaction ran an additional 30 min. at -78°C. The reaction was then diluted with EtOAc (200 mL) and quenched with sat. aq. Rochelle's Salt (200

mL). The solution was allowed to warm to RT and stirred vigorously overnight. The phases were then separated and the aq. phase was extracted with EtOAc (3 x 100 mL). The combined organic phases were dried over Na₂SO₄, filtered, and concentrated to give **2.45** (7.91, 99%) as a colorless oil. ¹H-NMR (400 MHz, CDCl₃) δ 5.09 (m, 2H), 4.23 (s, 2H), 4.14 (s, 2H), 2.71 (bs, 1H), 0.91 (s, 9H), 0.07 (s, 6H); ¹³C-NMR (100 MHz, CDCl₃) δ 147.7, 110.9, 65.0, 64.4, 26.0, -3.5, -5.3; FTIR (thin film) $\bar{\nu}$ (max) 3389, 2955, 2858, 1472 cm⁻¹; HRMS (ESI), *m/z*: 225.1283 (M+Na⁺), calc. for C₁₀H₂₂O₂SiNa: 225.1281.

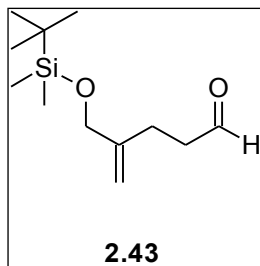
1-(Ethylidene)-2-methylidene-3-(*tert*-butyldimethylsiloxy)-1-propanol (**2.44**)



A 35-mL pressure tube equipped with a magnetic stir bar was charged with **2.45** (2.00 g, 9.88 mmol), [(PPh₃)AuCl] (0.098 g, 0.198 mmol), AgOAc (0.049 g, 0.296 mmol), and ethyl vinyl ether (9.46 mL, 72.11 mmol) and was sealed without exclusion of air and heated to 60°C for 18 hrs. The black

reaction mixture was directly transferred to a Si-gel column pre-treated with 1:1 hexane:EtOAc with 0.1% (v/v) NEt₃, and eluted with the same eluent to provide **2.44** (2.19 g, 97%) as a colorless oil. ¹H-NMR (400 MHz, CDCl₃) δ 6.37 (dd, *J*=6.8 Hz, 14 Hz, 1H), 5.15 (m, 1H), 5.05 (m, 1H), 5.01 (m, 1H), 4.18 (m, 3H), 4.11 (s, 2H), 0.91 (s, 9H), 0.07 (s, 6H); ¹³C-NMR (100 MHz, CDCl₃) δ 151.6, 144.3, 112.5, 111.2, 69.1, 64.0, 26.0, -3.4, -5.3; FTIR (thin film) $\bar{\nu}$ (max) 2953, 2929, 2857, 1471, 1463 cm⁻¹; HRMS (ESI), compound de-vinylates upon exposure to ESI field.

4-(*tert*-Butyldimethylsilyl)hydroxymethyl-4-pentaldehyde (**2.43**)



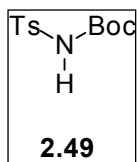
A 30-mL Biotage microwave vial equipped with a magnetic stir bar was charged with **2.44** (2.30 g, 10.07 mmol) and toluene (15 mL) and heated in a 150W microwave reactor for 15hrs at 150°C. The reaction mixture was cooled to RT and transferred to a Si-gel column and eluted with 100%

hexanes until the toluene was flushed through. The eluent was then changed to 1:1

hexane:EtOAc and the product was eluted, providing **2.43** as a light yellow oil (2.29 g, 99%).

$^1\text{H-NMR}$ (400 MHz, CDCl_3) δ 9.77 (t, $J=1.6$ Hz, 1H), 5.07 (s, 1H), 4.82 (s, 1H), 4.09 (s, 2H), 2.62 (dt, $J=7.6$ Hz, 1.6 Hz, 2H), 2.37 (t, $J=7.2$ Hz, 2H), 0.91 (s, 9H), 0.09 (s, 6H); $^{13}\text{C-NMR}$ (100 MHz, CDCl_3) δ 202.3, 147.0, 130.0, 66.2, 60.6, 42.0, 26.1, -3.4, -5.2; FTIR (thin film) $\bar{\nu}$ (max) 2954, 2928, 2856, 1733, 1472 cm^{-1} ; HRMS (ESI), m/z : 251.1446 ($\text{M}+\text{Na}^+$), calc. for $\text{C}_{12}\text{H}_{24}\text{O}_2\text{SiNa}$: 251.1438.

tert-Butoxycarbonyl-*p*-toluenesulfonamide (**2.49**)⁵⁷



A 250-mL round bottom flask equipped with a magnetic stir bar was charged with *p*-toluenesulfonamide (4.00 g, 23.36 mmol), DMAP (0.29 g, 2.34 mmol), and DCM

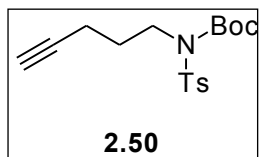
(50 mL). NEt_3 (3.58 mL, 25.70 mmol) was added to this solution at RT. A solution

of Boc_2O (6.17 mL, 26.86 mmol) in DCM (80 mL) was added to the solution over 10 minutes.

The reaction was stirred at RT for 30 minutes, then concentrated. The residue was dissolved in EtOAc (240 mL) and washed with 1N HCl (150 mL), H_2O (150 mL), brine (150 mL), and dried over MgSO_4 . Filtration and concentration gave **2.49** as a white powder (6.24 g, 98%). Product was further purified by recrystallization: Dissolve the product in hot Et_2O (50 mL), cool to RT,

layer the solution with hexane (175 mL) and allowing to diffuse overnight. Thusly, pure **2.49** was obtained as large, colorless hexagonal rods (5.22 g). An additional crop (0.76 g) was obtained by cooling the filtrate from isolation in a freezer over 3 days. This second crop is isolated as small, colorless needles. mp 124-125°C; ¹H-NMR (400 MHz, CDCl₃) δ 7.91 (d, *J*= 8.4 Hz, 2H), 7.55 (bs, 1H), 7.34 (d, *J*= 8.4 Hz, 2H), 2.45 (s, 3H), 1.39 (s, 9H); ¹³C-NMR (100 MHz, CDCl₃) δ 149.5, 144.9, 136.2, 129.7, 128.4, 84.3, 28.1, 21.9; FTIR (thin film) $\bar{\nu}$ (max) 3250, 2981, 2934, 1745, 1348, 1147, 1089 cm⁻¹; HRMS (ESI), *m/z*: 294.0769 (M+Na⁺), calc. for C₁₂H₁₇SNO₄Na: 294.0770.

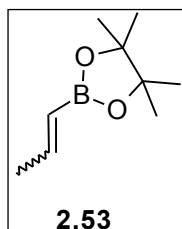
***tert*-Butoxycarbonyl-*p*-toluenesulfonamide (2.50)**



A 50-mL round bottom flask equipped with a magnetic stir bar was charged with 4-pentyn-1-ol (0.17 mL, 1.84 mmol) and THF (18.4 mL). The solution was stirred at RT as **2.49** (0.50 g, 1.84 mmol) was added, followed by PPh₃ (0.48 g, 1.84 mmol). Diisopropylazodicarboxylate (DIAD, 0.36 mL, 1.84 mmol) was added dropwise and the reaction ran at RT overnight. The reaction was then concentrated and the residue was dissolved in 4:1 hexane:EtOAc (10 mL) and stored, capped, in a freezer over 2 days. The crystallized diisopropylhydrazinedicarboxylate (white needles) was cold-filtered, and the filtrate was concentrated. The residue was purified by FCC (4:1 hexane:EtOAc) to give **2.50** as a light yellow oil (0.32 g, 51%). ¹H-NMR (400 MHz, CDCl₃) δ 7.78 (d, *J*= 8.4 Hz, 2H), .729 (d, *J*= 8 Hz, 2H), 3.79 (t, *J*= 7.6 Hz, 2H), 2.43 (s, 3H), 2.04 (s, 1H), 1.78 (q, *J*= 7.2 Hz, 2H), 1.33 (s, 9H), 0.96 (apparent t, *J*=7.2 Hz, 2H); ¹³C-NMR (100 MHz, CDCl₃) δ 151.2, 144.1, 137.8, 129.4, 128.0, 103.9, 84.1, 60.5, 48.8, 28.0, 23.6, 21.7, 11.2; FTIR (thin film) $\bar{\nu}$ (max) 2971, 2936, 2877,

1728, 1356, 1155 cm^{-1} ; HRMS (ESI), m/z : 360.1234 ($\text{M}+\text{Na}^+$), calc. for $\text{C}_{17}\text{H}_{23}\text{SNO}_4\text{Na}$:
360.1240.

***E/Z*-1-(4,4,5,5-Tetramethyl-1,3,2-dioxaboro)propene (2.53)**³⁶



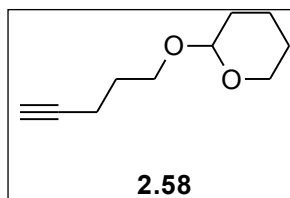
A 200-mL 2-neck round bottom flask equipped with a magnetic stir bar, addition funnel, and reflux condenser was charged with Mg turnings (1.22 g, 50.00 mmol) and THF (20 mL). This slurry was warmed to approx. 60°C, and a crystal of I_2 was added. A solution of *E/Z*-1-bromopropene (approx. 1:1 *cis:trans*, 6.00 mL, 70.00 mmol) in THF (80 mL) was added at moderate rate, over approx. 30 minutes. A light yellow color begins to develop after ~50% addition. After addition had completed, the reaction was heated to reflux until all of the Mg had reacted, about 3 hours.

A second, 500-mL round bottom flask equipped with a magnetic stir bar and an addition funnel was charged with trimethylborate (4.46 mL, 40.00 mmol) and Et_2O (10 mL). This solution was cooled to -78°C, and the warm (40-50°C) Grignard solution was transferred via cannula to the addition funnel. The solution was added warm (to prevent precipitation and clogging of the addition funnel neck), dropwise over 30 minutes. The reaction ran at -78°C for 1 hour, then was warmed to 0°C. Hydrolysis was initiated by addition of 30% HCl (70 mL) and the reaction ran for 30 minutes at 0°C, then was allowed to warm to RT. The reaction mixture was extracted with Et_2O (3 x 100 mL) and the combined organic phases were dried over Na_2SO_4 , filtered, and concentrated (bath temp $\leq 30^\circ\text{C}$) to give the crude boronic acid as a brown-yellow oil.

A 100-mL round bottom flask equipped a magnetic stir bar was charged with 4Å MS (5.00 g) and the sieves were flame-activated. After cooling to RT, Et_2O (50 mL) was added and

the reaction was charged with the crude boronic acid from the previous preparation (using some Et₂O to aid in transfer). The reaction stirred at RT while pinacol (7.09 g, 60.00 mmol) was added. The reaction ran overnight at RT, then was filtered through Celite and the filtrate was concentrated (bath temp ≤ 30°C). The orange residue was purified by FCC (9:1 pentane:Et₂O) to give **2.53** as a yellow oil (2:1 mixture of *cis:trans*, 2.93 g, 44%). ¹H-NMR (400 MHz, CDCl₃) δ *cis*: 6.52 (m, 1H), 5.34 (dt, *J*= 13.6 Hz, 3.2 Hz, 1H), 1.97 (dd, *J*= 7.2 Hz, 1.6 Hz, 3H), 1.26 (s, 12H, mixed with *trans* peak); *trans*: 6.65 (m, 1H), 5.45 (dt, *J*= 17.6 Hz, 1.6 Hz, 1H), 1.84 (dd, *J*= 6.4 Hz, 2 Hz, 3H), 1.26 (s, 12H, mixed with *cis* peak); ¹³C-NMR (100 MHz, CDCl₃) δ 149.8, 83.1, 25.0, 21.8, 18.7; FTIR (thin film) $\bar{\nu}$ (max) 2978, 2926, 2855, 1635, 1145 cm⁻¹.

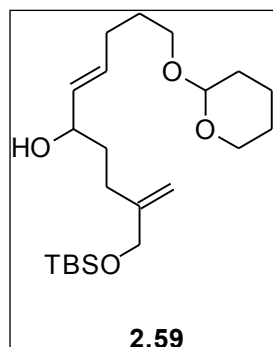
4-Pentyn-1-(tetrahydropyranyl)-ol (**2.58**)⁵⁸



A 200-mL round bottom flask equipped with a magnetic stir bar was charged with 4-pentyn-1-ol (5.53 mL, 59.44 mmol) and DCM (77.5 mL). The reaction was stirred at RT and Amberlyst-15 (0.305 g) was added in one portion. The reaction was heated to reflux and 2,3-dihydropyran (5.69 mL, 62.41 mmol) was added dropwise. The reaction stirred at reflux for 30 min, and then cooled to RT and filtered. The catalyst was washed with DCM (10 mL) and the filtrate was concentrated to give a yellow oil which was purified by FCC (9:1 hexane:Et₂O) gave **2.58** (9.915 g, 99%) as a colorless liquid. ¹H-NMR (400 MHz, CDCl₃) δ 4.60 (t, *J*=4 Hz, 1H), 3.83 (m, 2H), 3.49 (m, 2H), 2.32 (m, 2H), 1.95 (t, *J*=2.4 Hz, 1H), 1.82 (m, 3H), 1.71 (m, 1H), 1.54 (m, 4H); ¹³C-NMR (100 MHz, CDCl₃) δ 99.0, 84.2, 68.6, 66.0, 62.4, 30.8, 28.9, 25.7, 19.7, 15.5; FTIR (thin film) $\bar{\nu}$ (max) 2941, 2870, 2119 cm⁻¹; HRMS (ESI), *m/z*: 191.1051 (M+Na⁺), calc. for C₁₀H₁₆O₂Na: 191.1043.

9-[(*tert*-Butyldimethylsilyl)hydroxymethyl]-1-(tetrahydropyranyloxy)dec-4,9-dien-6-ol

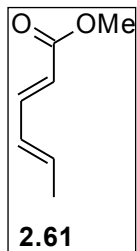
(2.59)



A 25-mL Schlenk flask equipped with a magnetic stir bar was charged with **2.58** (0.307 g, 1.825 mmol) and DCM (6.1 mL) and the reaction was purged with N₂. With stirring, the reaction was cooled to 0°C and Schwartz Reagent ([Cp₂Zr(H)Cl], 0.517 g, 2.008 mmol) was added in 5 portions over 20 minutes under a positive N₂ flow. The cloudy suspension was then warmed to RT and stirred until homogeneous (approx. 30 min. Reaction progression was checked by TLC using 4:1 hexane:EtOAc and *p*-anisaldehyde stain. The hydrozirconated product appears as a blue spot whereas the alkyne starting material appears as a red spot). The reaction was then cooled to -78°C and Me₂Zn (1.2 M in toluene, 1.76 mL) was added dropwise via syringe pump over 1 hr. The reaction was stirred at -78°C for an additional 30 min. then was warmed to 0°C and a solution of **2.43** (0.500 g, 2.19 mmol) in DCM (1.0 mL) was added via syringe pump over 1 hr. The reaction was stirred at 0°C for 6 hrs., then quenched with 5% aq. NaHCO₃ and extracted with Et₂O (3 x 10 mL, using solid NaCl to break up Zn aggregates when observed). The combined organic phases were washed with brine (10 mL), dried over Na₂SO₄, filtered, and concentrated. The crude product was purified by FCC (4:1 hexane:EtOAc, R_f= 0.25) to give **2.59** as a faintly yellow oil (0.298 g, 41%). ¹H-NMR (400 MHz, CDCl₃) δ 5.67 (dt, *J*=6.4 Hz, 15.6 Hz, 1H), 5.50 (dd, *J*=7.2 Hz, 15.6 Hz, 1H), 5.05 (s, 1H), 4.84 (s, 1H), 4.57 (t, *J*=2.4 Hz, 1H), 4.08 (s, 2H), 3.86 (m, 1H), 3.74 (m, 1H), 3.47 (m, 1H), 3.39 (m, 1H), 2.12 (m, 2H), 1.85 (m, 1H), 1.56 (m, 16H), 0.95 (s, 9H), 0.07 (s, 6H); ¹³C-NMR (100 MHz, CDCl₃) δ 148.4, 133.4, 131.7, 109.0, 99.1, 72.9, 67.0, 66.2, 62.5, 60.6, 34.7, 31.8, 29.1, 28.7, 26.1, 22.8,

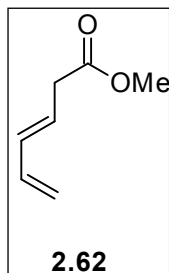
21.2, 19.9, 18.6, 14.4, 0.16, -5.2; FTIR (thin film) $\bar{\nu}$ (max) 3452, 2924, 2856, 1464, 1456 cm^{-1} ; HRMS (ESI), m/z : 421.2750 ($\text{M}+\text{Na}^+$), calc. for $\text{C}_{22}\text{H}_{42}\text{O}_4\text{SiNa}$: 421.2745.

Methyl sorbate (**2.61**)³⁸



A 500-mL round bottom flask equipped with a magnetic stir bar was charged with sorbic acid (10.00 g, 89.18 mmol) and MeOH (200 mL). The reaction was cooled to 0°C and SOCl_2 (14.31 mL, 196.20 mmol) was added dropwise. The reaction was allowed to warm to RT and then was heated to reflux for 3.5 hours. The reaction was concentrated, giving a dark red liquid which was purified by FCC (2% EtOAc in hexane) to give **2.61** as a yellow oil (9.12 g, 81%). Spectral data is consistent with the literature³⁸.

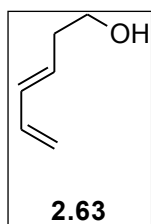
Methyl 3,5-hexadieneoate (**2.62**)⁵⁹



A 250-mL round bottom flask equipped with a magnetic stir bar was charged with diisopropylamine (6.67 mL, 47.56 mmol) and THF (80 mL). The reaction was cooled to -78°C and $n\text{BuLi}$ (2.5M in hexane, 19.02 mL, 47.56 mmol) was added slowly. HMPA (8.96 mL, 51.52 mmol) was added dropwise via addition funnel, at -78°C. The reaction ran for 30 minutes after addition, then **2.61** (5.00 g, 39.63 mmol) was added dropwise over 2 hours. The reaction ran at -78°C for an additional 1 hour, then was transferred slowly via cannula (as close to dropwise as possible) into a cooled (0°C) solution of AcOH (6.81 mL) in H_2O (150 mL). The yellow solution was extracted with pentane (3 x 50 mL) and the combined organic phases were washed with sat. aq. NaHCO_3 (50 mL), H_2O (50 mL), dried over MgSO_4 , filtered, and concentrated. Vacuum distillation (145°C bath temp, 110°C head temp) gave **2.62** as a yellow oil (2.28 g, 46%). $^1\text{H-NMR}$ (400 MHz, CDCl_3) δ 6.33 (dt,

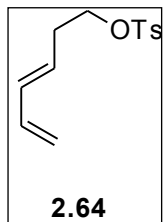
$J=6.8$ Hz, 17.2 Hz, 1H), 6.16 (m, 1H), 5.79 (m, 1H), 5.17 (dd, $J=1.6$ Hz, 16 Hz, 1H), 5.07 (dd, $J=0.4$ Hz, 10.4 Hz, 1H), 3.69 (s, 3H), 3.13 (d, $J=7.2$ Hz, 2H), 1.85 (d, $J=5.6$ Hz, 2H); ^{13}C -NMR (100 MHz, CDCl_3) δ 172.0 , 136.5 , 134.6 , 125.7 , 117.1 , 52.0 , 37.9 , 18.8 ; FTIR (thin film) $\bar{\nu}$ (max) 2952 , 2927 , 2855 , 1740 cm^{-1} ; HRMS (ESI), m/z : 127.1754 ($\text{M}+\text{H}^+$), calc. for $\text{C}_7\text{H}_{11}\text{O}_2$: 127.0754 .

3,5-Hexadiene-1-ol (**2.63**)⁵⁹



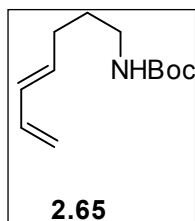
A 100 -mL round bottom flask equipped with a magnetic stir bar was charged with Et_2O (30.00 mL). The flask was cooled to 0°C and LiAlH_4 (0.527 g, 13.89 mmol) was added portionwise to the flask. The reaction was then charged with a solution of **2.62** (2.19 g, 17.36 mmol) in Et_2O (6.00 mL) dropwise. After 1 hour at 0°C , the reaction was quenched with $2:1$ $\text{THF}:\text{H}_2\text{O}$ (30 mL) followed by 1N HCl (30 mL). The product was extracted with EtOAc (2×10 mL) and the combined organic phases were washed with brine (15 mL), dried over MgSO_4 , filtered, and concentrated to give **2.63** as a yellow oil (1.70 g, quant.). ^1H -NMR (400 MHz, CDCl_3) δ 6.34 (dt, $J=10$ Hz, 17.2 Hz, 1H), 6.18 (m, 1H), 5.73 (m, 1H), 5.16 (dd, $J=1.6$ Hz, 16.8 Hz, 1H), 5.04 (dd, $J=2$ Hz, 10.4 Hz, 1H), 4.17 (d, $J=6$ Hz, 1H), 3.70 (t, $J=6$ Hz, 2H), 2.38 (q, $J=6.8$ Hz, 2H); ^{13}C -NMR (100 MHz, CDCl_3) δ 136.8 , 133.7 , 130.6 , 115.9 , 61.9 , 35.9 ; FTIR (thin film) $\bar{\nu}$ (max) 3345 , 2931 , 2878 cm^{-1} ; HRMS (ESI), m/z : 219.1352 ($2\text{M}+\text{Na}^+$), calc. for $\text{C}_{12}\text{H}_{20}\text{O}_2\text{Na}$: 219.1356 .

3,5-Hexadien-1-(*p*-toluenesulfonyl)-ol (**2.64**)



A 100-mL round bottom flask equipped with a magnetic stir bar was charged with **2.63** (1.70 g, 17.32 mmol), DCM (30 mL), NEt₃ (3.62 mL, 25.98 mmol), and DMAP (0.216 g, 1.732 mmol). The solution was cooled to 0°C and TsCl (3.63 g, 19.05 mmol) was added in portions over 10 minutes. The yellow solution was allowed to warm to RT and stir for 3 hours. The reaction was quenched by pouring into H₂O (50 mL) and the phases were separated. The organic phase was washed with sat. aq. NH₄Cl (30 mL), sat. aq. Na₂CO₃ (30 mL), dried over MgSO₄, filtered, and concentrated to give **2.64** as a brown oil (4.18 g, 96%). The material was used directly in the next step without further purification.

3,5-Hexadien-1-(*tert*-butoxycarbonyl)-amine (**2.65**)



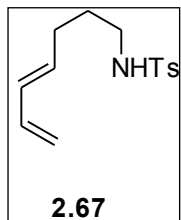
A 100-mL round bottom flask equipped with a magnetic stir bar was charged with crude **2.64** (4.18 g, 16.57 mmol) and DMSO (50 mL). With stirring, NaCN (1.22 g, 24.86 mmol) was added in one portion, with a rapid color change of orange to brown occurring. The reaction stirred at RT for 24 hours, then was diluted with H₂O (25 mL, EXOTHERMIC) and extracted with Et₂O (3 x 10 mL). The combined organic layers were washed with H₂O (60 mL), brine (60 mL), dried over Na₂SO₄, filtered, and concentrated to give the nitrile as a light orange oil (1.01 g, 57%). The material was taken forward without further purification.

A 50-mL round bottom flask equipped with a magnetic stir bar was charged with Et₂O (12.5 mL) and cooled to 0°C. LiAlH₄ (0.267 g, 6.99 mmol) was added in portions to the cooled solvent. The reaction was then charged with the crude nitrile from the previous preparation (1.01 g, 9.33 mmol) dropwise. The reaction ran at 0°C for 2 hours, then was quenched by the addition

of H₂O (1.5 mL), 15% aq. NaOH (1.5 mL), and H₂O (4.5 mL). The reaction was warmed to RT and MgSO₄ was added. The slurry was filtered and washed with Et₂O. The filtrate was concentrated to give the crude amine as a yellow oil which was taken forward without further purification.

A 200-mL round bottom flask equipped with a magnetic stir bar was charged with Boc₂O (2.36 mL, 10.26 mmol) and DCM (30 mL). The reaction was cooled to 0°C and NEt₃ (2.86 mL, 20.53 mmol) was added slowly. A solution of the crude amine from the previous preparation in DCM (30 mL) was added slowly, and the reaction was allowed to warm to RT. The reaction ran for 18 hours, then was quenched with 0.1M aq. citric acid (50 mL) and the phases were separated. The aq. phase was extracted with DCM (2 x 20 mL). The combined organic phases were washed with sat. aq. NaHCO₃ (30 mL), brine (30 mL), dried over MgSO₄, filtered, and concentrated. The orange residue was purified by FCC (4:1 hexane:EtOAc) to give **2.65** as a yellow liquid (1.40 g, 71% over two steps). ¹H-NMR (400 MHz, CDCl₃) δ 6.29 (dt, *J*= 10.4 Hz, 16.8 Hz, 1H), 6.05 (dd, *J*= 10.4 Hz, 15.2 Hz, 1H), 5.68 (dt, *J*= 6.8 Hz, 15.2 Hz, 1H), 5.08 (d, *J*=16.8 Hz, 1H), 4.96 (d, *J*= 10.4 Hz, 1H), 4.72 (bs, 1H), 3.12 (broad q, *J*= 6.8 Hz, 2H), 2.12 (apparent q, *J*= 6.8 Hz, 2H), 1.59 (m, 2H), 1.44 (s, 9H); ¹³C-NMR (100 MHz, CDCl₃) δ 146.9, 137.2, 134.1, 131.7, 115.2, 85.2, 60.4, 27.5, 21.1, 14.3; FTIR (thin film) $\bar{\nu}$ (max) 3420, 2982, 2936, 1811, 1758, 1716 cm⁻¹; HRMS (ESI), *m/z*: 234.1473 (M+Na⁺), calc. for C₁₂H₂₁O₂NNa: 234.1465.

3,5-Hexadien-1-(*para*-toluenesulfonyl)-amine (2.67)



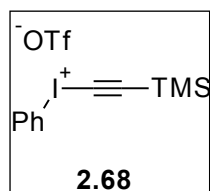
A 100-mL round bottom flask equipped with a magnetic stir bar was charged with crude **2.64** (4.63 g, 18.34 mmol) and DMSO (62 mL). With stirring, NaCN (1.35 g, 27.51 mmol) was added in one portion, with a rapid color change of orange to brown occurring. The reaction stirred at RT for 24 hours, then was diluted with H₂O (25 mL, EXOTHERMIC) and extracted with Et₂O (3 x 20 mL). The combined organic layers were washed with H₂O (60 mL), brine (60 mL), dried over Na₂SO₄, filtered, and concentrated to give the nitrile as a light orange oil (1.12 g, 57%). The material was taken forward without further purification.

A 50-mL round bottom flask equipped with a magnetic stir bar was charged with Et₂O (16 mL) and cooled to 0°C. LiAlH₄ (0.297 g, 7.84 mmol) was added in portions to the cooled solvent. The reaction was then charged with the crude nitrile from the previous preparation (1.12 g, 10.45 mmol) in Et₂O (5 mL) dropwise. The reaction ran at 0°C for 2 hours, then was quenched by the addition of H₂O (4.5 mL), 15% aq. NaOH (4.5 mL), and H₂O (4.5 mL). The reaction was warmed to RT and MgSO₄ was added. The slurry was filtered and washed with Et₂O. The filtrate was concentrated to give the crude amine as a yellow oil which was taken forward without further purification.

A 100-mL round bottom flask equipped with a magnetic stir bar was charged with the crude amine from the previous step and DCM (20 mL). Pyridine (2.54 mL, 31.35 mmol) was added and the solution was cooled to 0°C. TsCl (2.19 g, 11.50 mmol) was added slowly, with the orange solution turning deep red upon addition. After 24 hrs, the reaction was quenched with H₂O (20 mL) and extracted with Et₂O (3 x 20 mL). The combined organic phases were washed with brine (20 mL), dried over MgSO₄, filtered, and concentrated. The orange residue was

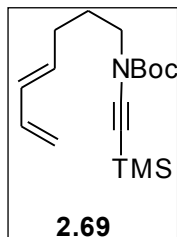
purified by FCC (10% EtOAc in hexanes → 15% EtOAc in hexanes) to give **2.67** as an orange oil (0.53 g, 19% over two steps). ¹H-NMR (400 MHz, CDCl₃) δ 7.72 (d, *J*=7.2 Hz, 2H), 7.26 (d, *J*=8 Hz, 2H), 6.21 (dt, *J*=16.8 Hz, 10.4 Hz, 1H), 5.94 (ddd, *J*=15.2 Hz, 10.4 Hz, 0.4 Hz, 1H), 5.23 (dt, *J*=14.4 Hz, 6.8 Hz, 1H), 5.03 (d, *J*=16.8 Hz, 1H), 4.92 (d, *J*=10.4 Hz, 1H), 4.90 (bs, 1H), 2.90 (q, *J*=6.8 Hz, 2H), 2.39 (s, 3H), 2.03 (q, *J*=7.2 Hz, 2H), 1.53 (p, *J*=7.2 Hz, 2H); ¹³C-NMR (100 MHz, CDCl₃) δ 143.5, 137.2, 137.1, 133.5, 132.1, 129.9, 127.3, 115.6, 42.8, 29.6, 29.2, 21.7; FTIR (thin film) $\bar{\nu}$ (max) 3284, 2931, 1326, 1159 cm⁻¹; HRMS (ESI), *m/z*: 288.1028 (M+Na⁺), calc. for C₁₄H₁₉O₂NSNa: 288.1029.

(2-Trimethylsilylethynyl)iodosobenzene triflate (2.68)⁶⁰



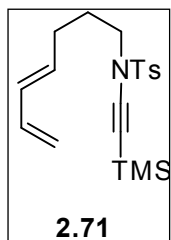
A 100-mL round bottom flask equipped with a magnetic stir bar was charged with PhI(OAc)₂ (8.05 g, 25.0 mmol) and DCM (25 mL). The reaction mixture was cooled to 0°C and set to stir, under N₂. Triflic anhydride (2.10 mL, 12.5 mmol) was added dropwise, resulting in a yellow slurry. The reaction was stirred for 30 min, then bis(trimethylsilyl)acetylene (5.66 mL, 25.0 mmol) was added dropwise, resulting in a homogeneous solution. After 2 hrs at 0°C, the reaction mixture was concentrated to a white paste and triturated with Et₂O. The white crystalline solid thus obtained was filtered and dried *in vacuo* to give **2.68** as white crystals (8.01 g, 71%). All melting point and spectral data are consistent with the literature.

3,5-Hexadien-1-(*tert*-butoxycarbonyl)-1-(2-trimethylsilylethyln)-amine (**2.69**)



A 25-mL round bottom flask equipped with a magnetic stir bar was charged with **2.65** (0.20 g, 0.947 mmol) and toluene (9.23 mL). The reaction was cooled to 0°C and KHMDS (0.91 M in THF, 1.26 mL, 1.14 mmol) was added dropwise, resulting in an orange solution. The reaction was stirred for 30 min, then **2.68** (0.256 g, 0.568 mmol) was added in small portions over 5 minutes. The reaction was allowed to warm to RT and stirred for 24 hrs. The reaction was then filtered through a plug of Si-gel using 1:1 Petroleum Ether:Et₂O as eluent. The filtrate was concentrated and the residue was purified by FCC (9:1 Petroleum Ether:Et₂O) to give **2.69** as an orange oil (0.060 g, 34%). ¹H-NMR (400 MHz, CDCl₃) δ 6.27 (dt, *J*=16.8 Hz, 10.4 Hz, 1H), 6.04 (ddd, *J*=14.4 Hz, 10.4 Hz, 0.8 Hz, 1H), 5.67 (dt, *J*=14.4 Hz, 6.8 Hz, 1H), 5.06 (d, *J*=16.4 Hz, 1H), 4.94 (d, *J*=10 Hz, 1H), 3.54 (t, *J*=7.6 Hz, 2H), 2.07 (q, *J*=7.2 Hz, 2H), 1.65 (t, *J*=2 Hz, 2H), 1.47 (s, 9H), 0.16 (s, 9H); ¹³C-NMR (100 MHz, CDCl₃) δ 152.8, 137.7, 134.3, 130.4, 127.6, 115.3, 82.3, 58.1, 46.3, 30.0, 28.6, 28.3, -0.3; FTIR (thin film) $\bar{\nu}$ (max) 2968, 2068, 1747, 1696, 1367, 1251, 1135, 884 cm⁻¹; HRMS (ESI), *m/z*: 330.1247 (M+Na⁺), calc. for C₁₇H₂₉O₂NSiNa: 330.1238.

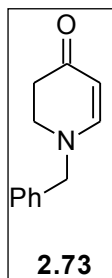
3,5-Hexadien-1-(*para*-toluenesulfonyl)-1-(2-trimethylsilylethyln)-amine (**2.71**)



The title compound was prepared as described for **2.69**, using **2.67** (0.20 g, 0.754 mmol), toluene (9.23 mL), KHMDS (0.91M in THF, 0.994 mL, 0.904 mmol), and **2.68** (0.204 g, 0.452 mmol). FCC (9:1 Petroleum Ether:Et₂O) gave **2.71** as an orange oil (0.056 g, 34%). ¹H-NMR (400 MHz, CDCl₃) δ 7.73 (d, *J*=8.4 Hz, 2H), 7.31 (d, *J*=8 Hz, 2H), 6.27 (dt, *J*=20.4 Hz, 10 Hz, 1H), 6.03 (ddd, *J*=15.2 Hz, 10.4 Hz, 0.8 Hz, 1H), 5.61 (dt, *J*=14.4 Hz, 6.8 Hz, 1H), 5.07 (d, *J*=16.8 Hz, 1H), 4.96 (d, *J*=10 Hz, 1H), 3.28 (t,

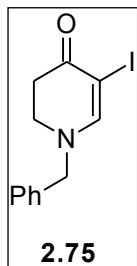
$J=7.2$ Hz, 2H), 2.43 (s, 3H), 2.09 (apparent q, $J=6.4$ Hz, 2H), 1.71 (apparent p, $J=7.2$ Hz, 2H), 0.13 (s, 9H); ^{13}C -NMR (100 MHz, CDCl_3) δ 205.0, 144.8, 137.7, 137.2, 133.4, 132.2, 130.4, 129.8, 128.0, 115.6, 50.9, 29.3, 27.6, 21.8, 0.3; FTIR (thin film) $\bar{\nu}$ (max) 2955, 2162, 1368, 1171, 844 cm^{-1} ; HRMS (ESI), m/z : 384.1435 ($\text{M}+\text{Na}^+$), calc. for $\text{C}_{19}\text{H}_{27}\text{O}_2\text{NSSiNa}$: 384.1424.

1-Benzyl-2,3-dihydro-4-pyridone (**2.73**)⁴⁶



A 250-mL round bottom flask equipped with a magnetic stir bar was charged with 1-benzyl-4-piperidone (1.00 mL, 5.39 mmol) and $\text{H}_2\text{O}:\text{EtOH}$ (2:1, 120 mL). With stirring at RT, $\text{Hg}(\text{OAc})_2$ (1.80 g, 5.66 mmol) was added in one portion and the solution became yellow and opaque immediately. EDTA (1.65 g, 5.66 mmol) was added in one portion and the reaction was heated to 80°C for 3 hours. The reaction was then cooled and the metallic Hg generated was filtered through Celite, washing with 2:1 $\text{H}_2\text{O}:\text{EtOH}$. The filtrate was diluted with sat. aq. NH_4Cl (50 mL) and extracted with DCM (3 x 30 mL). The combined organic phases were washed with H_2O (50 mL), brine (50 mL), dried over Na_2SO_4 , filtered, and concentrated to give **2.73** as an orange oil (0.50 g, 50%). ^1H -NMR (400 MHz, CDCl_3) δ 7.36 (m, 3H), 7.26 (m, 2H), 7.16 (d, $J=7.2$ Hz, 1H), 4.99 (d, $J=7.2$ Hz, 1H), 4.35 (s, 2H), 3.37 (t, $J=7.6$ Hz, 2H), 2.45 (t, $J=8$ Hz, 2H); ^{13}C -NMR (100 MHz, CDCl_3) δ 191.7, 154.5, 135.9, 129.2, 128.6, 127.8, 98.6, 60.0, 46.9, 35.7; FTIR (thin film) $\bar{\nu}$ (max) 3029, 2960, 1631, 1591 cm^{-1} ; HRMS (ESI), m/z : 188.1071 ($\text{M}+\text{H}^+$), calc. for $\text{C}_{12}\text{H}_{14}\text{ON}$: 188.1070.

1-Benzyl-3-iodo-5,6-dihydro-4-pyridone (**2.75**)⁴⁷



A 50-mL round bottom flask equipped with a magnetic stir bar was charged with **2.73** (0.10 g, 0.53 mmol), DMAP (0.13 g, 1.06 mmol), and DCM (12 mL). The reaction was wrapped in foil and set to stir at RT. A slurry of I₂ (0.16 g, 0.64 mmol) in DCM (5 mL) was added to the reaction, using additional DCM to ensure all I₂ crystals were transferred. The reaction was stirred for 18 hours, then was quenched by the addition of H₂O (10 mL). The phases were separated and the aq. phase was extracted with DCM (2 x 10 mL). The combined organic phases were washed with sat. aq. NH₄Cl (10 mL), H₂O (10 mL), sat. aq. Na₂S₂O₃ (10 mL), brine (10 mL), dried over Na₂SO₄, filtered, and concentrated. The residue was purified by FCC (1% NEt₃ in EtOAc) using a column pre-treated with the same eluent to give **2.75** as a yellow oil (0.15 g, 91%). ¹H-NMR (400 MHz, CDCl₃) δ 7.67 (s, 1H), 7.39 (m, 3H), 7.27 (m, 2H), 4.43 (s, 2H), 3.50 (t, *J* = 7.6 Hz, 2H), 2.66 (t, *J* = 7.6 Hz, 2H); ¹³C-NMR (100 MHz, CDCl₃) δ 185.3, 158.8, 135.2, 129.4, 128.9, 127.9, 60.1, 47.0, 34.7; FTIR (thin film) $\bar{\nu}$ (max) 3030, 2910, 1628, 1570 cm⁻¹; HRMS (ESI), *m/z*: 335.9861 (M+Na⁺), calc. for C₁₂H₁₂ONiNa: 335.9856.

2.8. References

- ¹ Ma, X., Gang, D.; *Nat. Prod. Rep.*, **2004**, *21*, 752-772.
- ² Besselièvre, M., Beugelmans, R., Husson, H. P.; *Tetrahedron Lett.*, **1976**, *38*, 3447-3450.
- ³ Heathcock, C., Kleinman, E., Binkley, E.; *J. Am. Chem. Soc.*, **1978**, *100*, 8036-8037.
- ⁴ Kin, S-W., Bando, Y., Takahashi, N., Horii, Z-I.; *Chem. Pharm. Bull.*, **1978**, *26*, 3150-3153.
- ⁵ Grieco, P., Dai, Y.; *J. Am. Chem. Soc.*, **1998**, *120*, 5128-5129.
- ⁶ Yang, H., Carter, R., Zakharov, L.; *J. Am. Chem. Soc.*, **2008**, *130*, 9238-9239; Yang, H., Carter, R.; *J. Org. Chem.*, **2010**, *75*, 4929-4938.
- ⁷ Yang, Y-F., Qu, S-J., Xiao, K., Jiang, S-H., Tan, J-J., Tan, C-H., Zhu, D-Y.; *J. Asian Nat. Prod. Res.*, **2010**, *12*, 1005-1009.
- ⁸ Witulski, B., Lumtscher, J., Bergsträßer, U.; *Synlett*, **2003**, No. 5, 708-710.

- ⁹ Witulski, B., Alayrac, C.; *Angew. Chem. Int. Ed.*, **2002**, *41*, 3281-3284; Witulski, B., Stengel, T.; *Angew. Chem. Int. Ed.*, **1999**, *38*, 2426-2430; Witulski, B., Gößmann, M.; *Chem. Commun.*, **1999**, 1879-1880.
- ¹⁰ Urata, H., Suzuki, H., Moro-oka, Y., Ikawa, T.; *Bull. Chem. Soc. Jpn.*, **1984**, *57*, 607-608.
- ¹¹ Tzeng, D., Weber, W.; *J. Org. Chem.*, **1981**, *46*, 265-267.
- ¹² Kohnen, A., Dunetz, J., Danheiser, R.; *Org. Synth.*, **2007**, *84*, p. 88.
- ¹³ Zhang, Y., Hsung, R., Tracey, M., Kurtz, K., Vera, E.; *Org. Lett.*, **2004**, *6*, 1151-1154.
- ¹⁴ Hamada, T., Ye, X., Stahl, S.; *J. Am. Chem. Soc.*, **2008**, *130*, 833-835.
- ¹⁵ Palucki, B.; Ph.D thesis under Danheiser, R.; **1997**, Massachusetts Institute of Technology, Boston, MA.
- ¹⁶ Chatterjee, A., Choi, T., Sanders, D., Grubbs, R., *J. Am. Chem. Soc.*, **2003**, *125*, 11360-11370.
- ¹⁷ Louge, M., Teng, K.; *J. Org. Chem.*, **1982**, *47*, 2549-2553.
- ¹⁸ Schmid, W., Klaps, E.; *J. Org. Chem.*, **1999**, *64*, 7537-7546; Yamamoto, Y., Fujiwara, N.; *J. Org. Chem.*, **1999**, *64*, 4095-4101; Kim, S., Lee, H., Kim, K., Kim, S., Kim, J.; *Tetrahedron*, **2010**, *66*, 7065-7076.
- ¹⁹ Fourgeaud, P., Midrier, C., Vors, J-P., Volle, J-P., Pirat, J-L., Virieux, D.; *Tetrahedron*, **2010**, *66*, 758-764.
- ²⁰ Tsui, G., Lautens, M.; *Angew. Chem. Int. Ed.*, **2010**, *49*, 8938-8941.
- ²¹ He, A., Yan, B., Thanavaro, A., Spilling, C., Rath, N.; *J. Org. Chem.*, **2004**, *69*, 8643-8651.
- ²² Clark, J., Griffiths, J., Diver, S.; *J. Am. Chem. Soc.*, **2013**, *135*, 3327-3330.
- ²³ **3.37** was synthesized from the bis-bromide by the procedure used for the mono-sulfone. The bis-bromide was synthesized according to the procedure of Musilek, K., Holas, O., Kuka, K., Jun, D., Dohnal, V., Opletalova, V., Dolezal, M.; *Bioorg. Med. Chem. Lett.*, **2007**, *17*, 3172-3176.
- ²⁴ For examples, see: Stivala, C., Gu, Z., Smith, L., Zakarian, A.; *Org. Lett.*, **2012**, *14*, 804-807; Venukadasula, P., Chegondi, R., Suryan, G., Hanson, P.; *Org. Lett.*, **2012**, *14*, 2634-2637.
- ²⁵ Vougioukalakis, G.; *Chem. Eur. J.*, **2012**, *18*, 8868-8880.
- ²⁶ BouzBouz, S., Simmons, R., Cossy, J.; *Org. Lett.*, **2004**, *6*, 3465-3467.
- ²⁷ Basavaiah, D., Reddy, B., Badsara, S.; *Chem. Rev.*, **2010**, *110*, 5447-5674.
- ²⁸ Nakamura, A., Tokunaga, M.; *Tett. Lett.*, **2008**, *49*, 3729-3732.
- ²⁹ Gupta, M., Paul, S., Gupta, R.; *Acta. Chim. Slov.*, **2009**, *56*, 749-764.
- ³⁰ Marcé, P., Díaz, Y., Matheu, I., Castellón, S.; *Org. Lett.*, **2008**, *10*, 4735-4738.
- ³¹ See: Katoh, T., Tanaka, R., Takeo, M., Nishide, K., Node, M.; *Chem Pharm. Bull.*, **2002**, *50*, 1625-1629; McMurry, J., Scott, W.; *Tett. Lett.*, **1983**, *24*, 979-982; Pandey, S., Greene, A., Poisson, J-F.; *J. Org. Chem.*, **2007**, *72*, 7769-7770.
- ³² Baraznenok, I., Nenajdenko, V., Balenkova, E.; *Tetrahedron*, **2000**, *56*, 3077-3119.
- ³³ Schomaker, J., Geiser, A., Huang, R., Borhan, B.; *J. Am. Chem. Soc.*, **2007**, *129*, 3794-3795.
- ³⁴ Xu, S., Lee, C-T., Rao, H., Negishi, E-I; *Adv. Synth. Catal.*, **2011**, *353*, 2981-2987.
- ³⁵ Kalinin, A., Scherer, S., Snieckus, V.; *Angew. Chem. Int. Ed.*, **2003**, *42*, 3399-3404.
- ³⁶ Morrill, C., Grubbs, R.; *J. Org. Chem.*, **2003**, *68*, 6031-6034.
- ³⁷ Takai, K., Nitta, K., Utimoto, K.; *J. Am. Chem. Soc.*, **1986**, *108*, 7408-7410; Andrus, M., Lepore, S., Turner, T.; *J. Am. Chem. Soc.*, **1997**, *119*, 12159-12169.
- ³⁸ Maeta, H., Hashimoto, T., Hasegawa, T., Suzuki, K.; *Tet. Lett.*, **1992**, *33*, 5965-5968.
- ³⁹ Wipf, P., Jahn, H.; *Tetrahedron*, **1996**, *52*, 12853-12910.

- ⁴⁰ Kitahara, T., Matsuoka, T., Kiyota, H., Warita, Y., Kutara, Y., Horiguchi, A., Mori, K.; *Synthesis*, **1994**, 692-694.
- ⁴¹ Lewis, F., Howard, D., Barancyk, S., Oxman, J.; *J. Am. Chem. Soc.*, **1986**, *108*, 3016-3023.
- ⁴² Kimura, M., Ezoe, A., Mori, M., Tamaru, Y.; *J. Am. Chem. Soc.*, **2005**, *127*, 201-209.
- ⁴³ Grieco, P., Galatsis, P., Spohn, R.; *Tetrahedron*, **1986**, *42*, 2847-2853.
- ⁴⁴ Kitamura, T., Zheng, L., Taniguchi, H.; *Tetrahedron Lett.*, **1993**, *34*, 4055-4058.
- ⁴⁵ Dempsey Hyatt, I., Croatt, M.; *Angew. Chem. Int. Ed.*, **2012**, *51*, 7511-7514.
- ⁴⁶ Flick, A., Padwa, A.; *Tet. Lett.*, **2008**, *49*, 5739-5741.
- ⁴⁷ Wang, X., Turunen, B., Leighty, M., Georg, G.; *Tetrahedron Lett.*, **2007**, *48*, 8811-8814.
- ⁴⁸ Luzung, M., Patel, J., Yin, J.; *J. Org. Chem.*, **2010**, *75*, 8330-8332.
- ⁴⁹ Šebesta, R., Pizzuti, M., Boersma, A., Minnaard, A., Feringa, B.; *Chem. Commun.*, **2005**, 1711-1713.
- ⁵⁰ Leroy, J.; *Org. Synth.*, **1998**, *Coll. Vol. 9*, 129.
- ⁵¹ Clasby, M., Craig, D., Slawin, A., White, A., Williams, D.; *Tetrahedron*, **1995**, *51*, 1509-1532.
- ⁵² White, J., Lincoln, C., Yang, J., Martin, W., Chan, D.; *J. Org. Chem.*, **2008**, *73*, 4139-4150.
- ⁵³ Schmid, W., Klaps, E.; *J. Org. Chem.*, **1999**, *64*, 7537-7546.
- ⁵⁴ Dappen, M., Pellicciari, R., Natalini, B., Monhan, J., Chiorri, C., Cordi, A.; *J. Med. Chem.*, **1991**, *34*, 161-168.
- ⁵⁵ Tsui, G., Lautens, M.; *Angew. Chem. Int. Ed.*, **2010**, *49*, 8938-8941.
- ⁵⁶ Crimmins, M., Jacobs, D.; *Org. Lett.*, **2009**, *11*, 2695-2698.
- ⁵⁷ Neustadt, B.; *Tet. Lett.*, **1994**, *35*, 379-380.
- ⁵⁸ Heitz, M-P., Wagner, A., Mioskowski, C.; *J. Org. Chem.*, **1989**, *54*, 500-503.
- ⁵⁹ Kimura, M., Ezoe, A., Mori, M., Tamaru, Y.; *J. Am. Chem. Soc.*, **2005**, *127*, 201-209.
- ⁶⁰ Kitamura, T.; *Synthesis*, **1998**, 1416-1418.

CHAPTER 3. ATTEMPTED TOTAL SYNTHESIS OF (+)-(*R*)-MYRICANOL

3.1. Introduction

In the pathology of AD, one of the hallmarks is the inability of neurotransmitters to migrate from one neuron to another. The facilitation of this movement is made possible by microtubules formed through tau protein-stabilized architecture. Tau protein binds to the various proteins involved in microtubule formation, and allows for the system to be structurally sound¹. In AD, tau protein tends to favor self-aggregation, very much like A β 1-42. When aggregated, tau protein is unable to stabilize these neurological microtubules, and the transmission of neurologically active molecules shuts down, leading to lapses in various functions of the brain, including memory, movement, and involuntary muscle control.

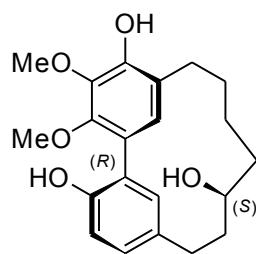
As previously discussed, AD and other neurological disorders are difficult to combat due to lack of fundamental understanding of mechanistic pathways with which pharmaceuticals can be attenuated. The tau protein aggregation pathway presents an alternative therapeutic target to the more traditional BACE-1 inhibitors or the direct A β aggregation diffusers. In addition to compounds which could feasibly prevent tau protein from aggregating, it may also be possible to “tag” advanced tau intermediates for clearance by proteases. This would not only enable direct targeting of tau intermediates which have not been shown to be beneficial at all, but would also allow for the body’s own defenses to naturally clear problematic protein tangles. Presumably, this would lead to lower compound toxicity, as the compound is essentially a suicide molecule used to label the destructive tau aggregate.

3.2. Tau Protein Aggregation Inhibitors

The tau protein contains a binding domain near the C-terminus for binding to the microtubule proteins. This binding domain is exposed in biologically active tau due to conformational configurations based around a repeat series of Ser/Thr, which are generally located next to a Pro residue². Nitrogen-dependant kinases phosphorylate these residues, causing conformational changes which expose alternative binding sites which favor homoprotein interactions over tau/microtubule interactions. It is thought that tau hyperphosphorylation is responsible for this, but that normal, regulated phosphorylation is necessary for functionality of the tau protein. Thus, it is difficult to find the “right balance” in the blocking of phosphorylation either by kinase inhibition or phosphatase activation.

3.3. (+)-*R*-Myricanol

Recently, researchers have found that extracts from the Bayberry root-bark promote tau aggregate clearance in biological assays³. Known compounds which were found in Bayberry that had tau clearance properties did not match to the observed levels, and it was eventually found that a diarylheptanoid, (+)-*aR*,11*S*-myricanol (Figure 3.1) was responsible for the activity. Interestingly enough, although the authors confirmed the structure by NMR comparisons, the optical rotation of the compound is opposite to the published value, suggesting that the enantiomer of the previously reported compound may be responsible.



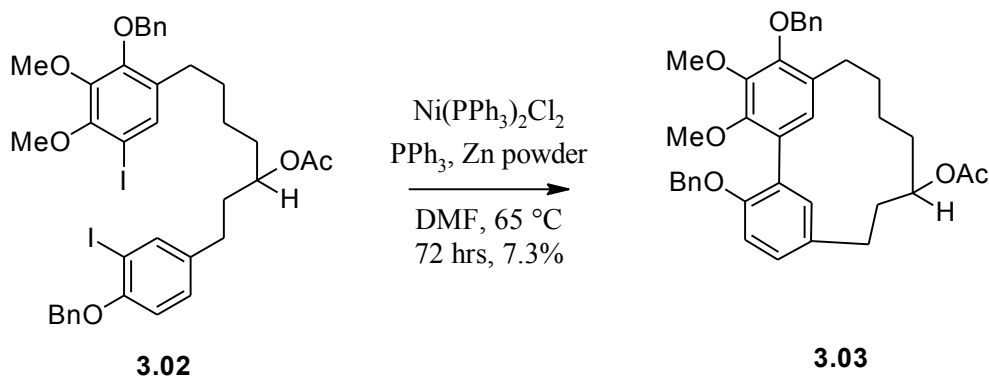
(aR,S)-3.01

Figure 3.1: Structure of the diarylheptanoid (+)-aR,11S-myricanol

This natural product has many interesting features aside from its beneficial biological activity. It is a diarylheptanoid, meaning that it possesses axial chirality, which is not seen as often in the pharmaceutical industry (the most notable exception being vancomycin). In addition, it possesses a chiral 2° alcohol on the carbocyclic side chain. The highly oxygenated ring structure of **3.01** also shares many similarities with compounds used as antioxidants. Reactive Oxygen Species (ROS), as described earlier, are implicated in many neurodegenerative disorders. Due to all of these interesting structural and biological features, we decided to undertake the total synthesis of **3.01**, keeping in touch with our goal of studying the synthetic approaches to anti-AD compounds.

3.4. Previous Approaches Towards Myricanol-Like Molecules

Reviewing the literature surrounding the diarylheptanoid family of myricanol, it was found that there are a number of potential methods for developing a racemic synthesis. Whiting and Wood developed a diastereoselective synthesis based on a Ni(0)-mediated oxidative coupling procedure of the electron rich aromatic rings of **3.02** (Scheme 3.1)⁴.



Scheme 3.1: Oxidative coupling of bisiodide **3.02** giving protected (\pm)-myricanol **3.03**

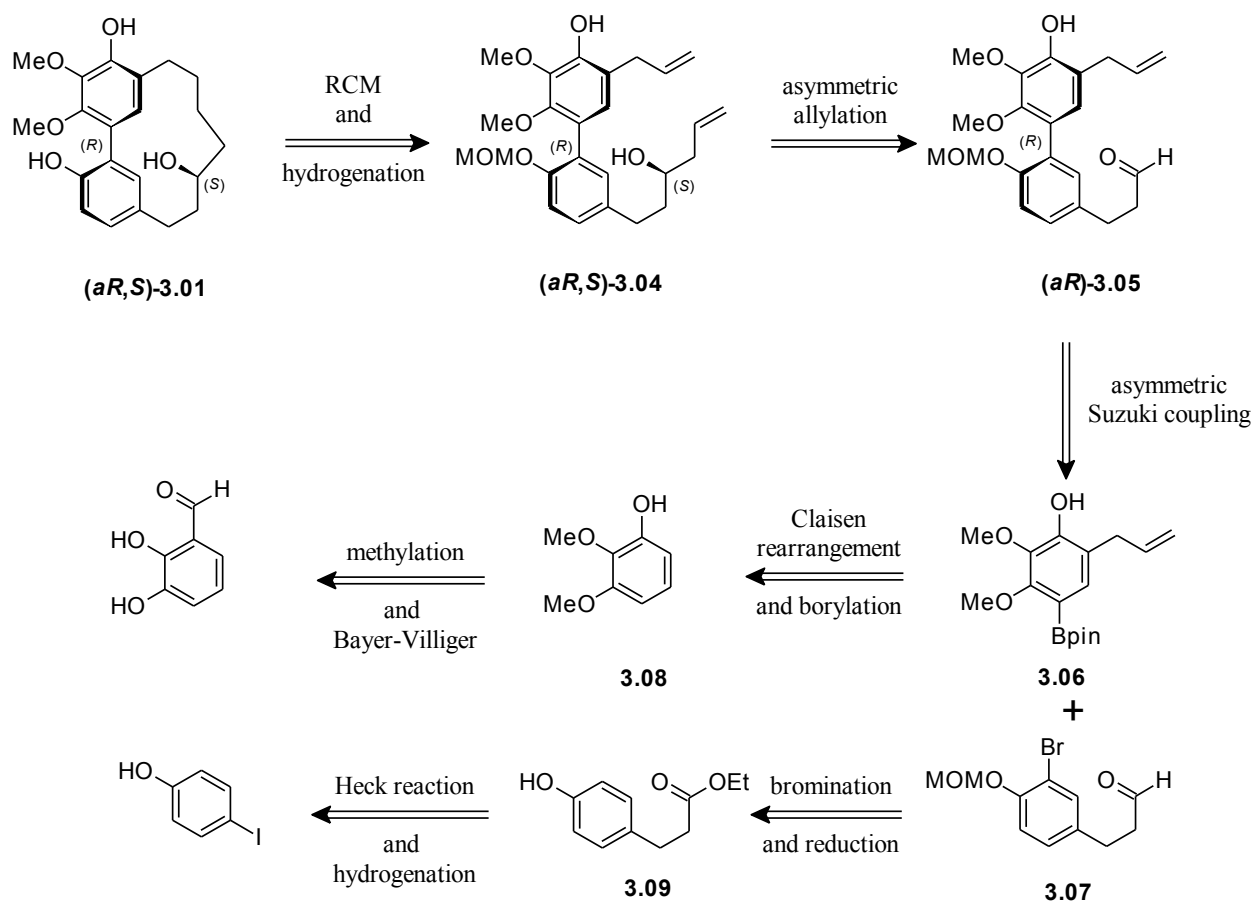
Although this procedure is quite low yielding, it shows that coupling protocols are approachable avenues for construction of the biaryl moiety. In fact, **3.03** is only the protected form of the racemic natural product. The initial isolation paper stated that the natural samples are generally racemic (only approx. 3% *ee*), but the active sample was scalemic (approx 86% *ee*). Generally speaking, this indicates a need for enantiocontrol over the formation of the biaryl functionality, as rotation about the joining bond would undermine resultant *ee* values, and thus erode the biological activity.

3.5. Retrosynthetic Analysis

Our approach to the retrosynthesis of (*R*)-myricanol (**3.01**) was to synthesize the carbocyclic, 13-membered ring lastly, using the now commonplace RCM reaction, giving **3.04**. The *cis* vs *trans* issue sometimes encountered by these reactions would be of little concern, as we would simply hydrogenate the product to get the saturated ring system. The southern metathesis partner could come from an asymmetric allylation of the parent aldehyde (**3.05**). It is our thought that the distance between the axially chiral biaryl moiety and the more mobile, freely rotating aldehyde would be too great to impart a great deal of stereochemical information.

However, using the biaryl group as a potential alignment tool for an asymmetric ligand (through π -stacking, most likely), may allow us to use the In(0)-mediated allylation that the Cook group has focused much of their research efforts. As a corollary to that promising idea, we would have to screen different ligands, because it is possible that the PhPyBOX ligand system we have developed (see Chapter 4) will not be as effective for the more flexible aliphatic aldehyde as it was for the more rigid isatin nucleus. It has been shown that simple amino alcohols can provide effective ligand control for these types of reactions⁵.

From the relatively less complex **3.05** we can envision an asymmetric Suzuki coupling, which has been shown to be effective for the synthesis of biaryl systems⁶. This provides aryl boronate **3.06** and aryl bromide **3.07**. The borylation can be made from the bromide, and the bromide may be installed from the bis-protected triphenol **3.08**. Installation of the allyl group to the *ortho* position must be accomplished prior to the installation of the bromine, otherwise there will be selectivity issues between *ortho* and *para* bromination, both of which are highly favorable due to the high electron density of the ring. Thankfully, this is easily accomplished through a Claisen rearrangement from the *O*-allyl ether. Triphenol **3.08** can be synthesized from 2,3-dihydroxybenzaldehyde, using a Bayer-Villiger oxidation followed by hydrolysis of the formate ester. Aryl bromide **3.07** can be synthesized from the aliphatic ester through electrophilic bromination and DIBAL-H reduction, giving **3.09**, which can easily be synthesized from 4-iodophenol through a Heck reaction/hydrogenation sequence (Scheme 3.2).

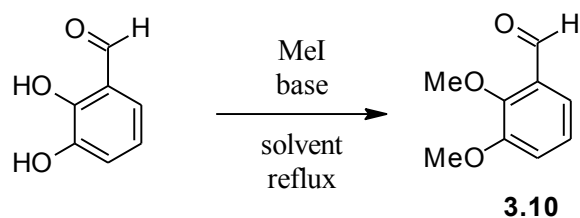


Scheme 3.2: Retrosynthetic analysis of myricanol

3.6. Forward Synthesis

Our convergent synthetic approach began with our attempt to synthesize aryl boronate **3.06**. We initially subjected 2,3-dihydroxybenzaldehyde to dimethylation using various protocols (Table 3.1). Our attempt was to optimize the first step to give us the most reliable yield and purity for the subsequent oxidation step.

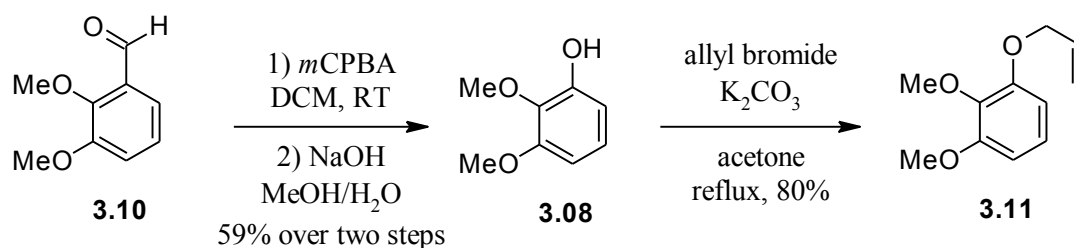
Table 3.1: Optimization of dimethylation reaction



Entry	Solvent	Base	Yield (%) ^a
1	DMF	K ₂ CO ₃	64
2	DMF	Cs ₂ CO ₃	59
3	Acetone	K ₂ CO ₃	25
4	Acetone	Cs ₂ CO ₃	0

^a: isolated yield, reactions run for 24 hrs.

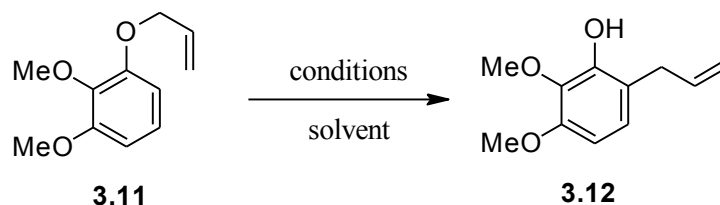
Using K₂CO₃ in DMF⁷, we were able to isolate the product as a white crystalline solid reproducibly. Acetone proved to be an inferior solvent under all circumstances for this reaction. This is most likely due to limited solubility of the base during the reaction. Bayer-Villiger oxidation of **3.10** with *m*CPBA and hydrolysis of the formate ester using NaOH in MeOH/H₂O gave the bis-protected triphenol **3.08**⁸. Alternatively, hydrolysis using more conventional LiOH produces similar results, but reproducibility varied based on the initial moisture content of the LiOH used. NaOH was far more consistent, even when an old bottle was used. Alkylation using allyl bromide as an electrophile proceeded smoothly using K₂CO₃/acetone to provide the allyl phenyl ether **3.11** (Scheme 3.3).



Scheme 3.3: *Synthesis of allyl phenyl ether 3.11*

We then turned our attention to the Claisen rearrangement of **3.11** to *ortho*-allyl phenol **3.12**. We attempted both a thermal and a microwave series of reactions, utilizing different solvents, as well as various additives (Table 3.2)⁹. Unfortunately, none of the reactions gave us any appreciable (>5%) yield. We suspect that the aromatic ring is too electron rich to participate in the rearrangement, since the small methoxy groups should not be sterically significant enough to interfere. We also never observed *para* rearrangement, which is sometimes possible if the *ortho* position is blocked¹⁰. There is little literature evidence to suggest possible reasons for the inability of **3.11** to undergo the Claisen rearrangement as written. A variety of solvents were screened, all showing no product formation, and in most cases no loss of starting material. Microwaves have been used to accelerate these reactions¹¹, and an application of this methodology did not provide any change to the initial results (Table 3.2, Entries 4 and 7). Lewis acid catalysts may also accelerate the Claisen rearrangement in certain cases¹², and efforts to use these also produced none of the desired product (Table 3.2, Entries 8 and 9). Finally, water is also a potential accelerant due to its ability to form hydrogen-bond networks with the substrate, encouraging conformations which promote rearrangement. However, even water (Table 3.2, Entry 7) could not produce the desired results.

Table 3.2: Attempted [3,3]-sigmatropic rearrangement of **3.11**



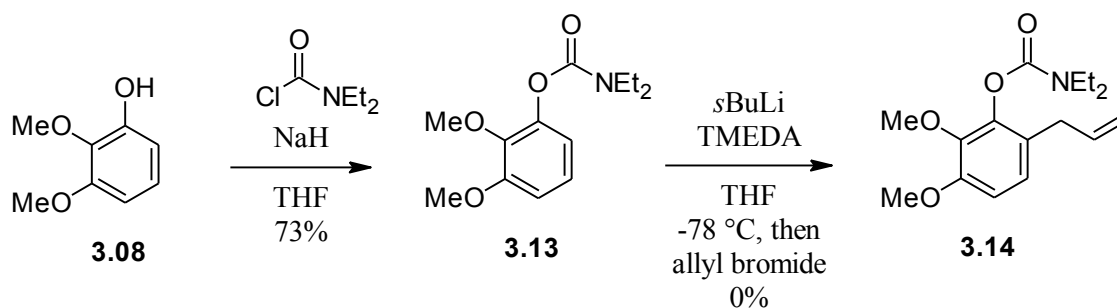
Entry	Conditions ^a	Solvent (temp)	Additive
1	A	toluene (80 °C)	none
2	A	toluene (reflux)	none
3	B	toluene (150 °C)	none
4	C	toluene (175°C)	none
5	A	<i>N,N</i> -diethylaniline (reflux)	none
6	B	<i>N,N</i> -diethylaniline (250 °C)	none
7	C	toluene (175 °C)	H ₂ O (3 eq.)
8	A	toluene (reflux)	BiCl ₃ (1.5 eq.)
9	A	<i>N,N</i> -diethylaniline (reflux)	BiCl ₃ (1.5 eq.)

Note: All reactions yielded no product, and were run for 24 hrs (thermal) or 6 hrs (μW)

^a: (A) thermal, traditional glassware; (B) thermal, sealed tube; (C) 150W μW

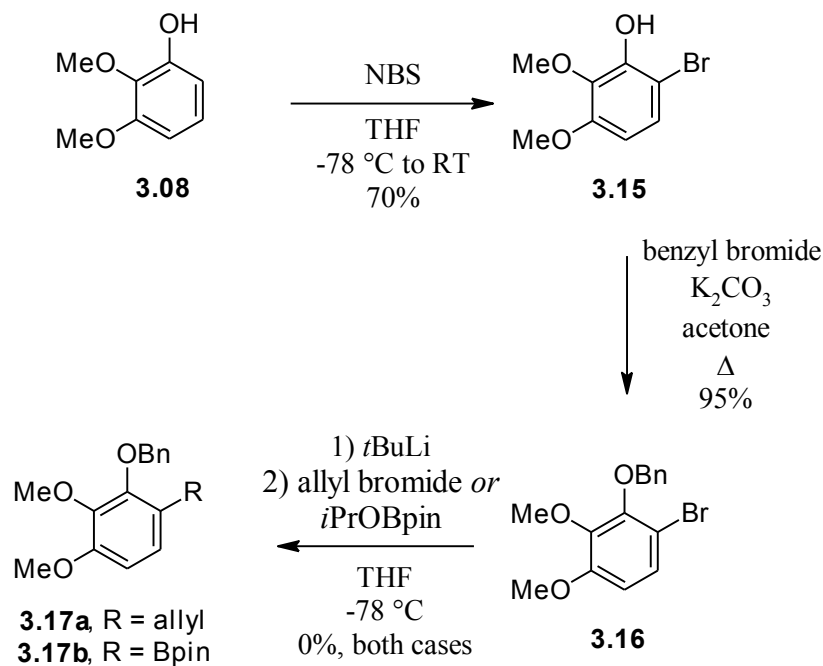
Since the Claisen rearrangement was unsuccessful, we next attempted to use an installed carbamate (**3.13**) to utilize Directed *ortho* Metalation (DoM)¹³. Unfortunately, the electron-rich nature of the substrate proved too much to overcome, and the metalation never occurred. Quantitative recovery of the starting carbamate was observed in all cases (Scheme 3.4). The large increase in electron density of the *ortho* position due to the deprotonation event leads to an increase in overall electron density of the ring current, which is already increased by the presence of the three phenolic groups. Additional electron density cannot therefore be accepted

into the ring current, and metalation does not occur. Modification of the initial DoM protocols using *t*BuLi did not produce any metalation either. Quenching of the reaction mixture with D₂O did not produce an *ortho* deuterium, supporting the observation that metalation is not occurring. In addition to these efforts, the series of butyl lithium reagents (*n*BuLi, *s*BuLi, *t*BuLi) were all screened in conjunction with TMEDA, *N,N,N',N'*-tetramethylpropyldiamine, and 12-crown-4 for deaggregation of the lithium species. None of these additives had any effect on the outcome of the reaction.



Scheme 3.4: Attempted DoM to install the C-6 allyl group

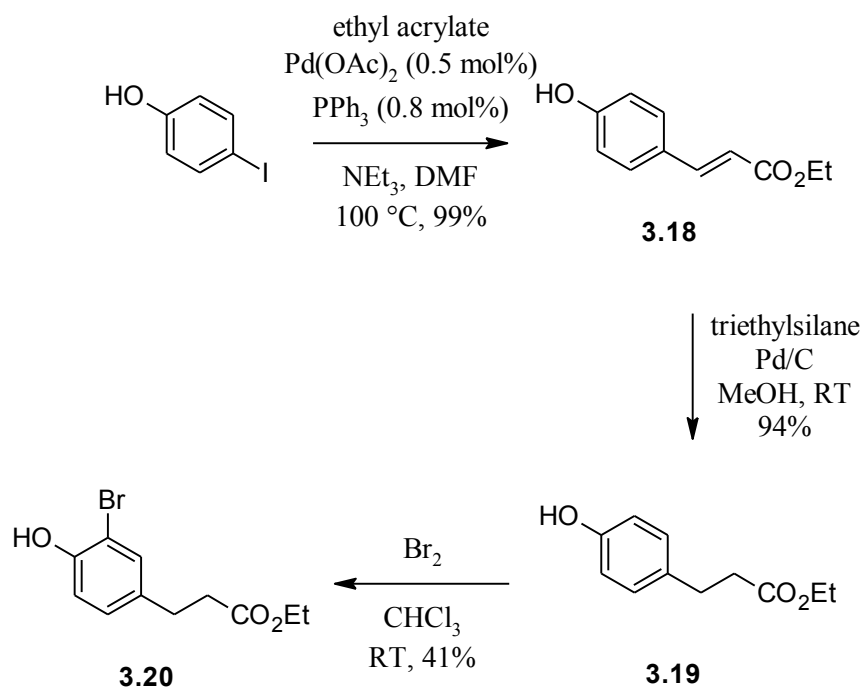
With the initial attempts to synthesize the allyl group having failed, we turned to a set of procedures using *t*BuLi to metalate the *ortho* bromine of **3.16**. Unfortunately, quenching with allyl bromide or the previously reported boron reagent failed to give useable product (Scheme 3.5)¹⁴. This suggested that even the more facile metal-halogen exchange was being blocked by the highly electron rich nature of the arene ring. This observation was supported by the presence of the bromine atom in all recovered starting material. Again, quenching of the reaction mixture with D₂O did not produce deuteration of the *ortho* position, but rather the starting material was recovered with the bromine intact, supporting that the initial metalation did not occur. Screening of the previously mentioned chelating agents also did not affect the reaction outcome.



Scheme 3.5: Attempted synthesis of the allyl group through metalation of **3.16**

With the synthesis of **3.06** stalled, we turned our attention to the synthesis of the southern portion **3.07**. Beginning with 4-iodophenol, we subjected it directly to basic Heck reaction conditions, providing **3.18** in excellent yield. Simple hydrogenation using H₂ gas over Pd/C solid support gave no product, but an alternative protocol using triethylsilane and Pd/C gave very high yields. This selective reactivity is attributed to the surface interactions of the silyl species generated during hydrogen abstraction by the Pd surface. This species, whose nature is unclear but is presumably of the form Pd-SiEt₃, operates to attract the chalcone to the surface, where the traditional Pd-H reduction takes place. Without this attracting agent, **3.18** does not interact with the surface of the Pd for long enough exposure times to affect the reduction. The main byproduct is Si₂Et₆, formed from either the recombination of two SiEt₃ radicals or the nucleophilic attack of an SiEt₃ anion to an SiEt₃ cation. Either of these scenarios could produce

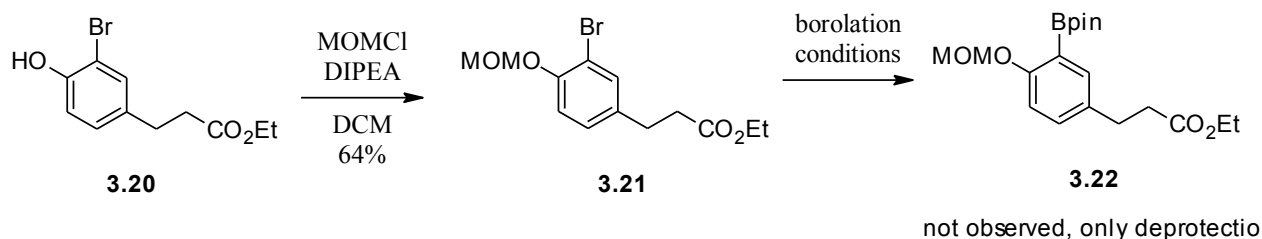
activating agents for the chalcone's carbonyl. Reproducibility of this reaction was found to be affected by the vendor of the triethylsilane. Yields with reagent purchased from the Acros Chemical company gave very high ($\geq 90\%$) yields, while reagent purchased from Sigma Aldrich chemical company gave consistently low ($\leq 30\%$) yields. The hydrogenated **3.19** was then subjected to bromination, giving **3.20** in moderate yield (Scheme 3.6).



Scheme 3.6: *Synthesis of 3.20*

Protection of the phenol as the MOM ether provided **3.21**. It is our belief that the MOM group will serve as adequate steric bulk to promote atropisomerism in the subsequent Suzuki cross coupling, while also acting as a directing group for the Pd in the aforementioned coupling reaction. Any attempts to introduce the boron moiety to **3.21** (or the benzoylated analog) gave only deprotection of the phenol (Scheme 3.7). We decided that our synthetic strategy would only be successful if the boron was included in the cross coupling partner **3.06**. The issue of

deprotection was also apparent if alternative protecting groups were used, such as benzoyl and benzyl. The proximity of the protected phenol seems to make the resultant boronate unstable. This is evidenced by the observation that if the conditions are changed to lithiation and quenching of the lithiate with a boron compound, similar results are observed, even though lithiation was confirmed through D₂O quenching.



Scheme 3.7: Final synthesis of **3.21**

In several experiments, we found that reduction of the ester to an aldehyde as desired (**3.07**) gave poor yields. DIBAL-H reductions are difficult to control completely, and a complete reduction is most likely the more efficient pathway, with a reoxidation occurring to enable allylation of the resulting aldehyde. We decided to perform the final reduction after the cross coupling was performed. We renewed our efforts to synthesize the allyl group onto the C-6 position of **3.08**, but all of our efforts were unsuccessful. It is possible that our mistake was oxidizing the original aldehyde to the phenol. Perhaps the electron withdrawing nature of the aldehyde would provide us with acceptable electronics for subsequent reactions. We regretted the choice to discontinue the project due to lack of forward progress and lack of personelle to perform the reactions.

3.7. Implications and Conclusions of the Synthesis

While our synthetic efforts did not yield the natural product, we are confident that our synthetic strategy is viable, provided **3.06** could be synthesized. We have no reason to believe that the cross coupling will not work as described, and we believe our *ortho* position groups (MOM protected phenol in **3.21** and methoxy in **3.06**) would give us enough steric crowding to promote atropisomerism with the addition of a known chiral ligand¹⁵. We performed a simple experiment using hydrocinnamaldehyde and our allyl indium protocol (see Chapter 4) and found that our PhPyBOX ligand system is ineffective at providing a chiral alcohol as in **3.04**. The yield is quantitative, but there is no *ee*. This issue would require either a large screening of other types of ligands, or the use of other allylation methods such as Brown allylation.

3.8. Experimental Section

3.8.1. General Reaction Considerations

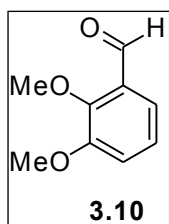
All reactions were conducted in oven-dried (100°C) glassware, and were run under an atmosphere of argon, unless otherwise stated. DCM was dried by passing the degassed solvent through a column of activated Cu/alumina under N₂ immediately before use. MeOH was distilled from Mg turnings and stored over 3Å MS. Acetone was used as HPLC-grade. Allyl bromide was purified by washing with sat. aq. NaHCO₃ followed by distilled H₂O, drying over CaCl₂, and distilling under reduced pressure. Chromatography was performed on EMD silica gel (40-60 microns) using air pressure, unless otherwise specified. All other solvents and reagents were purchased at the highest level of purity and were used as received.

NMR spectra were obtained on a Varian INOVA NMR instrument, at the indicated field strength in the indicated deuterated solvent. NMR spectra are referenced to internal

tetramethylsilane. HRMS were collected on a Bruker BIOTOF III instrument with a positive ESI mode and are referenced to appropriate PEG or NaTFA standards. FTIR spectra were collected on a Bruker Dalton FTIR instrument. Melting points were collected on a Fisher-Johns apparatus and are uncorrected.

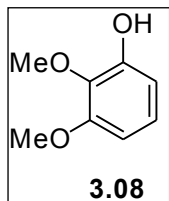
3.7.2. Experimental Details

2,3-Dimethoxybenzaldehyde (**3.10**)¹⁶



A 3-neck, 250-mL round bottom flask equipped with a mechanical stirrer, stopper, and condenser was charged with 2,3-dihydroxybenzaldehyde (5.00 g, 36.2 mmol) and DMF (40 mL). The reaction was stirred as methyl iodide (5.41 mL, 86.7 mmol) was added, followed by solid K_2CO_3 (20.00 g, 144.9 mmol) in portions as to not impede the stirring by addition. The reaction slurry was heated to reflux for 24 hours, then cooled to RT, diluted with H_2O (250 mL), and extracted with EtOAc (3 x 100 mL). The combined organic phases were washed with H_2O (200 mL), brine (150 mL), dried over $MgSO_4$, filtered, and concentrated. The residue was purified by FCC (3:2 hexane:EtOAc) to give **3.10** as white crystals (3.85 g, 64%). 1H -NMR (400 MHz, $CDCl_3$) δ 10.40 (s, 1H), 7.38 (dd, $J=2.8$ Hz, 6.8 Hz, 1H), 7.08-7.14 (m, 2H), 3.96 (s, 3H), 3.88 (s, 3H); ^{13}C -NMR (100 MHz, $CDCl_3$) δ 190.3, 153.2, 152.9, 130.0, 124.3, 119.4, 118.3, 62.5, 56.2; FTIR (thin film) $\bar{\nu}$ (max) 2964, 2873, 2749, 1688 cm^{-1} ; HRMS (ESI), m/z : 189.0529 ($M+Na^+$), calc. for $C_9H_{10}O_3Na$: 189.0522.

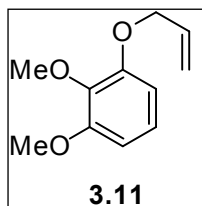
2,3-Dimethoxyphenol (**3.08**)⁸



A 100-mL round bottom flask equipped with a magnetic stir bar was charged with **3.10** (1.25 g, 7.52 mmol) and DCM (25 mL). *m*CPBA (approx. 50% wt/wt, 5.20 g, 15.04 mmol) was added in one portion and the reaction ran at RT for 18 hours.

The resultant slurry was filtered and the filter cake (*m*-chlorobenzoic acid) was washed with DCM. The filtrate was concentrated and the residue was dissolved in MeOH (25 mL). A solution of NaOH (0.65 g, 16.40 mmol) in H₂O (0.88 mL) was added dropwise and the reaction ran at RT for 2.5 hours. The mixture was concentrated and the residue was suspended in 1:1 sat. aq. NH₄Cl:brine and extracted with EtOAc (2 x 50 mL). The combined organic layers were dried over MgSO₄, filtered, and concentrated. The residue was purified by FCC (1% MeOH in DCM) to give **3.08** as a brown oil (0.68 g, 59%). ¹H-NMR (400 MHz, CDCl₃) δ 10.40 (s, 1H), 6.90 (t, *J* = 8.4 Hz, 1H), 6.58 (d, *J* = 8.4 Hz, 1H), 6.45 (d, *J* = 8.4 Hz, 1H), 5.88 (bs, 1H), 3.87 (s, 3H), 3.84 (s, 3H); ¹³C-NMR (100 MHz, CDCl₃) δ 152.9, 149.9, 136.1, 124.2, 108.6, 104.3, 61.0, 55.9; FTIR (thin film) $\bar{\nu}$ (max) 3528, 2944, 2840 cm⁻¹; HRMS (ESI), *m/z*: 267.1394 (M+Na⁺), calc. for C₁₂H₂₄O₃SiNa: 267.1387.

1-Allyloxy-2,3-dimethoxybenzene (**3.11**)

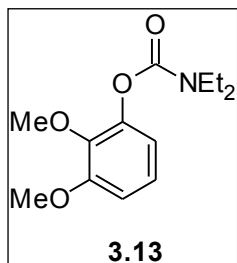


A 50-mL round bottom flask equipped with a magnetic stir bar was charged with **3.08** (2.20 g, 14.27 mmol), K₂CO₃ (2.96 g, 21.41 mmol), and acetone (25 mL). Allyl bromide (1.36 mL, 15.70 mmol) was then added and the reaction

was heated to reflux for 18 hrs. The reaction mixture was then cooled to RT and filtered through Celite, rinsing with acetone. The filtrate was concentrated and the residue purified by FCC (4:1 Hexane:EtOAc) to give **3.11** as a colorless oil (2.22 g, 80%). ¹H-NMR (400 MHz, CDCl₃) δ

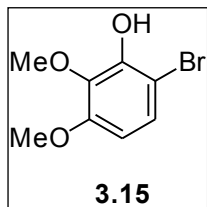
6.89 (dt, $J=8.4$ Hz, 1.2 Hz, 1H), 6.52 (dd, $J=8.4$ Hz, 1.2 Hz, 2H), 6.01 (m, 1H), 5.36 (dq, $J=17.2$ Hz, 0.8 Hz, 1H), 5.21 (dt, $J=10.8$ Hz, 1.6 Hz, 1H), 4.54 (m, 2H), 3.82 (s, 3H), 3.79 (s, 3H); ^{13}C -NMR (100 MHz, CDCl_3) δ 153.9, 152.7, 138.9, 133.7, 123.7, 117.5, 107.4, 105.7, 70.0, 60.9, 56.2; FTIR (thin film) $\bar{\nu}$ (max) 2937, 2836, 1596, 1495, 1476 cm^{-1}

2,3-Dimethoxy-1-*N,N*-diethylcarbamoylphenol (**3.13**)



A 50-mL round bottom flask equipped with a magnetic stir bar was charged with NaH (60% in oil, 88 mg, 2.2 mmol) and THF (2 mL). The reaction was cooled to 0°C and stirred for 10 min. A solution of **3.08** (300 mg, 2.0 mmol) in THF (2 mL) was then added dropwise. After 1 hr, *N,N*-diethylcarbamoyl chloride (0.30 mL, 2.2 mmol) was added in one portion and the reaction mixture was allowed to warm to RT and stirred overnight. The reaction was quenched with sat. aq. NH_4Cl and the phases were separated. The aqueous phase was extracted with EtOAc (3 x 5 mL). The combined organic phases were washed with brine (10 mL) and dried (Na_2SO_4). Filtration and concentration gave a brown residue which was purified by FCC (1% MeOH in DCM) to give **3.13** as an orange oil (370 mg, 73%). ^1H -NMR (400 MHz, CDCl_3) δ 6.90 (t, $J=8.4$ Hz, 1H), 6.67 (m, 2H), 3.76 (s, 6H), 3.34 (m, 4H), 1.14 (m, 6H); ^{13}C -NMR (100 MHz, CDCl_3) δ 171.1, 153.9, 145.3, 141.7, 123.3, 115.9, 109.8, 60.7, 60.5, 56.2, 42.3, 14.2, 13.5; FTIR (thin film) $\bar{\nu}$ (max) 2974, 2938, 2837, 1720, 1599, 1494, 1471 cm^{-1}

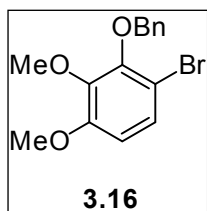
6-Bromo-2,3-dimethoxyphenol (**3.15**)¹⁴



A 50-mL round bottom flask equipped with a magnetic stir bar was charged with **3.08** (0.57 g, 3.7 mmol) and THF (15 mL). The reaction was cooled to -78°C and NBS (recrystallized, 0.66 g, 3.7 mmol) was added in one portion.

The reaction stirred at -78°C for 4 hrs, then was allowed to warm to RT overnight. The reaction was then concentrated and the residue was dissolved in DCM (20 mL) and washed with H₂O (20 mL) and brine (20 mL). The organic phase was dried (MgSO₄), filtered, and concentrated. The residue was purified by FCC (19:1 Petroleum Ether:Et₂O) to give **3.15** as a thick, orange oil (0.60 g, 70%). ¹H-NMR (400 MHz, CDCl₃) δ 7.13 (d, *J*=8.8 Hz, 1H), 6.39 (d, *J*=8.8 Hz, 1H), 5.98 (bs, 1H), 3.89 (s, 3H), 3.83 (s, 3H); ¹³C-NMR (100 MHz, CDCl₃) δ 152.2, 147.0, 136.6, 127.0, 105.4, 100.5, 61.3, 56.3; FTIR (thin film) $\bar{\nu}$ (max) 3515, 2942, 2837, 1494, 1466, 908, 733 cm⁻¹.

1-Benzoyloxy-6-bromo-2,3-dimethoxybenzene (**3.16**)¹⁴

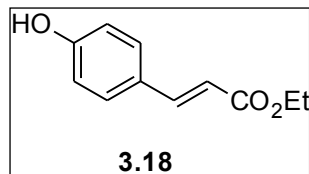


A 50-mL round bottom flask equipped with a magnetic stir bar was charged with **3.15** (583 mg, 2.50 mmol), K₂CO₃ (519 mg, 3.75 mmol), and acetone (25 mL). The reaction was stirred as benzyl bromide (0.47 mL, 2.75 mmol) was

added, and the reaction was set to stir at reflux for 4 hrs. The reaction was cooled to RT and concentrated. The paste-residue was suspended in DCM (20 mL) and washed with H₂O (15 mL), brine (15 mL), dried (MgSO₄), filtered, and concentrated. The residue was purified by FCC (19:1 Petroleum Ether:Et₂O) to give **3.16** as a colorless solid (768 mg, 95%). m.p. 71-73°C; ¹H-NMR (400 MHz, CDCl₃) δ 7.55 (dd, *J*=7.6 Hz, 1.2 Hz, 2H), 7.36 (m, 3H), 7.21 (d, *J*=8.8 Hz, 1H), 6.59 (d, *J*=9.2 Hz, 1H), 5.06 (s, 2H), 3.87 (s, 3H), 3.84 (s, 3H); ¹³C-NMR (100

MHz, CDCl₃) δ 153.6, 150.1, 144.0, 137.3, 128.8, 128.6, 128.4, 127.1, 109.1, 75.6, 61.4, 56.4; FTIR (thin film) $\bar{\nu}$ (max) 2936, 2836, 1574, 1478, 1092, 1009 cm⁻¹; HRMS (ESI), m/z : 345.0085, 347.0070 (M+Na⁺), calc. for C₁₅H₁₅O₃BrNa: 345.0097, 347.0078.

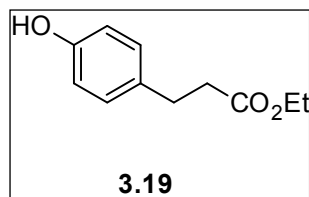
Ethyl 4-hydroxy-*trans*-cinnamaic acid (**3.18**)¹⁷



A 250-mL round bottom flask equipped with a magnetic stir bar was charged with 4-iodophenol (2.00 g, 9.08 mmol), Pd(OAc)₂ (10.2 mg, 0.045 mmol, 0.5 mol%), and PPh₃ (23.8 mg, 0.091 mmol, 0.8 mol%).

The flask was sealed under argon and charged with DMF (28 mL), NEt₃ (3.80 mL, 27.60 mmol), and ethyl acrylate (4.00 mL, 36.8 mmol). The reaction mixture was set to stir at 100°C for 24 hrs. The reaction was then cooled to RT and diluted with 2:1 EtOAc:Et₂O (75 mL). The solution was washed with 1N HCl (50 mL), brine (50 mL), dried (Na₂SO₄), filtered, and concentrated. Purification of the residue by FCC (4:1 hexane:EtOAc) gave **3.18** as yellow crystals (1.76 g, 99%). m.p. 69-72°C; ¹H-NMR (400 MHz, CDCl₃) δ 7.61 (d, J =16 Hz, 1H), 7.39 (d, J =8.4 Hz, 2H), 6.85 (dd, J =10 Hz, 8.4 Hz, 2H), 6.27 (d, J =16 Hz, 1H), 4.25 (q, J =7.2 Hz, 2H), 1.32 (t, J =7.2 Hz, 3H); ¹³C-NMR (100 MHz, CDCl₃) δ 168.7, 158.8, 145.4, 130.3, 126.8, 116.2, 115.1, 61.0, 14.5; FTIR (thin film) $\bar{\nu}$ (max) 3335, 2981, 1684, 1604, 1515 cm⁻¹; HRMS (ESI), m/z : 215.0646 (M+Na⁺), calc. for C₁₁H₁₂O₃Na: 215.0679.

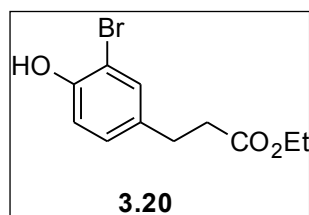
Ethyl 4-hydroxy-hydrocinnamaic acid (**3.19**)¹⁸



A 100-mL round bottom flask equipped with a magnetic stir bar was charged with **3.18** (2.20 g, 11.40 mmol), Pd/C (0.18 g, 15 wt%), and MeOH (21 mL). The reaction was sealed under argon and a bubbling

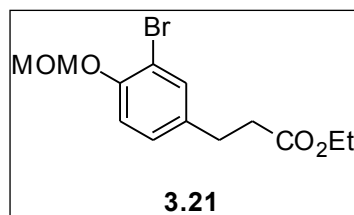
outlet was affixed. Triethylsilane (18.10 mL, 116.50 mmol) was added dropwise, with vigorous hydrogen gas evolution occurring upon addition. The reaction was allowed to stir at RT for 72 hrs before filtering through Celite, rinsing with MeOH. The filtrate was concentrated and the residue was purified by FCC (4:1 hexane:EtOAc) to give **3.19** as a yellow oil, which on occasion has solidified to give pale yellow crystals (2.08 g, 94%). ¹H-NMR (400 MHz, CDCl₃) δ 7.01 (d, *J*=8.8 Hz, 2H), 6.85 (bs, 1H), 6.75 (d, *J*=8.4 Hz, 2H), 4.11 (q, *J*=7.2 Hz, 2H), 2.85 (t, *J*=7.6 Hz, 2H), 2.58 (t, *J*=8.4 Hz, 2H), 1.21 (t, *J*=7.2 Hz, 3H); ¹³C-NMR (100 MHz, CDCl₃) δ 174.3, 154.7, 132.2, 129.6, 115.6, 61.0, 36.6, 30.4, 14.3; FTIR (thin film) $\bar{\nu}$ (max) 3393, 2982, 2936, 1707, 1597 cm⁻¹.

Ethyl 3-bromo-4-hydroxy-hydrocinnamaic acid (**3.20**)



A 50-mL round bottom flask equipped with a magnetic stir bar was charged with **3.19** (0.70 g, 5.12 mmol) and CHCl₃ (7 mL). The reaction was cooled to 0°C and Br₂ (neat, 0.15 mL, 2.92 mmol) was added dropwise over 5 min. The reaction was allowed to warm to RT and stirred for 4 hrs. The reaction mixture was directly washed with 1N HCl (5 mL), brine (5 mL), dried (Na₂SO₄), filtered, and concentrated. The residue was purified by FCC (4:1 hexane:EtOAc) to give **3.20** as a yellow oil (0.40 g, 41%). ¹H-NMR (400 MHz, CDCl₃) δ 7.26 (m, 1H), 6.99 (dd, *J*=8.4 Hz, 2 Hz, 1H), 6.88 (d, *J*=8.4 Hz, 1H), 5.73 (bs, 1H), 4.09 (q, *J*=11.6 Hz, 2H), 2.82 (t, *J*=7.6 Hz, 2H), 2.54 (t, *J*=8 Hz, 2H), 1.20 (t, *J*=6.8 Hz, 3H); ¹³C-NMR (100 MHz, CDCl₃) δ 173.1, 151.0, 134.3, 132.1, 131.9, 129.2, 60.8, 36.2, 30.0, 14.3; FTIR (thin film) $\bar{\nu}$ (max) 3406, 2982, 2936, 1727, 1497, 1184, 1041 cm⁻¹; HRMS (ESI), *m/z*: 295.0002, 296.9992 (M+Na⁺), calc. for C₁₁H₁₃O₃BrNa: 294.9940, 296.9921.

Ethyl 3-bromo-4-(methoxymethoxy)-hydrocinnamaic acid (**3.21**)



A 50-mL round bottom flask equipped with a magnetic stir bar was charged with **3.20** (0.30 g, 1.09 mmol) and DCM (7.5 mL). With stirring at RT, *N,N*-diisopropylethylamine (DIPEA, 0.28 mL, 1.65 mmol) was added, followed by chloromethyl methyl ether (MOMCl, 0.12 mL, 1.65 mmol) resulting in a white gas formation. The reaction was allowed to stir for 18 hrs at RT, then was diluted with Et₂O (10 mL) and washed with H₂O (10 mL), brine (10 mL), dried (Na₂SO₄), filtered, and concentrated. The residue was purified by FCC (4:1 hexane:EtOAc) to provide **3.21** as a colorless oil (0.22 g, 64%). ¹H-NMR (400 MHz, CDCl₃) δ 7.34 (s, 1H), 7.03 (m, 2H), 5.18 (s, 2H), 4.09 (q, *J*=7.2 Hz, 2H), 3.48 (s, 3H), 2.84 (t, *J*=7.6 Hz, 2H), 2.54 (t, *J*=8 Hz, 2H), 1.20 (t, *J*=6.8 Hz, 3H); ¹³C-NMR (100 MHz, CDCl₃) δ 172.8, 152.4, 135.9, 133.3, 128.5, 116.5, 113.0, 95.4, 60.7, 56.5, 36.0, 30.0, 14.4; FTIR (thin film) $\bar{\nu}$ (max) 2984, 2906, 1727, 1495, 1244, 1044 cm⁻¹; HRMS (ESI), *m/z*: 339.0193, 341.0181 (M+Na⁺), calc. for C₁₃H₁₇O₄BrNa: 339.0202, 341.0183.

3.8. References

- ¹ Drubin, D., Kirshner, M.; *J. Cell. Biol.*, **1986**, *103*, 2739-2746.
- ² Buée, L., Bussière, T., Buée-Scherrer, V., Delacourte, A., Hof, P.; *Brain Res. Rev.*, **2000**, *33*, 95-130.
- ³ Jones, J., Lebar, M., Jinwal, U., Abisambra, J., Koren, J., Blair, L., O'Leary, J., Davey, Z., Trotter, J., Johnson, A., Weeber, E., Eckman, C., Baker, B., Dickey, C.; *J. Nat. Prod.*, **2011**, *74*, 38-44.
- ⁴ Whiting, D., Wood, A.; *J. Chem. Soc. Perkin Trans. I*, **1980**, 623-628.
- ⁵ Haddad, T., Hirayama, L., Singaram, B.; *J. Org. Chem.*, **2010**, *75*, 642-649.
- ⁶ Baudoin, O.; *Eur. J. Org. Chem.*, **2005**, 4223-4229. Heravi, M., Hashemi, E.; *Tetrahedron*, **2012**, *68*, 9145-9178.
- ⁷ Gill, G., Grobelny, D., Chaplin, J., Flynn, B.; *J. Org. Chem.*, **2008**, *73*, 1131-1134.

- ⁸ McElroy, W., DeShong, P., *Tetrahedron*, **2006**, *62*, 6945-6954.
- ⁹ Sreedhar, B., Swapna, V., Sridhar, C.; *Synth. Commun.*, **2004**, *34*, 1433-1440.
- ¹⁰ Castro, A.; *Chem. Rev.*, **2004**, *104*, 2939-3002.
- ¹¹ Gupta, M., Paul, S., Gupta, R.; *Acta. Chim. Slov.*, **2009**, *56*, 749-764.
- ¹² Sreedhar, B., Swapna, V., Sridhar, C.; *Synth. Commun.*, **2004**, *34*, 1433-1440.
- ¹³ Kauch, M., Hoppe, D.; *Synthesis*, **2006**, 1575-1577; Sibi, M., Snieckus, V.; *J. Org. Chem.*, **1983**, *48*, 1937-1938.
- ¹⁴ Donohoe, T., Jones, C., Barbosa, L.; *J. Am. Chem. Soc.*, **2011**, *133*, 16418-16421.
- ¹⁵ Buchwald, S., Huang, X., Zim, D.; *US Patent No 20040171833A1*, **2004**. BINAP has also been shown to be effective for asymmetric Suzuki couplings. See: Baudoin, O.; *Eur. J. Org. Chem.*, **2005**, 4223-4229. Heravi, M., Hashemi, E.; *Tetrahedron*, **2012**, *68*, 9145-9178.
- ¹⁶ Grudzień, K., Malinska, M., Barbasiewicz, M.; *Organometallics*, **2012**, *31*, 3636-3646.
- ¹⁷ Park, J., Lackey, H., Onrusek, B., McQuade, D.; *J. Am. Chem. Soc.*, **2011**, *133*, 2410-2413.
- ¹⁸ Sauerberg, P., Olsen, G., Jeppesen, L., Mogensen, J., Pettersson, I., Jeppesen, C., Daugaard, J., Galsgaard, E., Ynddal, L., Fleckner, J., Panajotova, V., Polivka, Z., Pihera, P., Havranek, M., Wulff, E.; *J. Med. Chem.*, **2007**, *50*, 1495-1503.

CHAPTER 4. TOTAL SYNTHESIS OF (+)-CONVOLUTAMYDINE E AND ATTEMPTED
TOTAL SYNTHESIS OF RELATED 3-HYDROXYINDOLIN-2-ONE NATURAL
PRODUCTS

4.1. Introduction

The total synthesis of natural products has been a highly useful tool for organic chemists to showcase their methodologies, identify new candidates for pharmaceutical development, and expand the capabilities of modern chemistry. A wide range of natural products exist, with a diverse range of functional groups and biological activities as well as complex structural scaffolds. This is exemplified in the total synthesis of vancomycin (Figure 4.1) by the Nicolaou group¹. The total syntheses of these types of molecules have opened up a wide array of synthetic tools for the modern organic chemist in the form of established chemical reactions.

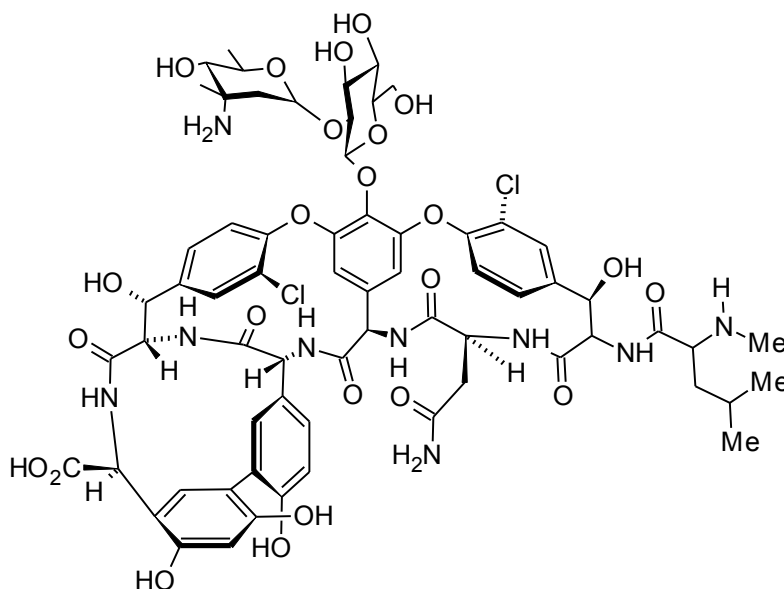


Figure 4.1: *Vancomycin*

4.1.1. Allyl Groups as Functional Handles for Organic Synthesis

Allylation is a key synthetic strategy in organic synthesis. The allyl group can be used as a transformative synthon for a wide number of other functional groups (Figure 4.2).

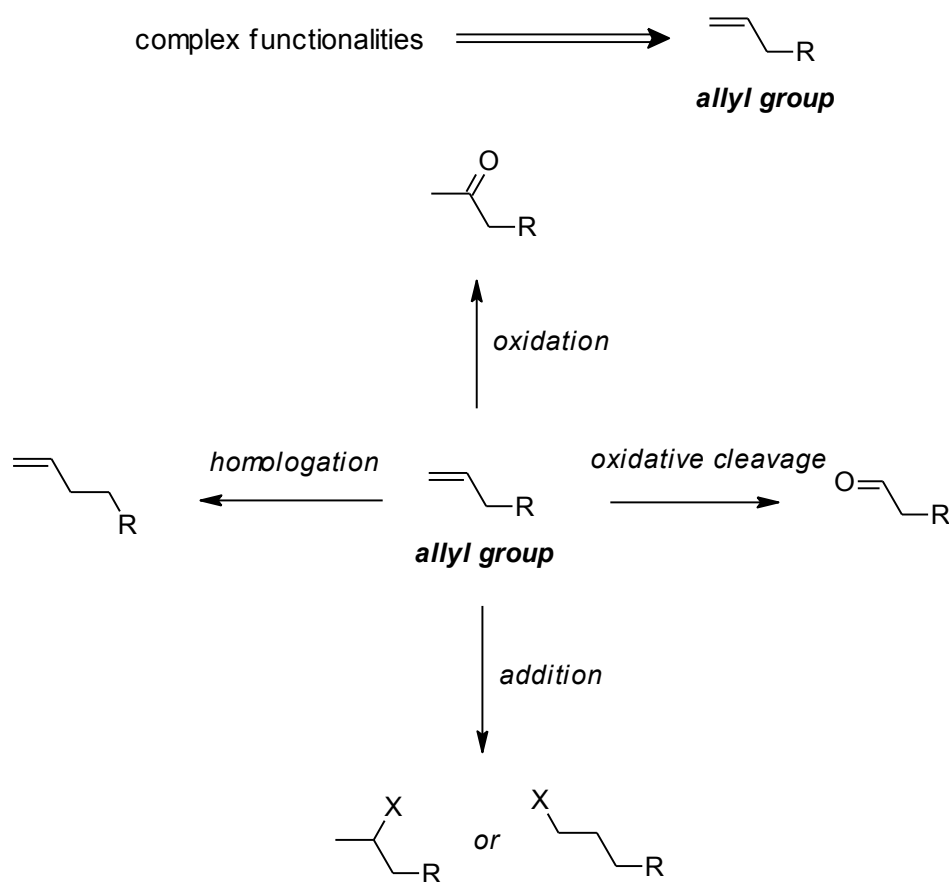
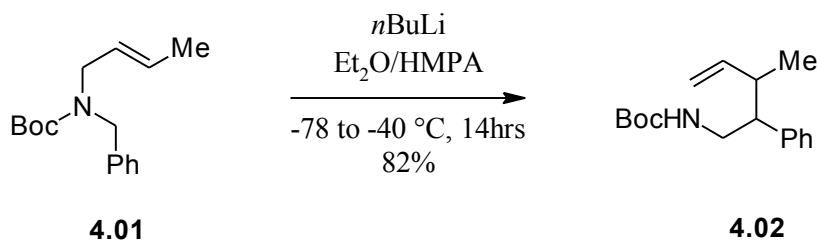


Figure 4.2: Synthetic utility of the allyl group

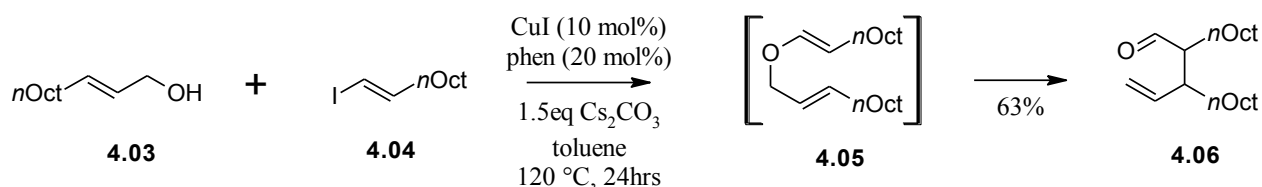
A large number of synthetic strategies centered on the allyl group have been developed. The allyl group, being a 3-carbon unit, provides access to [2,3] and [3,3]-sigmatropic rearrangements such as the [2,3]-Wittig rearrangement and Claisen rearrangement. By incorporating the allyl group as a side chain of Boc-protected benzyl amine **4.01**, Anderson, *et*

al. were able to deprotonate the benzylic position and facilitate the thermal [2,3]-Wittig rearrangement to **4.02**² (Scheme 4.1).



Scheme 4.1: Example of a [2,3]-Wittig rearrangement

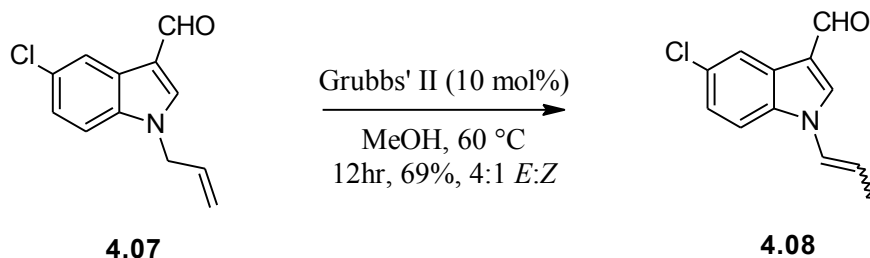
Claisen rearrangements are also highly useful reactions where allyl groups play an integral role. Buchwald and co-workers have developed an *O*-vinylation using Cu-catalyzed cross coupling of allylic alcohol **4.03** and vinyl iodide **4.04**, resulting in the cross coupled product **4.05**. The allyl vinyl ether, under the thermal reaction conditions, undergoes [3,3]-sigmatropic rearrangement to give the homoallylic aldehyde **4.06**³ (Scheme 4.2).



Scheme 4.2: Example of [3,3]-sigmatropic rearrangement (Claisen rearrangement) of an allyl vinyl ether

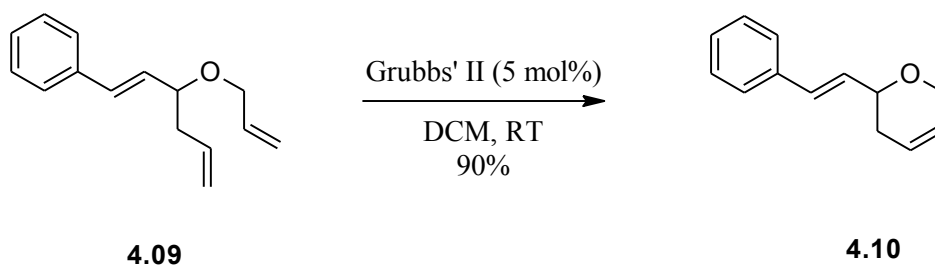
Allyl groups can also be isomerized into internal alkenes through transition metal catalyzed C-H bond functionalization. By isomerizing the allyl group, it can then be subjected to

numerous other reactions where the internal substitutions can be utilized. For example, a Rh-catalyzed alkene isomerization using the Grubb's 2nd generation catalyst readily isomerizes allyl groups to the internal alkenes, which can allow for compounds such as *N*-allyl indole **4.07** to be converted into the enamine **4.08**, which can then be easily deprotected (Scheme 4.3)⁴.



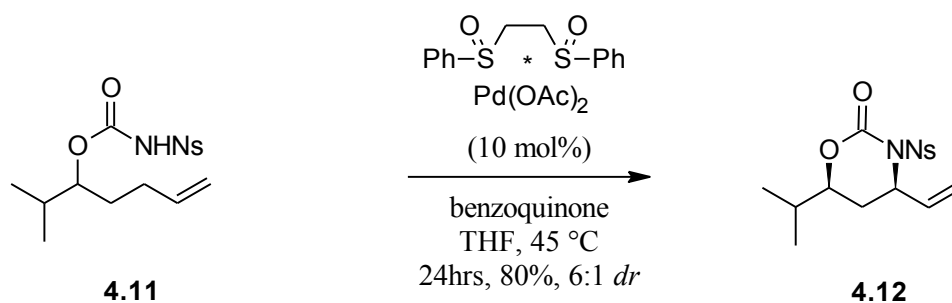
Scheme 4.3: Example of an allyl group isomerization catalyzed by Rh

Allyl groups can also be subjected to Ring-Closing Metathesis (RCM) or Cross-Metathesis (CM) via the same catalyst (Grubbs' II), but in a different solvent (CH₂Cl₂). Using this catalyst system, bis allyl ether **4.09** is subjected to RCM, providing dihydropyran **4.10** in a very good yield (Scheme 4.4)⁵.



Scheme 4.4: Example of allyl groups participating in RCM

The allyl group also has been utilized recently in the explosion of C-H bond activation chemistry. Using the allyl's alkene pi system as a “docking handle” for transition metals, the allylic C-H bonds become readily accessible for functionalization. In work pioneered separately by M. Christina White and J. DuBois, Pd or Rh can be used to similar effect to functionalize the C-H bonds of the allylic carbon. As an example, from the White group, homoallylic carbamate **4.11** can be ring closed onto the allylic C-H position by Pd-catalyzed C-H activation, providing cyclic carbamate **4.12** in good yields and with moderate diastereoselectivity (Scheme 4.5)⁶.



Scheme 4.5: Example of allylic C-H bond functionalization using Pd catalysis

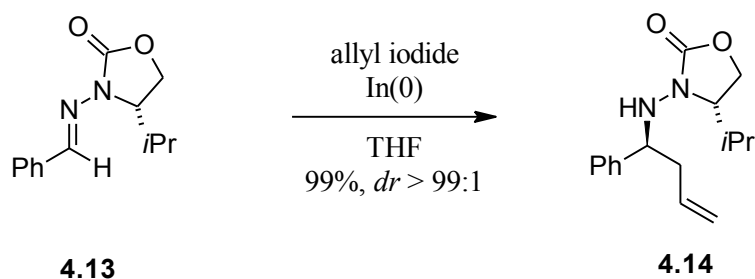
Allylation has become one of the premier tools in the organic chemist's toolbox, not only for its ease of incorporation into molecular structures, but for its robust reactivity profile. All of the aforementioned reactions can be applied to virtually any terminal olefin, and the allyl group provides that, but also provides access to synthetically powerful rearrangements which require a three-carbon unit.

4.1.2. Allylation and the Cook Group Methodologies

A rapidly developing caveat of organic chemistry is the need to be environmentally friendly with our choices of reagents, solvents, and reaction conditions⁷. In this light, our

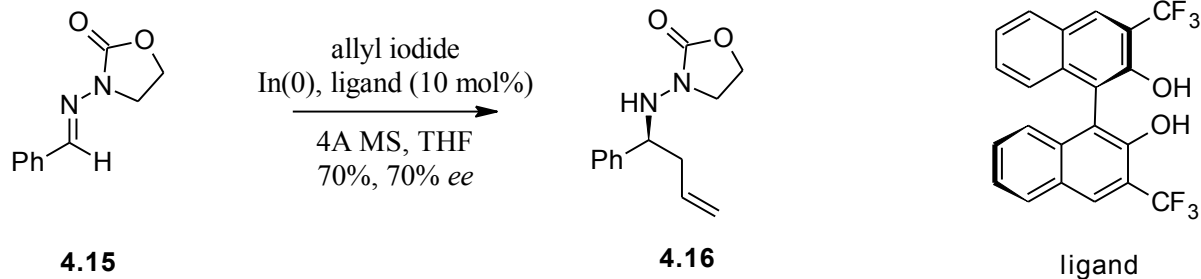
research group has sought to bring new chemistry to the forefront, based around Indium and Bismuth as organometallic precursors. We have shown that In(0) can be an efficient metal for Barbier-type allylations using convenient allyl iodides and bromides⁸.

The reactions were first utilized on chiral hydrazones, using allyl iodide and the stereocontrol was achieved through an adjacent chiral center on the hydrazone's oxazolidinone auxiliary. Thus, hydrazone **4.13** was allylated using allyl iodide and In(0) in THF to produce allylated hydrazone **4.14** in near quantitative yield and diastereomeric ratio (Scheme 4.6)⁹.



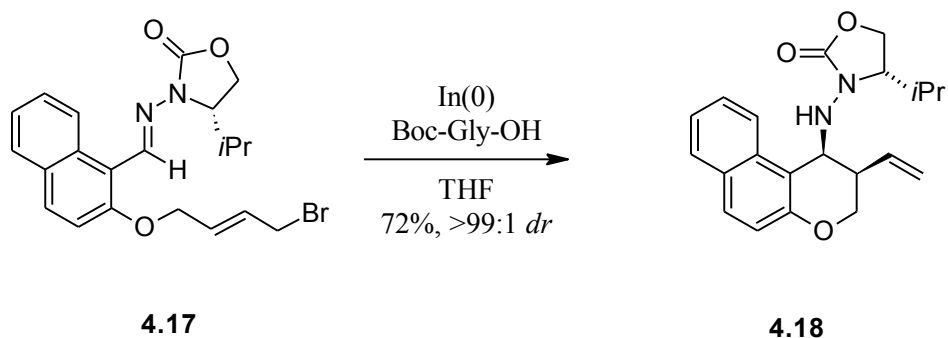
Scheme 4.6: Cook Group methodology for diastereoselective allylation of hydrazones

The allylation can also be achieved with ligand control by utilizing an atrop-chiral BINOL-derived ligand and the addition of 4Å molecular sieves (MS). The analogous hydrazone **4.15** can be effectively allylated using these conditions, giving the allylated product **4.16** in good yield with moderate-to-good enantioselectivities (Scheme 4.7)¹⁰.



Scheme 4.7: Cook group ligand control of enantioselective hydrazone allylation

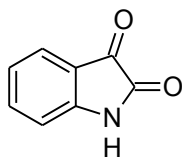
Changing the ligand to have a more electron withdrawing nature allowed the allyl iodide to be replaced with the easier to use and less reactive allyl bromide¹¹. The reactions give higher yields (around 85%) and much better enantioselectivities (90-97% *ee*). This allowed for more applicability towards different reactions, as allyl bromides are relatively easier to synthesize or are commercially available. One of the ways in which the methodology was applied was towards the intramolecular allylation of hydrazones, most notably in the formation of aminochromanes. In this case, a Boc-protected glycinol was used as a ligand, and the substrate controlled the diastereoselectivity. The hydrazone/allyl bromide **4.17** was cyclized via and In(0)-mediated allylation to give the aminochromane **4.18** in a good yield with excellent diastereoselectivity (Scheme 4.8)¹².



Scheme 4.8: *Highly diastereoselective intramolecular allylation of hydrazones leading to aminochromanes*

4.1.3. Current Cook Group Allylation Methodologies

Due to our interest in the allylation of hydrazones and other imine-type substrates, our group has expanded its methodologies to include ketone bodies. The model substrate for these investigations has been isatin, **4.19** (Figure 4.3).

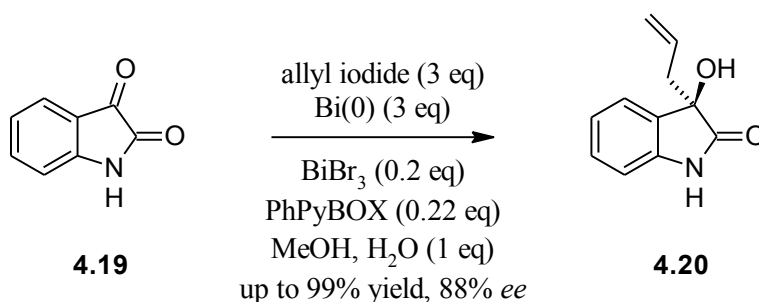


4.19

Figure 4.3: *Isatin*

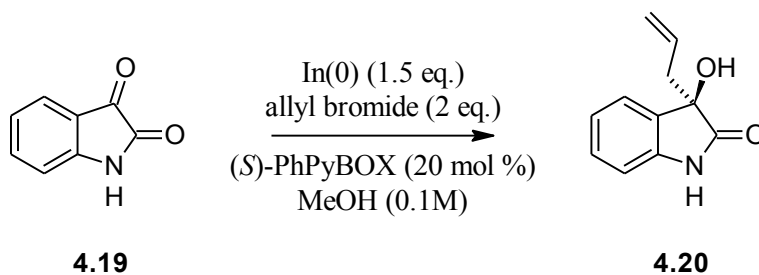
Isatin is unique in that the reactive ketone is completely planar, meaning that any asymmetric reactions would have to be controlled exclusively from the reagent. Also, the unique placement of the ketone and the amide carbonyl allows for very efficient binding to Lewis acids, forming the thermodynamically preferred five-membered ring chelate. In research already established in the Cook group, isatin has been allylated using similar conditions to the hydrazone

series. Thus, isatin (**4.19**) has been allylated using allyl iodide and Bi(0), using (*S*)-PhPyBOX as a ligand. In this case a Lewis acid is needed to coordinate to both the chiral ligand and the isatin substrate, and so BiCl₃ was chosen, providing 3-allyl-3-hydroxyindolin-2-one **4.20** in good yields with moderate enantioselectivities (Scheme 4.9)¹³. Most notably, this reaction is operationally simple, with little purification necessary to isolate the product from the reaction mixture.



Scheme 4.9: *Allylation of isatin using Bi(0)/BiCl₃ conditions*

This methodology led to the experimentation of the allylation conditions directly from the hydrazone chemistry, using In(0) as the Barbier-type metal. Interestingly, the generated allyl indium species was Lewis acidic enough to eliminate the need for an additional Lewis acid additive. Using the ligand optimized for the earlier bismuth allylation chemistry, the methodology was developed in earnest until an optimized protocol was achieved. Isatin was allylated using In(0) in methanol using allyl bromide and (*S*)-PhPyBOX to give the allylated product in high yield and good enantioselectivities (Scheme 4.10)¹⁴.

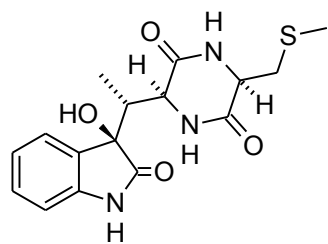


Scheme 4.10: Alkylation of isatin using *In(0)*-mediated conditions

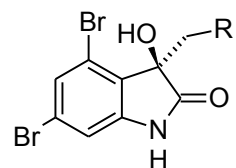
While this methodology is very robust and highly effective, there was little support for its incorporation into a larger synthesis. In this light, it was decided to pursue a project of total synthesis devoted to specific natural products with the 3-hydroxyindolin-2-one core.

4.2. Selection of Natural Products for Total Synthesis

There are many natural products which contain the desired 3-hydroxyindolin-2-one structural motif, but many were deemed too complicated for simple transformations from the allyl group. It was envisioned that the results of the alkylation efforts towards **4.19** would allow us to utilize the chemically diversifiable allyl group to complete these syntheses. In this light, several natural products were identified as possible targets for a total synthesis project (Figure 4.4)¹⁵.

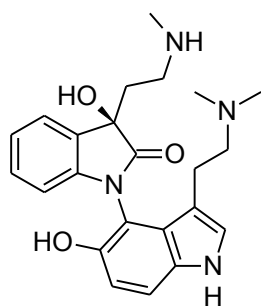


4.21

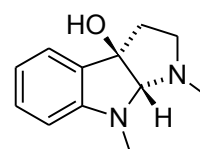


4.22, R = COMe

4.23, R = CH₂OH



4.24



4.25

Figure 4.4: Possible synthetic targets for total synthesis in support of the Cook group allylation methodology

Firstly considered was Maremycin B (**4.21**), which was attractive because of the C-10 methyl group, which we envisioned could come from a crotyl addition to **4.19**, as opposed to an allylation (i.e. C-10 would be CH₂). However, this was eliminated as a possible choice due to the inconsistencies of the crotylation methodologies, as well as the highly complex 2,5-piperazinedione moiety, which could not be retrosynthesized in an efficient way from the crotyl's terminal double bond. Secondly, we considered Convolutamydine A (**4.22**) and Convolutamydine E (**4.23**), both of which can be synthesized easily from the terminal olefin of the allyl group. The only problem we envisioned was the presence of the 4,6-dibromoindolin-2-one core, which possesses bromines on positions not typically found to be substituted in this class

of natural products. We also examined Arundaphine (**4.24**) as a possible target. It possesses a potentially atrop-isomeric *N*-aryl bond, which was not defined in the literature, as well as methylamino and *N,N*-dimethylserotonin moieties. Early experimentation showed the difficulty in creating the *N*-aryl bond through established methodologies¹⁶. Finally, we considered the tricyclic CPC-1 (**4.25**), which could be generated by cyclization of a pendant *N*-methylamine (derived from the allyl group's olefin) onto the isatin core's amide carbonyl. This molecule was dropped from consideration due to time limitations during the syntheses of some of the other compounds.

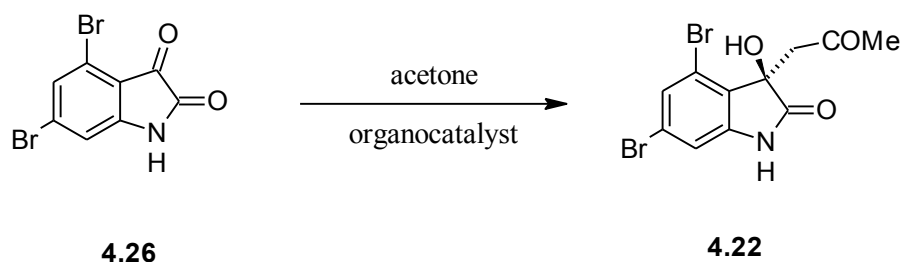
4.3. Previous Syntheses of (*R*)-Convolutamydines A and E

4.3.1. (*R*)-Convolutamydine A

The compound (*R*)-convolutamydine A was isolated from the Floridian marine bryozoans *Amathia convolute* in 1995. It is a potent inhibitor of HL-60 human leukemia cell lines, with an active concentration of 0.1-25 µg. It specifically inhibits adhesiveness to the culture plate, arrests growth, and induces phagocytosis of latex particles¹⁷. Structurally, it possesses two bromine atoms, a methyl ketone, and a fully substituted chiral carbon at C-3 in addition to the indolin-2-one core.

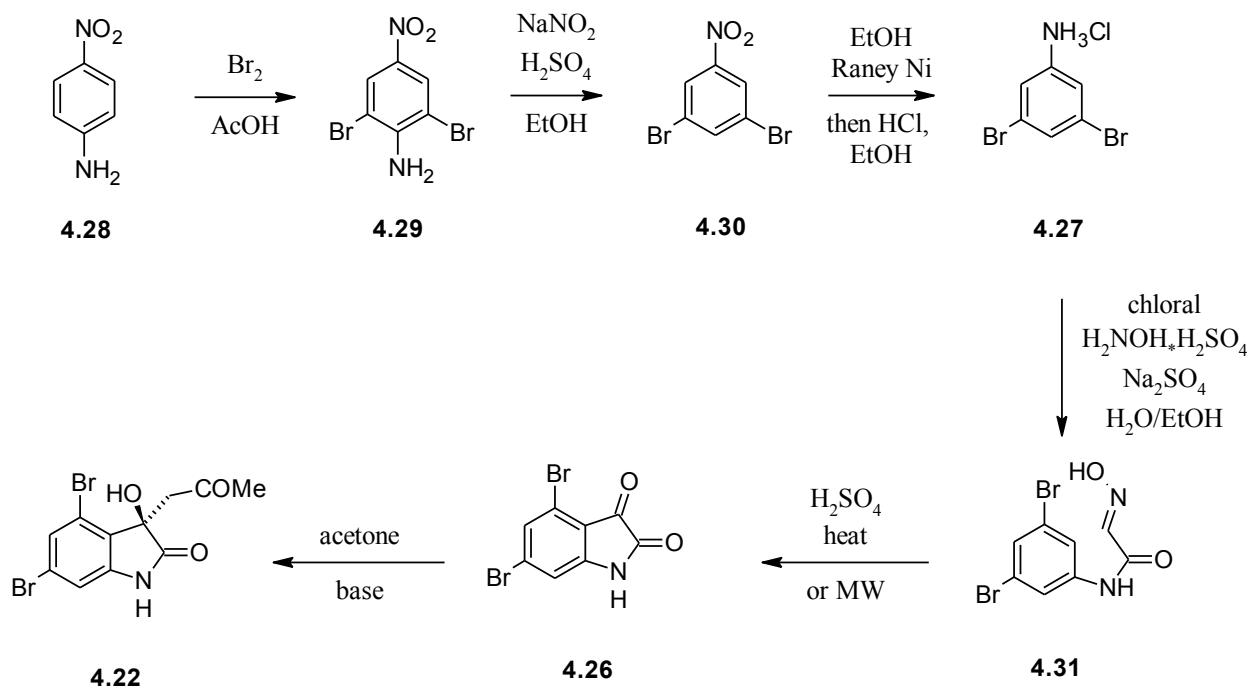
Since the appendage of convolutamydine A (**4.22**) is a methyl ketone, and the chiral carbon is generally derived from the starting ketone (4,6-dibromoisatin **4.26**), it is understandable that many people have used this molecule as a total synthesis target to showcase asymmetric Aldol reactions. Generally, these are organocatalytic, as strong bases usually associated with traditional Aldol reactions would decompose the indolin-2-one ring. Specific

examples use acetone as a nucleophile and some derivative of L-Proline as an organocatalyst (Scheme 4.11)¹⁸.



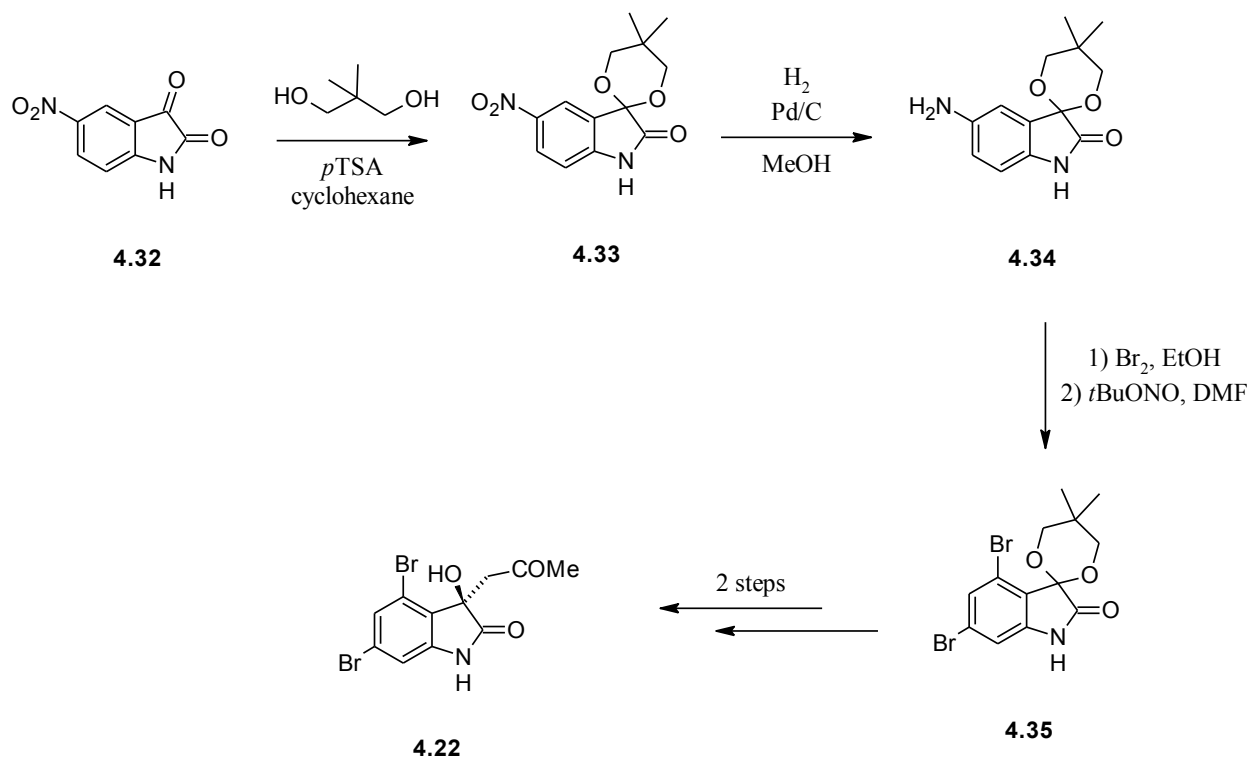
Scheme 4.11: General organocatalytic approach to the total synthesis of (R)-convolutamydine A

In addition to these syntheses, many people have tried to focus their synthetic attention on the synthesis of **4.26**, which is relatively more complicated to synthesize. Mainly, the syntheses of **4.26** begin with 3,5-dibromoaniline (**4.27**), which can be made from *p*-nitroaniline (**4.28**) through a simple sequence of electrophilic bromination, diazotization/reduction, and reduction of the remaining nitro group (Scheme 4.12)¹⁹. Bromination of **4.28** gives the doubly directed dibromination product **4.29**. Diazotization under strongly acidic conditions allows for the *ipso*-protonation of the diazonium salt, giving the bis-*meta* brominated nitrobenzene **4.30**. Reduction using Raney Ni, and trapping of the aniline as its HCl salt gives **4.27**. A multicomponent reaction involving chloral and hydroxylamine under acidic conditions gives the isonitrosoanilide **4.31**, which is cyclized under fairly hard acidic/thermal conditions to give **4.26**. The synthesis is carried forward to the natural product by the previously described routes.



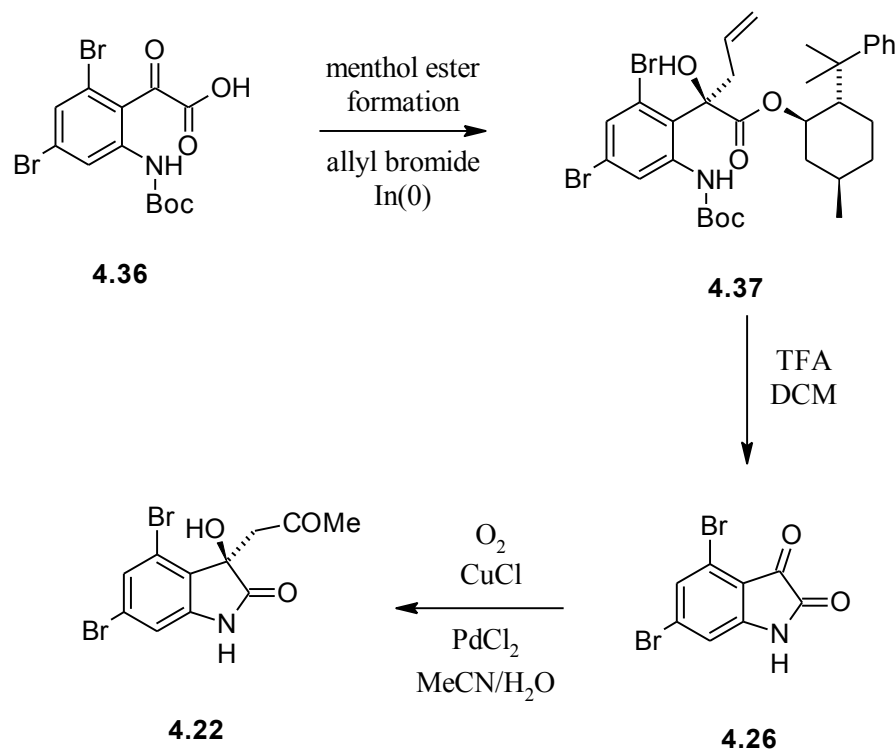
Scheme 4.12: Previous total synthesis of (R)-convolutamydine A

Another synthetic strategy, which is related to the previous strategy, is to brominate an isatin core directly. In order to achieve this, protection of the isatin ketone must be enacted, and an electrophilic aromatic substitution directing group must be present at C-5. The Deshpande group, which successfully applied microwaves to the synthesis in the previously mentioned strategy, has achieved this synthesis from 5-nitroisatin (**4.32**). Protection of the 3-keto moiety as its 2,2-dimethylpropane-1,3-diol ketal provides **4.33**, which is reduced to the 5-aminoisatin derivative **4.34**. Electrophilic bromination is achieved under neutral conditions, with the amino group being diazotized off, akin to the previous syntheses, giving the deaminated, protected dibromoisatin **4.35**. Deprotection and Aldol reaction with acetone completes the natural product (Scheme 4.13)²⁰.



Scheme 4.13: Total synthesis of (R)-convolutamydine A without forming the isatin directly

Interestingly enough, there are few examples where the methyl ketone of **4.22** is not synthesized from an Aldol reaction. Cravotto, *et al* synthesized **4.22** from a dibromophenylglyoxylic acid derivative (**4.36**) and, using the menthol ester, added allyl bromide by way of the allyl indium species to generate the diastereomeric allylated compound **4.37**. Deprotection of the Boc-aniline allowed for amidation of the menthol ester, closing the indolin-2-one ring and forming the 3-allyl-3-hydroxy isatin derivative **4.38** (Scheme 4.14)²¹.



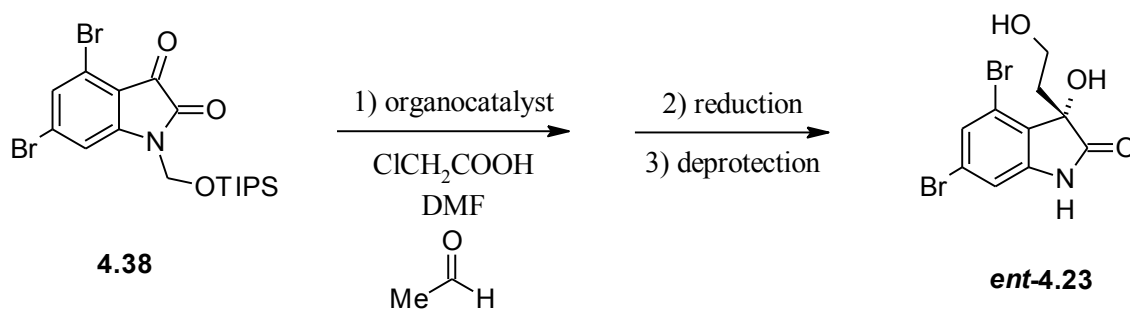
Scheme 4.14: Total synthesis of (*R*)-convolutamydine A using *In*-mediated diastereoselective allylation

4.3.2. Previous Syntheses of (*R*)-Convolutamydine E

(*R*)-convolutamydine E (**4.23**) has been less studied as a target of total synthesis, most likely due to its lack of significant biological activity as compared with some of the other members of the convolutamydine family. It was isolated from the same bryozoa as the other members of the convolutamydine family, and possesses a one-carbon shorter side chain than convolutamydine A, with a terminal hydroxyl group²².

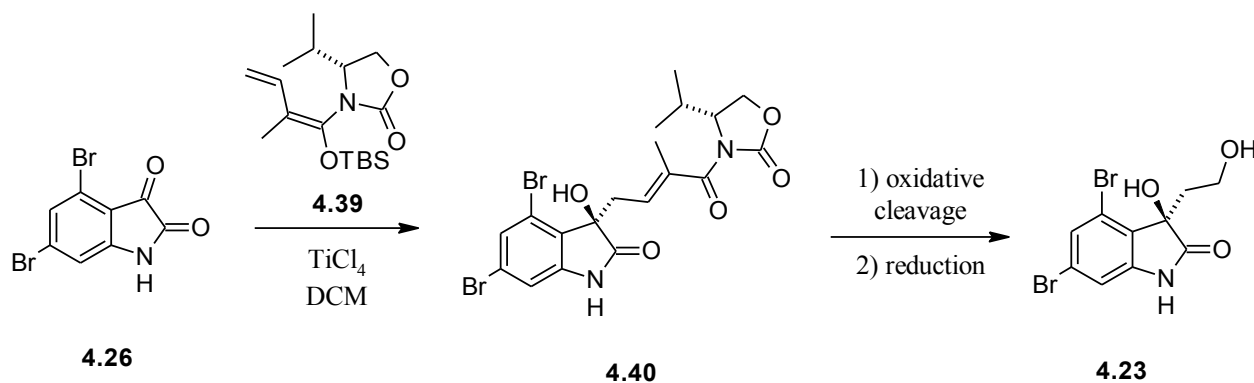
Synthetically, the few efforts towards **4.23** have been centered around the Aldol reaction. Hayashi and co-workers have used a 3-hydroxy-L-prolinol organocatalyst to facilitate the Aldol reaction between *N*-protected 4,6-dibromoisatin **4.38** and acetaldehyde. The resultant aldehyde

was then reduced to the natural product. Unfortunately, this methodology provided only the enantiomer of the naturally occurring molecule (Scheme 4.15)²³.



Scheme 4.15: Organocatalytic total synthesis of (*R*)-convolutamydine *E*

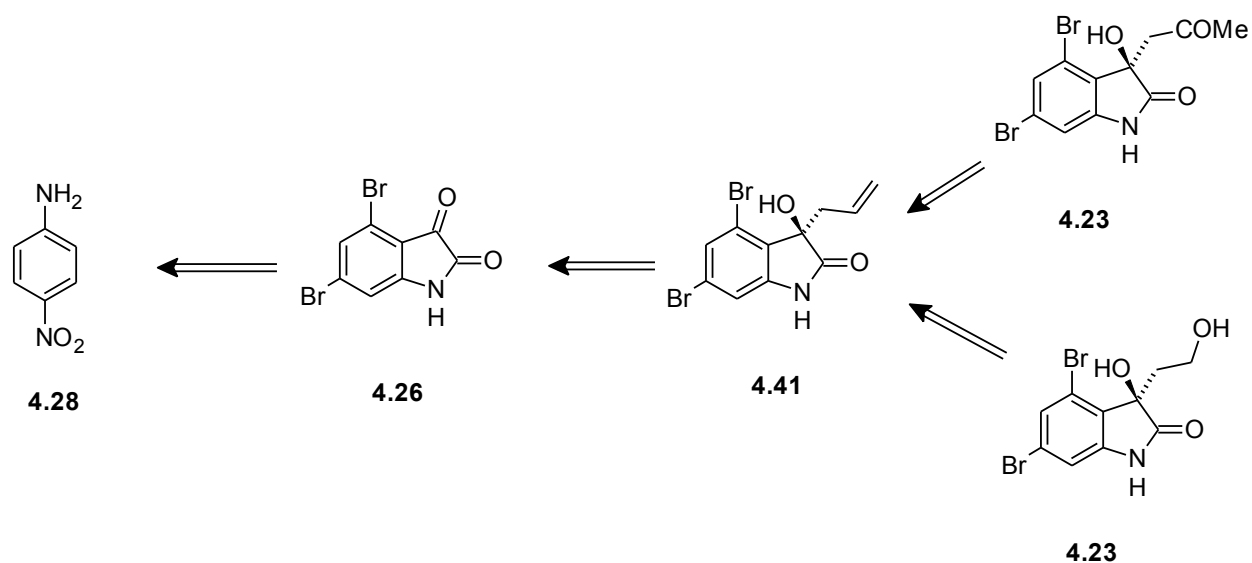
The Kobayashi group has also reported a total synthesis which involves a vinylogous Mukaiyama Aldol reaction, where silyl enol ether **4.39** is reacted with **4.26** under Lewis acidic conditions to give an allylated-type of product, **4.40**. This is oxidatively cleaved to provide the aldehyde, which is reduced to the primary alcohol giving **4.23** (Scheme 4.16)²⁴.



Scheme 4.16: Vinylogous Mukaiyama Aldol reaction leading to (*R*)-convolutamydine *E*

4.4. Retrosynthetic Analysis for Convolutamydines A and E

In planning a retrosynthetic analysis of **4.22** and **4.23**, the common precursor that was envisioned was the 3-allyl-3-hydroxy-dibromoisatin, **4.41**. Wacker oxidation of the allyl group would provide **4.22** and oxidative cleavage with a reductive work-up would provide **4.23**. The allylated material would come from **4.26** via the Cook group's established In(0)-mediated allylation of isatins. The starting material, **4.26**, would come from the known method starting from **4.28** (Scheme 4.17).

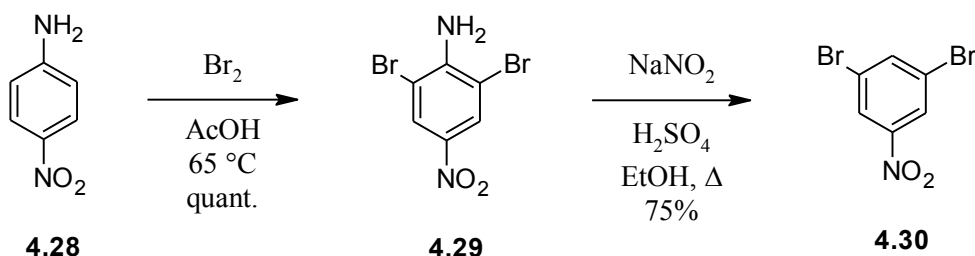


Scheme 4.17: *Proposed retrosynthetic analysis of convolutamydines A and E*

4.5. Attempted Synthesis of (*R*)-Convolutamydine A

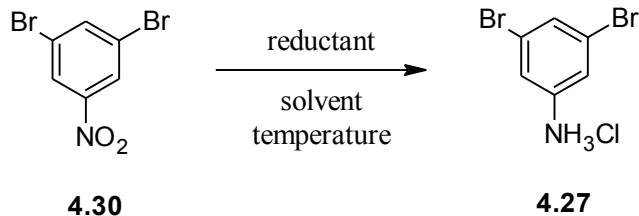
The synthesis began with the bromination of **4.28** using the established conditions (Br_2 in AcOH)²⁵, giving the dibrominated **4.29** in quantitative yield. It was also attempted to use direct bromination methods of nitrobenzene²⁶. These methods were all unsuccessful due to the highly deactivating nature of the nitro group on the aromatic ring. The literature reports good yields

and simple protocols, but all reagents were recovered unchanged in our hands. Diazotization of **4.29** under acidic conditions provided **4.30** (Scheme 4.18)²⁷.



Scheme 4.18: *Synthesis of 3,5-dibromonitrobenzene (4.30)*

Reduction of the nitro group proved to be more difficult than originally anticipated. The literature showed several options, but all failed to give useful amounts of product when attempted. Only SnCl_2 (Table 4.1-Entry 5) acted as an acceptable reduction agent, which provided the HCl salt **4.27** in good yields (Table 4.1)²⁸. The protocol involving Raney-Ni was unsuccessful in our hands. The electronic nature of **4.30** requires that a precise matching of the reduction potential of the reducing metal be achieved.

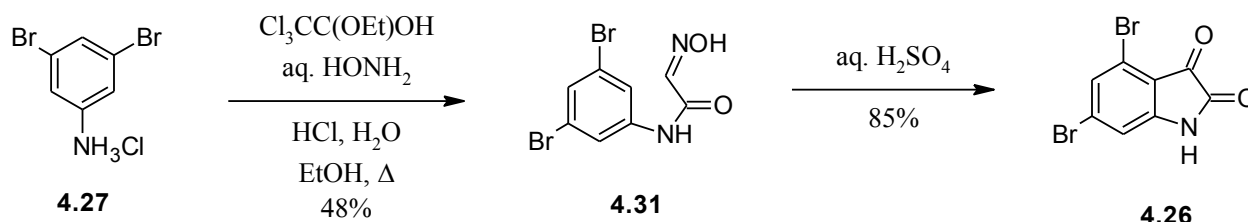
Table 4.1: *Trials for the reduction of 4.30 to 4.27*

Entry	Reducing Agent	Solvent	Temperature (°C)	Additive	% Yield (isolated) ^a
1	Fe(0)	AcOH	25	-	15
2	Fe(0)	AcOH	25	Ac ₂ O	10 ^b
3	Fe(0)	AcOH	80	H ₂ O	2
4	Sn/HCl	H ₂ O	80	-	0
5	SnCl₂	EtOH	95	-	87

^a: Yields are an average of two trials ^b: Product was isolated as the acetyl-protected aniline

To synthesize the required isonitrosoanilide (**4.31**), the literature utilizes chloral, which is a regulated substance according to the Drug Enforcement Agency (DEA). Due to the lack of DEA approval for purchasing chloral, two alternatives were explored. The isonitrosoanilide could be prepared from α,α -bis(acetoxy)acetyl chloride in a mildly basic solution along with hydroxylamine²⁹. Attempts to synthesize the acetyl chloride lead to low yields of an impure product which could not be readily purified by distillation. Analysis of the literature yielded 1,1,1-trichloro-2-ethoxyethanol, a convenient chloral surrogate for use in the preparation of isonitrosoanilides. Reaction of **4.27** with 1,1,1-trichloro-2-ethoxyethanol and hydroxylamine in an acidic, aqueous environment provided the isonitrosoanilide **4.31**. Interestingly, the addition of Na₂SO₄ (as referenced in the original procedures) was found to be a detriment to product isolation. During the final filtration, the product was adherent to the solid sulfate, and could not

be isolated directly. Upon removal of the sulfate, the reaction proceeded as previously, but the material was able to be identified by $^1\text{H-NMR}$. Compound **4.31** was cyclized using the acidic conditions described in the precedent syntheses to give 4,6-dibromoisatin **4.26** (Scheme 4.19). The cyclization reaction is extremely sensitive to both temperature and concentration of the acid. Precise control of both allowed for a good yield of **4.26** to be isolated (Table 4.2-Entry 6).



Scheme 4.19: Synthesis of 4,6-dibromoisatin **4.26**.

Table 4.2: Cyclization of **4.31** to **4.26** – acid concentration and reaction time experiments

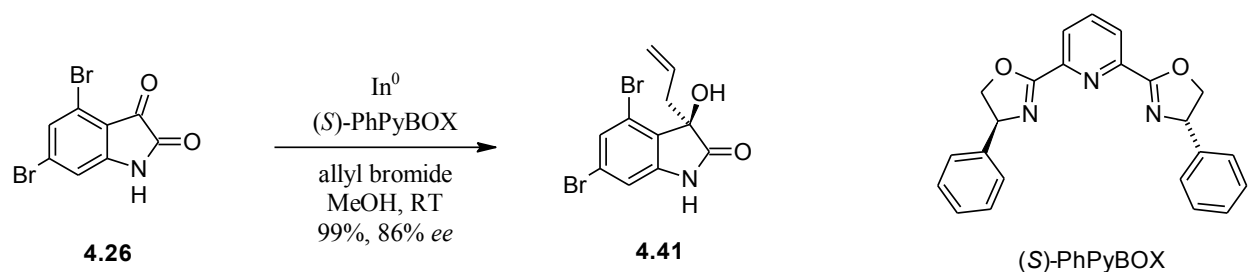
Entry	H ₂ SO ₄ conc. (%) ^a	Rxn Temp (°C) ^b	Rxn Time (min) ^b	% Yield (isolated)
1	98	75	10	0
2	98	75	20	7
3	98	85	10	0
4	98	85	20	0
5	98	80	10	25
6	80	80	10	85

^a: % H₂SO₄ refers to wt/wt % in H₂O.

^b: The substrate was added in portions to the acid at 55°C in all cases.

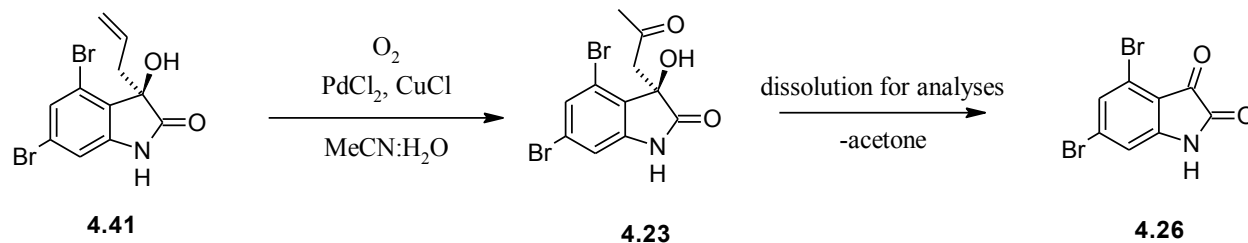
The reaction was then warmed to the indicated temperature and stirred for the indicated time.

After synthesizing **4.26**, it was subjected to the In(0) mediated allylation conditions established by the Cook group. It was found that an additional equivalent of allyl bromide (bringing the total equivalency to 3) was necessary for complete conversion. Thus, treating **4.26** with 3 eq. allyl bromide and 1.5 eq. In(0) using 20 mol% (*S*)-PhPyBOX as a ligand in MeOH provided the allylated **4.41** in near quantitative yield with 86% *ee* (Scheme 4.20).



Scheme 4.20: *In(0)*-mediated allylation of **4.26**

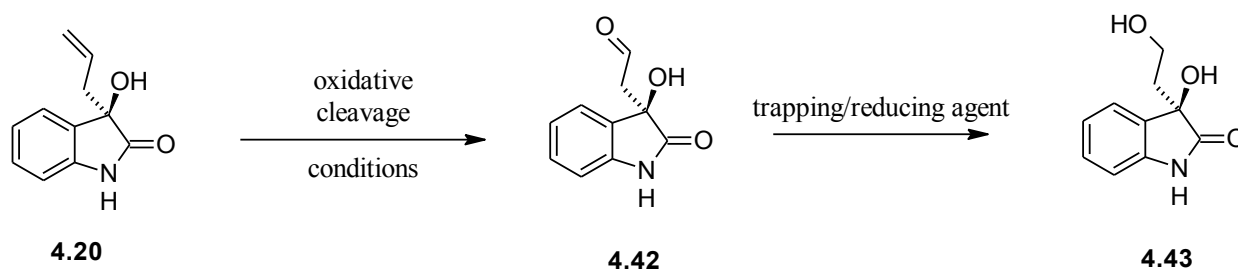
In order to complete the total synthesis of (*R*)-convolutamydine A, a Wacker oxidation was to be performed. Oxidation using standard catalytic PdCl₂ and CuCl using molecular oxygen as a re-oxidant gave a white solid compound which appeared identical to the reported convolutamydine A, but underwent retro-Aldol to give **4.26** and acetone immediately upon entering any solution in preparation for analysis. As such, HRMS and HPLC data could not be obtained, and the product could not be unambiguously confirmed for structure or optical activity (Scheme 4.21).



Scheme 4.21: Attempted Wacker oxidation of **4.41** to give **4.23**

4.6. Synthesis of (*R*)-Convolutamydine E

Due to the extreme similarities between **4.23** and **4.24**, the synthesis of **4.24** was initiated from the dibrominated allyl isatin **4.41**. Initial attempts to oxidatively cleave the allyl group of simple allyl isatin **4.20**, used as a model system, were met with immediate decomposition of the formed aldehyde (Scheme 4.22 and Table 4.3). The decomposition was so rapid that even the *in situ* addition of a reducing agent (i.e. without isolation of the aldehyde) did not yield the desired primary alcohol. Even more active ozonolysis conditions using pyridine as an accelerant provided no product (Table 4.3, Entry 3)³⁰.



Scheme 4.22: Attempted oxidative cleavage of model system **4.20**

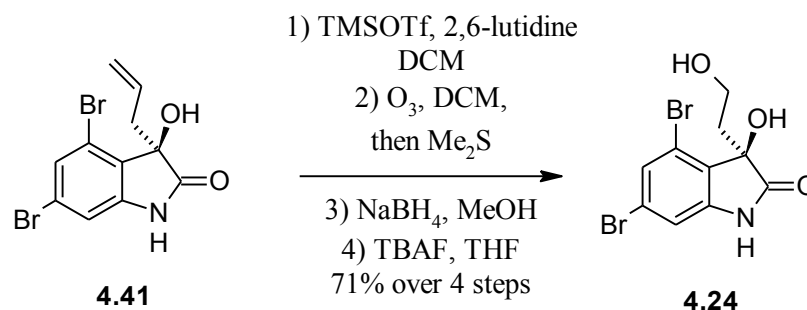
Table 4.3: Attempts to oxidatively cleave 4.20

Entry	Reagent	Rxn Solvent	Trapping/Reducing agent	% SM remaining ^a	% isolated yield ^b
1	O ₃	MeOH	Me ₂ S	0	0
2	O ₃	MeOH	NaBH ₃ CN	0	0
3	O ₃	EtOAc/Pyr ^c	NaBH ₃ CN	0	0
4	OsO ₄ /NMO/NaIO ₄	<i>t</i> BuOH/H ₂ O	NaBH ₃ CN ^d	0	0

^a: As monitored by TLC. ^b: After chromatography. ^c: Pyridine was chosen as a co-solvent due to its ability to accelerate ozonolysis reactions. ^d: NaBH₃CN was used to trap the intermediate aldehyde as opposed to an ozonide.

Although none of the oxidative cleavage protocols yielded product, all of them very clearly converted **4.20** (as observed by TLC). It was hypothesized that the 3° alcohol in **4.42** was somehow trapping either the ozonide or the aldehyde, and thus making a highly unstable ring system, which underwent the observed decomposition. After carefully examining the literature for the previous syntheses, it was discovered that one had used oxidative cleavage, the report by Kobayashi, *et al*²². In order to preserve the 3° alcohol center, they protected it as its TMS ether. It was not discussed as to why this was done, but presumably they observed the same interference in their ozonolysis and came to the same conclusion. By adopting their final strategy, **4.41** was protected as its TMS-ether. Isolation of this compound gave a 59% yield, but the material is relatively unstable and decomposes rapidly. Direct input of the material isolated after rapid purification into the ozonolysis reaction provided the aldehyde (detectable by ¹H-NMR), which was also unstable in solution. Direct input of the rapidly purified aldehyde into the reduction reaction gave the mono-protected diol after an extractive work-up. While this diol is more stable, the TMS-ether does not allow for long-term storage and analyses, and so the

crude mono-protected diol was subjected directly to TBAF deprotection, which provided **4.24** in 71% yield over the four steps (Scheme 4.23).



Scheme 4.23: Oxidative cleavage of **4.41** to yield **4.24**

4.7. Conclusions

Although the synthesis of (*R*)-convolutamydine A was partially unsuccessful, it did demonstrate the utility of the In(0)-mediated allylation strategy developed by the Cook group. The group methodologies which have been focused on green chemistry-based approaches toward synthesis have provided a rapid means to these interesting structural motifs. The total synthesis of (*R*)-convolutamydine E was much more successful, and provided a unique environment to attempt the oxidative cleavage. While the exact structure is fairly unique, the presence of the 3° alcohol at both a benzylic position and a homoallylic position makes for an interesting argument for the widespread utility of this reaction. It shows that it is possible to use the allylic group as a reactive handle for the synthesis of more complicated molecules, while still maintaining the 3° alcohol and that center's stereochemistry. The ozonolysis challenge also showcased the reactivity of these groups within the strain of the planar isatin core, which brings the alcohol and the resultant electrophilic carbon together.

4.8. Experimental Section

4.8.1. General Reaction Considerations

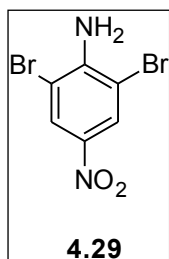
All reactions were conducted in oven-dried (100°C) glassware, and were run under an atmosphere of argon, unless otherwise stated. EtOH is used as an absolute solution. (*S*)-PhPyBOX was prepared according to a previously reported procedure³¹. Indium powder was purchased from Strem Chemicals. Allyl bromide was purified by washing with sat. aq. NaHCO₃ followed by distilled H₂O, drying over CaCl₂, and distilling under reduced pressure. MeOH was distilled from Mg(0). TMSOTf was distilled under N₂ immediately prior to use. 2,6-lutidine was dried over KOH for 24hrs prior to use. DCM and THF were dried by passing the degassed solvent through a column of activated Cu/alumina under N₂ immediately before use.

Chromatography was performed on EMD silica gel (40-60 microns) using air pressure, unless otherwise specified. Preparative TLC was performed on EMD 10 μm silica gel plates. All other solvents and reagents were purchased at the highest level of purity and were used as received.

NMR spectra were obtained on a Varian INOVA NMR instrument, at the indicated field strength in the indicated deuterated solvent. NMR spectra are referenced to internal tetramethylsilane. HRMS were collected on a Bruker BIOTOF III instrument with a positive ESI mode and are referenced to appropriate PEG or NaTFA standards. FTIR spectra were collected on a Bruker Dalton FTIR instrument. Melting points were collected on a Fisher-Johns apparatus and are uncorrected.

4.8.2. Experimental Details

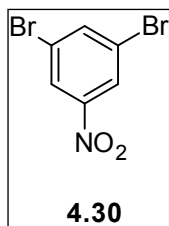
2,6-Dibromo-4-nitroaniline (4.29)



A 500-mL, 3-neck round bottom flask equipped with a magnetic stir bar, condenser, stopper, and addition funnel was charged with *p*-nitroaniline (15.00 g, 0.11 mol) and glacial acetic acid (180 mL). This slurry was set to stir at 65°C, and the addition funnel was charged with a solution of bromine (11.27 mL, 0.22 mol)

in glacial acetic acid (140 mL). This solution was added dropwise, with a heavy precipitate forming upon addition. After approx. 10% of the bromine solution had been added, warm H₂O (15 mL) was added to redissolve the precipitate. The use of additional water did not aid in the dissolving of further precipitates. After the bromine addition was complete, the reaction continued at 65°C for 1.5 hrs, then was cooled to RT. The resultant slurry was poured into a stirring solution of ice (25 g) in water (250 mL), and the resultant yellow precipitate was filtered and air dried to give **4.29** as a fluffy yellow solid (30.64 g, 94%). m.p. 193-195°C (lit. 204-206°C³²); ¹H-NMR (400 MHz, DMSO-*d*₆) δ 6.75 (bs, 2H, NH₂), 8.25 (s, 2H, Ar-*H*, symm.); ¹³C-NMR (100 MHz, DMSO-*d*₆) δ 110.77, 133.43, 141.92, 154.63. FTIR (thin film): $\bar{\nu}$ (max): 3584, 3372, 2293, 2853, 1605, 1457 (d), 1300, 1128 cm⁻¹; HRMS (ESI), *m/z*: 318.8518 (M+Na⁺), calc. for C₆H₄N₂O₂Br₂Na: 318.8511.

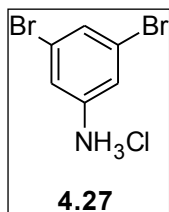
3,5-Dibromo-1-nitrobenzene (4.30)



A 50-mL, 2-neck round bottom flask equipped with a magnetic stir bar, condenser, and stopper was charged with **4.29** (1.92 g, 6.5 mmol), EtOH (22 mL), and concentrated H₂SO₄ (10% v/v, 2.2 mL). This solution was set to stir at reflux, and powdered NaNO₂ (1.44 g, 20.93 mmol) was added slowly through the open neck of the flask.

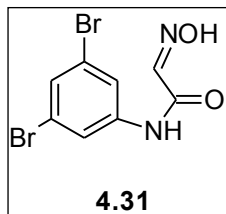
Vigorous frothing was observed upon addition, and the rate of addition was slowed accordingly to allow for this to subside. After the addition was complete, the reaction ran at reflux for 24 hrs, upon which time TLC (60:40 EtOAc:hexanes) showed complete consumption of SM. Reaction was cooled to RT, and poured onto crushed ice (25 g) in water (25 mL), and the resultant brown precipitate was filtered and air dried to give **4.30** (1.37 g, 75%), which was used without further purification. m.p. 102-107°C (lit. 104°C)³³; ¹H-NMR (400 MHz, CDCl₃) δ 8.00 (s, 1H, Ar-*H*), 8.33 (s, 2H, Ar-*H*); ¹³C-NMR (100 MHz, CDCl₃) δ 123.69, 125.80, 140.27. FTIR (thin film): $\bar{\nu}$ (max): 2293, 2853, 1462 (d) cm⁻¹.

3,5-Dibromoaniline hydrochloride (**4.27**)



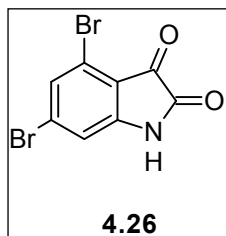
A 10-mL round bottom flask equipped with a magnetic stir bar was charged with **4.30** (1.0 g, 3.56 mmol), SnCl₂ (3.37 g, 17.80 mmol), and EtOH (absolute, 10mL). This mixture was brought to reflux, with the appearance changing from a brown slurry to a dark brown solution after approx. 1 min of heating. The reaction continued at reflux for 4 hrs, when TLC (60:40 EtOAc:hexanes) determined complete consumption of the SM. The reaction was cooled to RT, poured onto crushed ice (10 g), and diluted with H₂O (10 mL). The resultant solution was extracted with EtOAc (2 x 25 mL), with some hazy tin salts being observed in the organic phase. The resultant organic slurry was filtered through Celite, and the filtrate was dried over MgSO₄. Filtration of the drying agent and concentration gave **4.27** as a tan/yellow solid (0.89g, 87%). m.p. >190°C (dec.); ¹H-NMR (500 MHz, CDCl₃) δ 7.03 (s, 1H, Ar-*H*), 6.84 (s, 2H, Ar-*H*), 3.75 (bs, 2H, NH₂); ¹³C-NMR (125 MHz, CDCl₃) δ 148.9, 123.9, 123.6, 119.6, 119.0, 116.8; FTIR (thin film): $\bar{\nu}$ (max): 3384 (broad), 2923 cm⁻¹; HRMS (ESI), *m/z*: 251.8836 (M+H⁺), calc. for C₆H₆NBr₂: 251.8841.

3,5-Dibromoisourosulfonamide (4.31)



A 50-mL round bottom flask equipped with a magnetic stir bar and a condenser was charged with **4.27** (1.44 g, 5.0 mmol), H₂O (15 mL), EtOH (10 mL), and concentrated HCl (0.15 mL). To this solution was added hydroxylamine (50% in H₂O, 0.5 mL, 7.5 mmol), and 1,1,1-trichloro-2-ethoxyethanol (1.16 g, 6.0 mmol), in that order. The resultant mixture was brought to reflux for 4 hrs, at which time TLC (60:40 EtOAc:hexanes) showed complete consumption of the SM. The reaction mixture was allowed to boil without the condenser for 10 min., then was cooled to RT and filtered. The filter cake was washed with H₂O and dried in a dessicator over silica gel to yield **4.31** as a light yellow/off-white solid (1.13 g, 44%). The product was taken forward to the next step without further purification.

4,6-Dibromoisatin (4.26)

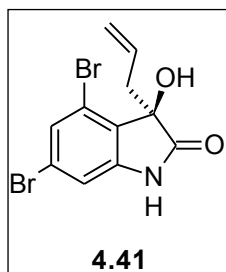


A 2-dram vial equipped with a magnetic stir bar was charged with 80% H₂SO₄ (1 mL), and warmed to 55°C. Solid **4.31** (0.2 g, 0.62 mmol) was added in portions over 15 min, then the now deep red solution was carefully heated to 80°C (anything higher than 80°C results in rapid decomposition) and then the reaction mixture was poured into 20 g crushed ice and allowed to sit for 30 min. The precipitate was filtered and washed with water to give **4.26** as a light brown solid (176 mg, 87%). Recrystallization from EtOAc gave fine brown needles. mp 253°C (dec.); ¹H-NMR (400 MHz, DMSO-*d*₆) δ 11.23 (s, 1H), 7.47 (dd, *J*=1.6 Hz, 3.6 Hz, 1H), 7.01 (dd, *J*=1.6 Hz, 3.6 Hz, 1H); ¹³C-NMR (100 MHz, DMSO-*d*₆) δ 216.6, 191.7, 159.3, 153.7, 132.0, 129.2, 120.9, 114.8;

FTIR (thin film): $\bar{\nu}$ (max): 3682, 3019, 2400, 1711, 1523, 1423, 1221, 1214, 784, 735 cm^{-1} ;

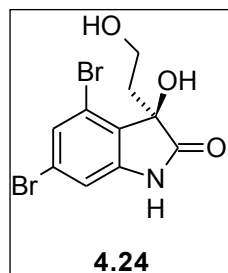
HRMS (ESI) m/z : 327.8407 ($\text{M}+\text{Na}^+$)⁺, calc. for $\text{C}_8\text{H}_3\text{NO}_2\text{Br}_2\text{Na}$: 327.8403.

(R)-3-Allyl-4,6-dibromo-3-hydroxy-2-oxindole (4.41)



A 20-mL scintillation vial equipped with a magnetic stir bar was charged with **4.26** (0.1 g, 0.33 mmol), (*S*)-PhPyBOX (20 mol%, 24 mg, 0.066 mmol), In powder (56 mg, 0.49 mmol), and MeOH (6 mL). To this stirring slurry at RT was added allyl bromide (57 μL , 0.66 mmol) via syringe, and the reaction proceeded for 5 hrs, after which time TLC (60:40 EtOAc:hexanes) showed complete consumption of SM. The volatiles were removed *in vacuo* and the residue was triturated with 60:40 EtOAc:hexanes and passed as a slurry through a plug of silica gel, using 5 column volumes to wash the plug. The resultant solution was concentrated to give **4.41** as a brown-orange solid (64 mg, 99%), which was shown by chiral HPLC (AD-3 column, 10% *iso*-propanol in hexane, 1mL/min) to have an *ee* of 87%. $[\alpha]_D^{25}$: 2.400 (*c* 0.5, MeOH); $^1\text{H-NMR}$ (400 MHz, CDCl_3) δ 8.81 (bs, 1H), 7.31 (d, $J=1.6$ Hz, 1H), 6.94 (d, $J=1.2$ Hz), 5.34 (m, 1H), 5.07 (dd, $J=1.6$ Hz, 17.2 Hz, 1H), 4.97 (dd, $J=1.6$ Hz, 10Hz. 1H), 3.67 (bs, 1H), 2.95 (ddd, $J=7.2$ Hz, 10.8 Hz, 162 Hz, 2H); $^{13}\text{C-NMR}$ (100 MHz, CDCl_3) δ 179.1, 143.5, 129.6, 129.5, 127.1, 124.0, 121.1, 120.2, 113.3, 78.2, 40.0; FTIR (EtOH) $\bar{\nu}$ (max): 3355, 2974, 2889, 1734, 1610, 1381, 1090, 1050, 881, 735 cm^{-1} ; HRMS (ESI), m/z : 369.8873 [$\text{M}+\text{Na}^+$]⁺, calc. for $\text{C}_{11}\text{H}_9\text{O}_2\text{NBr}_2\text{Na}$: 369.8872.

(R)-4,6-Dibromo-3-(2-hydroxyethyl)-3-hydroxy-2-oxindole (convolutamydine E, 4.24)



A solution of **4.41** (87.5 mg, 0.252 mmol), in dry DCM (1.5 mL) was cooled to -30°C , under argon. With stirring, 2,6-lutidine (0.18 mL, 1.54 mmol) was added, dropwise. After addition, freshly distilled TMSOTf (0.15 mL, 0.635 mmol) was added, dropwise. After addition was complete, the reaction mixture was warmed to 0°C and allowed to stir for 3 hrs, when TLC (60:40 EtOAc:hexane) showed complete consumption of starting material. The reaction was then quenched with sat. aq. NaHCO_3 at that temperature, and allowed to warm to RT, then extracted with DCM (2 x 5 mL). The combined organic phases were washed with brine (10 mL), dried (Na_2SO_4), filtered, and concentrated. The residue was purified by flash column chromatography using a short column of silica gel (N_2 pressure, 60:40 EtOAc:hexane, $R_f = 0.98$) to give the TMS-protected compound as an off-white solid. This was carried forward without further purification.

The TMS-protected material was dissolved in dry DCM (3.5 mL), and a stream of O_3 was bubbled through the solution, with stirring, at -78°C . After approx. 5 min, the solution had turned blue, and the O_3 was continued for an additional 2 min, then argon was bubbled through the solution to remove any excess O_3 . To the resultant pale solution was added Me_2S (0.3 mL) and the reaction was warmed, with stirring, to 0°C , and kept there for 15 additional minutes. The reaction was concentrated to give a light orange oil, which was dissolved in MeOH (1.5 mL), and powdered NaBH_4 (7.7 mg, 0.204 mmol) was added to the stirring solution at 0°C , under a stream of N_2 . The reaction ran for 2hrs, and then was quenched with sat. aq. NH_4Cl , and extracted with EtOAc (3 x 5 mL). The combined organic phases were washed with brine (10 mL), dried (Na_2SO_4), filtered, and concentrated to give the desired monoprotected diol as a light yellow sticky solid, which was taken forward without further purification.

The monoprotected diol was dissolved in dry THF (4 mL), and cooled to 0°C, under argon. With stirring, a commercial solution of tetra-*n*-butylammonium fluoride (TBAF, 1.0 M in THF, 0.197 mL, 1.27 mmol) was added dropwise. The solution turned to a lighter shade of yellow upon addition. After 30 minutes at 0°C, the reaction was quenched with the addition of sat. aq. NH₄Cl, and extracted with ether (2 x 5 mL). The combined organic layers were washed with brine (10 mL), dried (Na₂SO₄), filtered, and concentrated. Purification by preparative TLC using 2:1 EtOAc:hexane as eluent furnished the desired product, convolutamydine E (**4.24**), as a white solid (38.5 mg, 71% over 4 steps). m.p. 132-134°C; ¹H-NMR (400 MHz, acetone-*d*₆) δ 9.44 (bs, 1H), 7.19 (dd, *J*=0.8 Hz, 0.8 Hz, 1H), 6.94 (dd, *J*=0.8 Hz, 0.8 Hz, 1H), 5.12 (bs, 1H), 5.05 (s, 1H), 3.37 (dt, *J*=6 Hz, 2.4 Hz, 2H), 2.32 (m, 2H, coupling of 0.8 Hz is observed); ¹³C-NMR (100 MHz, acetone-*d*₆) δ 185.6, 144.3, 143.2, 138.2, 135.5, 127.8, 127.7, 72.7, 52.9, 35.5; FTIR (thin film) $\bar{\nu}$ (max) 3430, 2960, 2925, 2848, 1728, 1608 cm⁻¹; HRMS (ESI), *m/z*: 371.8859, 373.8811, 375.8810 [M+Na⁺], calc. for C₁₀H₉O₃NBr₂Na: 371.8841, 373.8821, 375.8802.

4.9. References

- ¹ Nicolaou, K.C., Li, H., Boddy, C., Ramanjulu, J., Yue, T-Y., Natarajan, S., Chu, X-J., Bräse, S., Rübsam, F.; *Chem. Eur. J.*, **1999**, *5*, 2584-2601; Nicolaou, K.C., Boddy, C., Li, H., Koumbis, A., Hughes, R., Natarajan, S., Jain, N., Ramanjulu, J., Bräse, S., Solomon, M.; *Chem. Eur. J.*, **1999**, *5*, 2602-2621.
- ² Anderson, J., Roberts, C.; *Tetrahedron Letters*, **1998**, *39*, 159-162.
- ³ Buchwald, S., Nordmann, G.; *J. Am. Chem. Soc.*, **2003**, *125*, 4978-4979.
- ⁴ Hanessian, S., Giroux, S., Larsson, A.; *Org. Lett.*, **2006**, *8*, 5481-5484.
- ⁵ Schmidt, B.; *Eur. J. Org. Chem.*, **2003**, 816-819.
- ⁶ Qi, Xiangbing, Rice, G., Lall, M., Plummer, M., White, M.C.; *Tetrahedron*, **2010**, *66*, 4816-4828.
- ⁷ Horváth, I., Anastas, P.; *Chem. Rev.*, **2007**, *107*, 2167-2168; Walsh, P., Li, H., Anaya de Parrodi, C.; *Chem. Rev.*, **2007**, *107*, 2503-2545.
- ⁸ Cook, G., Kargbo, R., Maity, B.; *Org. Lett.*, **2005**, *7*, 2767-2770; Kargbo, R., Takahashi, Y., Bhor, S., Cook, G., Lloyd-Jones, G., Shepperson, I.; *J. Am. Chem. Soc.*, **2007**, *129*, 3846-3847.
- ⁹ Cook, G., Maity, B., Kargbo, R.; *Org. Lett.*, **2004**, *6*, 1741-1743.
- ¹⁰ Cook, G., Kargbo, R., Maity, B.; *Org. Lett.*, **2005**, *7*, 2767-2770.

- ¹¹ Kargbo, R., Takahashi, Y., Bhor, S., Cook, G., Lloyd-Jones, G., Shepperson, I.; *J. Am. Chem. Soc.*, **2007**, *129*, 3846-3847.
- ¹² Samanta, D., Kargbo, R., Cook, G.; *J. Org. Chem.*, **2009**, *74*, 7183-7186.
- ¹³ Song, Xixi; Bismuth-Mediated, Barbier-type Asymmetric Allylation of Activated Imines and Ketones, M.S. Thesis, May 2008, North Dakota State University; *manuscript in preparation*; Balasubramanian, Ganesh; Stereoselective Carbon-Carbon Bond Forming Reactions Using Indium and Bismuth: New Approaches in Green Chemistry, Ph.D. Thesis, August 2012, North Dakota State University; *manuscripts in preparation*.
- ¹⁴ Balasubramanian, Ganesh; Stereoselective Carbon-Carbon Bond Forming Reactions Using Indium and Bismuth: New Approaches in Green Chemistry, Ph.D. Thesis, August 2012, North Dakota State University; *manuscripts in preparation*.
- ¹⁵ Peddibhotla, S.; *Curr. Bioactive Compounds*, **2009**, *5*, 20-38.
- ¹⁶ Antilla, J., Klapars, A., Buchwald, S.; *J. Am. Chem. Soc.*, **2002**, *124*, 11684-11688; Jiang, J., Koehl, J., Mehdi, S., Moorcroft, N., Musick, K., Weintraub, P., Eastwood, P.; US 2005/0054631 A1, **2005**
- ¹⁷ Kamana, Y., Zhang, H., Ichihara, Y., Kizu, H., Komiyama, K., Pettit, G.; *Tett. Lett.*, **1995**, *36*, 2783-2784.
- ¹⁸ Malkov, A., Kabeshov, M., Bella, M., Kysilka, O., Malyshev, D., Pluháčková, K., Kočovský, P.; *Org. Lett.*, **2007**, *9*, 5473-5476; Nakamura, S., Hara, N., Nakashima, H., Kubo, K., Shibata, N., Toru, T.; *Chem. Eur. J.*, **2008**, *14*, 8079-8081.
- ¹⁹ Garden, S., Torres, J., Ferreira, A., Silva, R., Pinto, A.; *Tetrahedron Letters*, **1997**, *38*, 1501-1504; Jnaneswara, G., Bedekar, A., Deshpande, V.; *Synth. Commun.*, **1999**, *29*, 3627-3633.
- ²⁰ Jnaneshwar, G., Deshpande, V.; *J. Chem. Res.*, **1999**, 632-633.
- ²¹ Cravotto, G., Giovenzana, G., Palmisano, G., Penoni, A., Pilati, T., Sisti, M., Stazi, F.; *Tetrahedron: Asymmetry*, **2006**, *17*, 3070-3074.
- ²² Kamano, Y., Kotake, A., Hashima, H., Hayakawa, I., Hiraide, H., Zhang, H-P., Kizu, H., Komiyama, K., Hayashi, M., Pettit, G.; *Collect. Czech. Chem. Commun.*, **1999**, *64*, 1147-1153.
- ²³ Itoh, T., Ishikawa, H., Hayashi, Y.; *Org Lett.*, **2009**, *11*, 3854-3857.
- ²⁴ Nakamura, T., Shirokawa, S., Hosokawa, S., Nakazaki, A., Kobayashi, S.; *Org. Lett.*, **2006**, *8*, 677-679.
- ²⁵ Chanteau, S., Tour, J.; *J. Org. Chem.*, **2003**, *68*, 8750-8766.
- ²⁶ Rajesh, K., Somasundaram, M., Saiganesh, R., Balasubramanian, K.; *J. Org. Chem.*, **2007**, *72*, 5867-5869.
- ²⁷ See Ref. 23, as well as: Carlin, R., Forshey, W.; *J. Am. Chem. Soc.*, **1950**, *72*, 793-801.
- ²⁸ This protocol was used in Ref. 23's prep of the material; however it became immediately clear that additional steps were necessary to isolate the product. The reference's authors describe the isolation of the free aniline from the concentrated reaction mixture, while I was only ever able to isolate the HCl salt from the organic layer (presumably the salt is still soluble in the organic phase due to the location of the bromine atoms). Also, a large amount of Sn salts were present in the work-up. See Experimental Details.
- ²⁹ Rewcastle, G., Sutherland, H., Weir, C., Blackburn, A., Denny, W.; *Tetrahedron Letters*, **2005**, *46*, 8719-8721.
- ³⁰ Li, F., Tartakoff, S., Castle, S.; *J. Org. Chem.*, **2009**, *74*, 9082-9093.
- ³¹ Nishiyama, H., Kondo, M., Nakamura, T., Itoh, K.; *Organometallics*, **1991**, *10*, 500-508.
- ³² Shepard, R.; *J. Org. Chem.*, **1947**, *12*, 275.

³³Kubiczak, G., Oesch, F., Borlakoglu, J., Kunz, H., Robertson, L.; *J. Agric. Food Chem.*, **1989**, *37*, 1160-1164.

CHAPTER 5. FINAL CONCLUSIONS AND FUTURE WORK

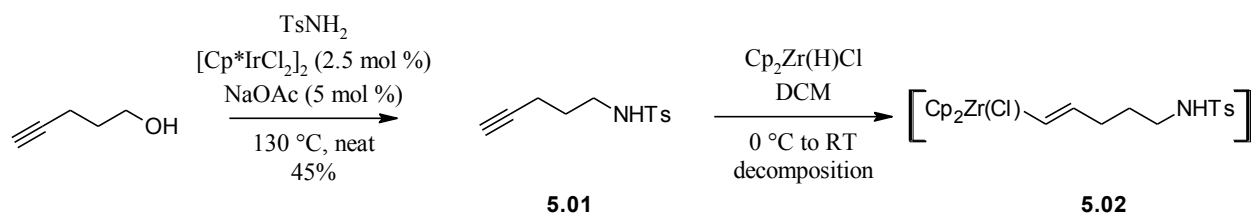
5.1. Attempted Total Synthesis of Huperzine X

In the monumental effort to synthesize this complex and complicated molecule, many reactions and potential pathways were explored. Many of these did not yield usable products, performed significant side reactions, or simply did not react under the literature reported conditions. However, the use of these reactions as well as the reactions which produced the desired products has allowed for a broader view of the synthesis and the implications for the future of the project.

5.1.1. The Main Synthesis

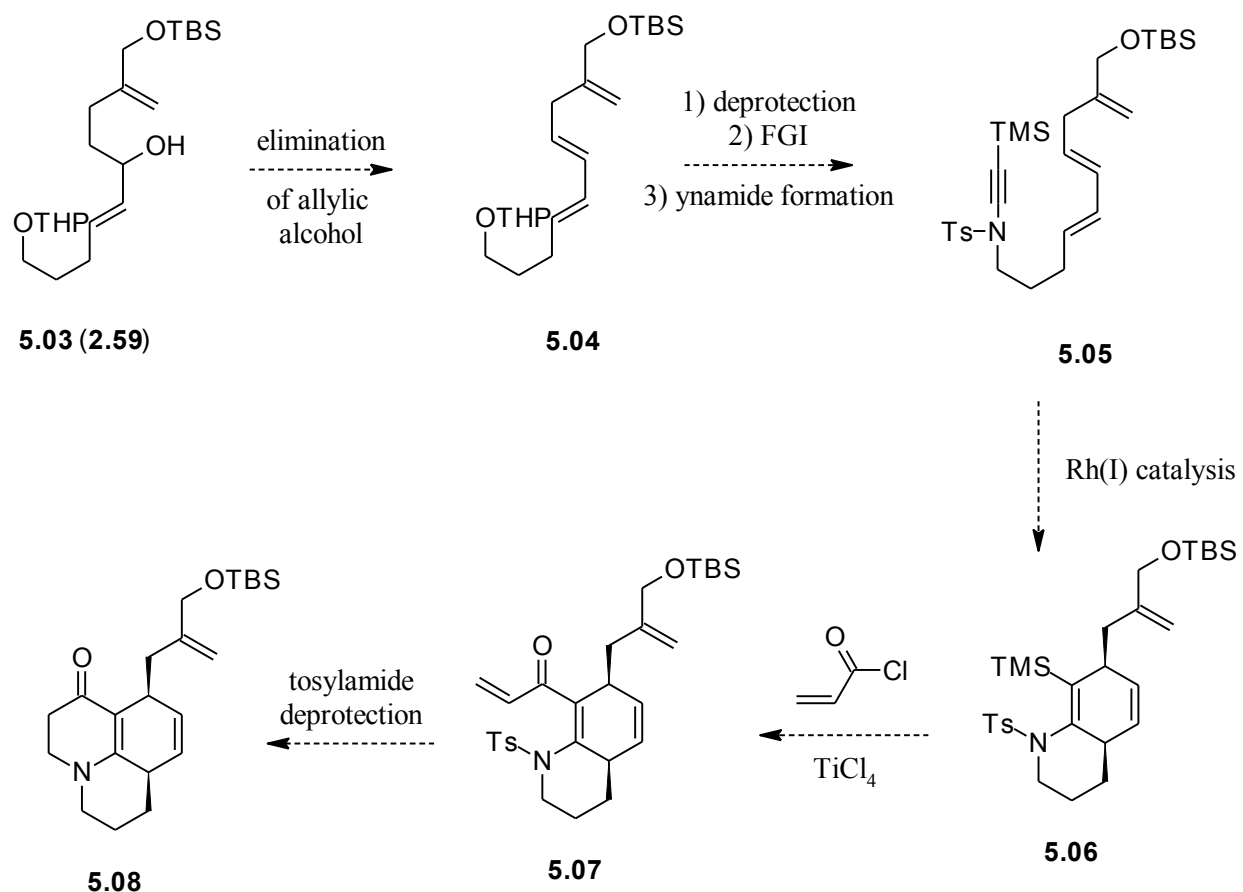
While the carbon backbone of the main Huperzine X was successfully synthesized, it has not been completed. Initial screenings of conditions to eliminate the allylic alcohol and produce the desired 1,3-diene motif have been unsuccessful at both acquiring the desired structure in a reasonable yield as well as achieving high *trans* selectivity. The issue is primarily the “loose” carbon chain, which cannot be held into a rigid structure in order to facilitate selectivity. The solution to such a problem is unclear. It does seem clear that direct elimination of the allylic alcohol is not going to result in the desired selectivity. Another issue is the incorporation of the nitrogenous functionality. As currently proposed, the nitrogen must be installed through a nucleophilic displacement of the parent alcohol with azide. Reduction of this azide and protection with tosylate provides a long route to the desired structure. It may be possible to utilize tosylamide as a starting material and couple the nitrogen directly using iridium catalysis¹. In generalized studies, this was found to be possible to install the tosylamide directly onto 4-

pentyn-1-ol, but the tosylamide **5.01** was found to be highly competitive to hydrozirconation under the established conditions. While this is due in large part to the acidic hydrogen of the tosylamide, sulfonylated amines are generally poor substrates for hydrozirconation (Scheme 5.1).



Scheme 5.1: Attempted use of Ir-catalyzed nitrogenous coupling to produce viable transmetalation partner **5.02**

If the alcohol problem can be solved and the nitrogen installed, the work already done on the Diels-Alder model system shows that the ynamide can be formed using the alkynyl iodonium triflate chemistry. The cationic Rh(I) [4+2] cycloaddition will lead to the formation of the B and D rings simultaneously. If work can be completed on an enantioselective variant of the reaction (see Section 5.1.2), the major stereocenters of Huperzine X can be installed in one step (Scheme 5.2). Quenching of the reactive vinyl silane with acryloyl chloride using a halogen source to facilitate reformation of the olefin should prove straightforward². Tosylamide deprotection is often problematic, and the recent surge in the use of SmI₂ will almost certainly be hazardous to the other functionality in **5.07**³, so the use of a more functional group tolerant approach will be necessary, as exemplified by Nayak with the use of low-valent Ti species⁴. Provided the deprotection does not alter the free olefins or the 1,4-cyclohexadiene structure, the liberated amine will undergo Michael addition, resulting in **5.08**.



Scheme 5.2: Projected synthesis of the tricyclic core of Huperzine X

With the A ring synthesized, efforts will be focused on transforming the OTBS group to the more reactive TMS group. This can be accomplished through first a deprotection of the silyl ether, followed by acetylation of the allylic alcohol. The acetylation should not affect the nitrogenous functionality, due to its conjugation as an enamine. The allylic acetate should be able to be converted to the allylic TMS compound through now standard Pd-catalyzed chemistry⁵. Our proposed intramolecular allylation can then be performed. The final stages of the synthesis are more straightforward; the critical goal of creating the central *lycopodine* core will at this point have been successful.

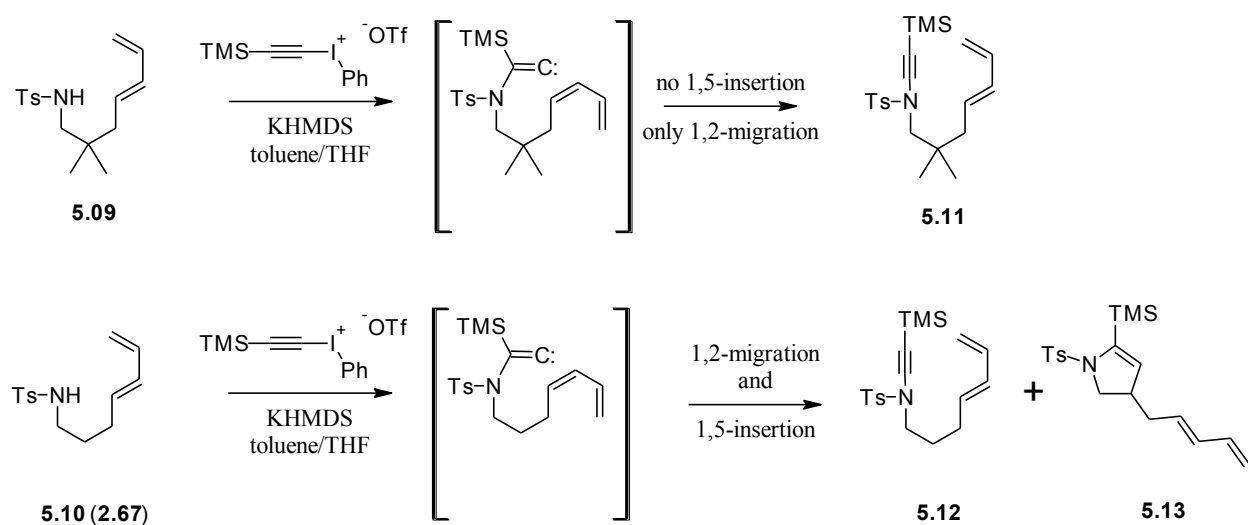
5.1.2. Diels-Alder Model System

There are two major areas of improvement for the Diels-Alder model system. The most important is the optimization of the cationic Rh(I)-catalyzed intramolecular ynamide Diels-Alder chemistry. Isolation of only 20% yield indicated that formation of the 6,6-fused ring system was problematic. As the reaction is under kinetic control, and this does not favor 6,6-ring formations, it is possible that an increase in reaction temperature might facilitate this structure's formation. As such, a screening of various temperatures may lead to optimization of the reaction. It appears that the silver salt and solvents (DCE and toluene) are optimum for reactivity and solubility, and are thus not expected to change. The use of Wilkenson's catalyst is also optimum as it is relatively inexpensive and is able to survive prolonged storage without purification.

If the yield can be improved, it is theoretically possible to add a chiral ligand to induce a chiral preference in the reaction. The model system's product possesses only one chiral center, making the added issues of *syn/anti* selectivity in the Diels-Alder reaction nonexistent. Research has shown that Rh(I) catalyzed (both cationic and neutral metal centers) cycloadditions can be influenced to a large extent by simple chiral ligands such as BINAP⁶ and H₈-BINAP⁷. Most significant of these previous examples is the precedent set by Shibata and co-workers, using BINAP to effect [4+2] cycloadditions between 1,3-dienes and acetylenedicarboxylates, which share many similarities to our proposed ynamide Diels-Alder chemistry⁸. In this light, we have confidence that a ligand of the BINAP family will be effective at controlling stereochemistry for our desired 1,4-cyclohexadiene product.

A side project that has been designed for examination as a model system is to synthesize **5.09**, a dimethylated analog of the previously shown **5.10 (2.67)**. This molecule can be used to

test the theory that the low yield of the ynamide formation is due to 1,5-insertion of the transient vinylidene carbene created by the attack of the tosylamide nitrogen onto the iodonium alkyne and subsequent loss of iodobenzene (Scheme 5.3). It is thought that blocking these positions will shut down the 1,5-insertion and increase the yield. The two methyl groups should be far enough away from the reactive center that they shouldn't directly interfere with the ynamide formation, but should only serve as insertion blocking groups.



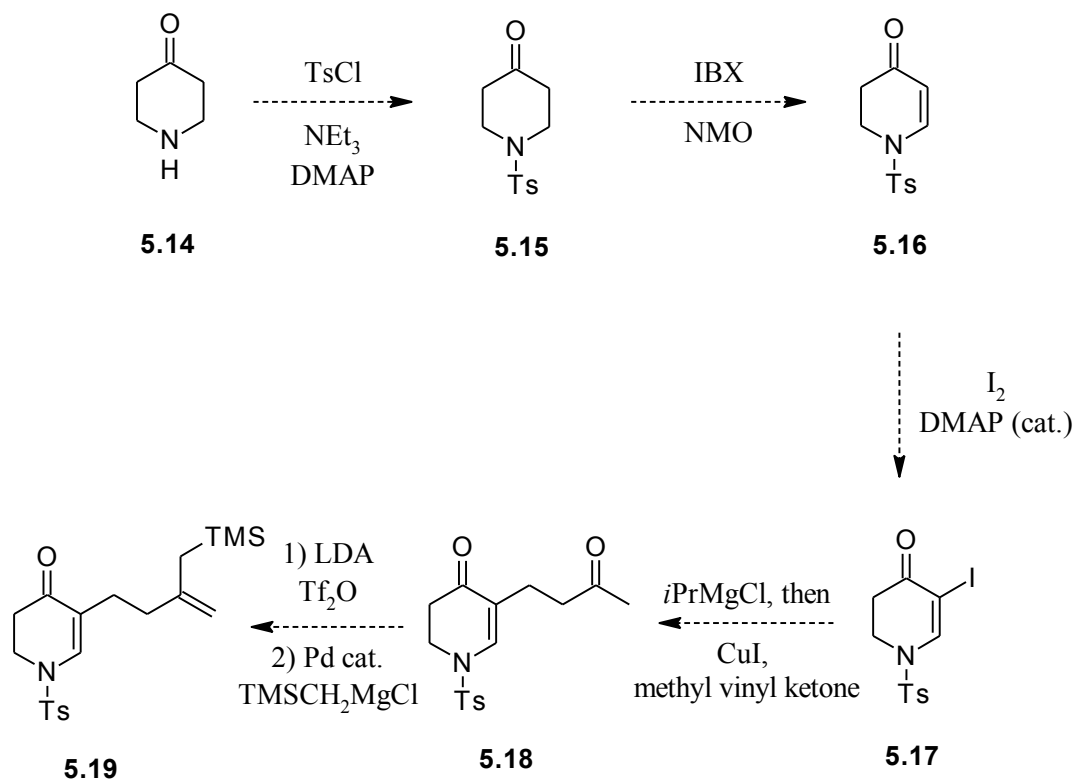
Scheme 5.3: *Alternative experiments to determine cause of low yield in ynamide formation*

While it is possible for both **5.11** and **5.12** to undergo [2+1] cycloaddition with the internal olefin of the 1,3-diene moiety, it is thought that this pathway is unfavorable due to the formation of a larger fused ring system (7,3). The product of such a formation would also be difficult to detect, as it would be a vinyl cyclopropane, and thus likely to rearrange.

With the creation of an optimized, enantioselective ynamide Diels-Alder reaction and better understanding of how to increase the yield of the initial ynamide formation, the Diels-Alder model system will provide excellent support for the campaign to complete Huperzine X.

5.1.3. Allylation Model System

While we were unable to cause allyltrimethylsilane to react with 2,3-dihydro-4-pyridones protected with benzyl groups, it was thought that a more electron withdrawing group such as a tosyl might improve reactivity. Tosylation of 4-piperidone (**5.14**) followed by IBX oxidation is reported⁹. Although it is not reported, 2,3-dihydro-4-pyridone **5.16** should be able to be functionalized at the α position using reported iodination chemistry¹⁰. Our studies have shown that metalation using *i*PrMgCl and subsequent CuI-mediated 1,4-addition of these types of α -iodo-2,3-dihydro-4-pyridones onto methyl vinyl ketone is very effective (Scheme 5.4). Standard triflation of the kinetic enolate and subsequent Kumada coupling is projected to produce the desired intramolecular allylalliton system. The conditions for allylation promotion can be screened as an intermolecular variant using **5.16** and allyltrimethylsilane.



Scheme 5.4: Projected synthesis of a more reactive intramolecular allylation model system

If the final allylation step can be optimized, the prospect of forming the C ring of the final natural product becomes illuminated. All that remains is to complete the synthesis of the remaining rings to set up the intramolecular allylation and set the stage for the end-game of the total synthesis effort.

5.1.4. Final Conclusions

If the problems facing the Diels-Alder model system and the allylation model system can be ironed out, the remainder of the total synthesis will be set. The primary problem facing the

main synthesis is the presence of the allylic alcohol after the vinyl addition to the intermediate aldehyde. If this alcohol can be eliminated in a *trans* fashion, the installation of the nitrogen functionality should be trivial. Formation of the ynamide has already been demonstrated, and has the possibility to be optimized further. The cationic Rh(I)-catalyzed Diels-Alder is effective at creating the B and D rings simultaneously. *Ips*o substitution of the produced vinyl silane with acryloyl chloride will cleanly produce the desired enone, and deprotection of the tosylamide will produce *in situ* Michael addition to form the A ring. Finally, the C ring can be closed by transforming the OTBS group into a reactive allylic TMS group, which can undergo promoted quenching of the set-up iminium ion generated by polarization of the 2,3-dihydro-4-pyridone functionality. With all of the rings set, differential oxidation of the olefins generates the penultimate structure, with a final methylation of the C-ring ketone completing the proposed total synthesis of Huperzine X.

5.2. Attempted Total Synthesis of (*R*)-Myricanol

The attempt made to synthesize the diarylheptanoid, (*R*)-myricanol, requires only two significant optimizations to reach a potential completion stage of the research. Initially, the issue of how to install an allyl group to the *ortho* position of the northern arene ring is the most significant challenge. Secondly, the optimization of the In(0)-mediated allylation onto the aliphatic aldehyde of the southern fragment to be enantioselective must be addressed.

5.2.1. Synthesis of the Northern Fragment

While our efforts have been significant in the attempt to install the allyl group to the northern fragment, there are alternatives that were not explored for the lack of time. These alternatives could hold the key to successfully completing this important scaffold. One alternative to the Claisen rearrangement or metalation strategies is to add the allyl group as a nucleophile, rather than an electrophile. Mal and co-workers have demonstrated the ability of allyl indium reagents to add to oxidized phenols¹¹. The products of this reaction quickly decompose to liberate MeOH and reform the aromatic ring, with transfer of the allyl group to the *ortho* position. Not only will this chemistry allow us access to the elusive products we desire, it is also possible that the *para* position will be functionalized with a methoxy group, which can be selectively deprotected to give a more useful phenol that can be transformed into a boronate through Miyaura borylation.

5.2.2. Synthesis of the Southern Fragment

The southern fragment was synthesized quite effectively with our initial attempts. The most significant drawback of the synthesis (detailed in Chapter 3) is that it is difficult to achieve complete selectivity in the bromination of ethyl 4-hydroxy-dihydrocinnamate. Through serendipitous experimentation, it was discovered that careful extraction with diethyl ether allowed for the selective removal of the dibrominated material by solvating the monobrominated compound in the mixture. Extraction with EtOAc did not produce this effect. While the low yield of this reaction can be attributed to the formation of dibrominated products as well as the desired monobrominated species, the extractive work-up allows for isolation of the

monobrominated compound selectively. The yield does not seem to be improved by changing the bromine source. While Br₂ gave the best results, NBS and benzyltrimethylammonium tribromide (BnN(CH₃)₃Br₃) gave similar results, with no observed selectivity for monobromination. Direct installation of the boron for cross-coupling also was unsuccessful. Regardless of these observations, the final MOM-protected bromophenol was obtained in acceptable yields.

5.2.3. Biaryl Formation and Completion Steps

Upon completion of the northern fragment, it is thought that previously reported asymmetric Suzuki coupling can produce the desired atropisomeric biaryl moiety¹². Asymmetric Suzuki coupling can occur with high stereoselectivity with either enantiomer of the BINAP ligand¹³, or with more electron rich binaphthylamino-phosphines¹⁴. The binaphthylamino-phosphines can be synthesized racemically¹⁴, then resolved to isolate either enantiomer¹⁵, thus enabling access to either potential atropisomer of the natural product. This is desirable because it is unclear which ligand will produce which enantiomer of the biaryl system. The MOM group of the southern fragment and the methoxy group of the northern fragment should be sufficiently bulky enough to force restricted rotation about the biaryl bond, thus preventing degradation of any achieved enantiomeric excess. After the asymmetric Suzuki coupling, DIBAL-H reduction of the ester group followed by reoxidation (as described in Section 5.1.1) to the aldehyde will set up an asymmetric allylation. The Cook group's In(0)-mediated allylation is quite functional for aliphatic aldehydes, and can be performed without exclusion of moisture or air, and represents an attractive alternative to more sensitive asymmetric allylation methodologies. However, currently

there is no ligand which provides enantioselectivity for this transformation. While it is desired to find an appropriate ligand for the *in situ* generated indium Lewis acid, it may not be possible to achieve strong coordination to the aliphatic aldehyde. There is partial support of this by the Cook groups' unpublished work on aliphatic α -ketoamides, where the enantioselectivity is partially eroded by the lack of an aromatic ring near the reaction center, suggesting a π -stacking interaction as partially responsible for initial ligand association with the substrate. Studies with hydrocinnamaldehyde have shown that the aromatic ring is too far away from the aldehyde for any π -stacking associative mechanism to be effective. Previous research in the group on achiral aliphatic hydrazones has shown that chiral triflone BINOL-type ligands are effective at transferring chirality, and these ligands may provide the enantioselectivity desired for aliphatic aldehydes. An alternative option is the use of chiral phosphoric acids, using a BINOL-style platform. These species possess chiral discriminating groups on the naphthyl rings *ortho* to the phosphoric acid group, which can be used to shield one face of the aldehyde after initial protonation of said aldehyde. The ion pair's proximity to the reactive center would allow for stereochemical information to be transferred. One drawback is that these phosphoric acid catalysts have not been screened against the In(0)-mediated allylation, and may create problems associated with the initial formation of the In(III)-Lewis acid generated during the allyl indium reagent formation.

The final stages of the synthesis are quite straightforward. Ring-closing metathesis (RCM) of the two terminal olefins will produce the macrocyclic structure, while standard hydrogenation methods will reduce the new internal olefin to the saturated analog. Subsequent deprotection of the two arene rings will unmask the natural product. The southern half's now exposed hydroxyl group may not be sterically large enough to prevent rotation around the biaryl

bond, but the locking of the structure with the formation of the saturated macrocyclic ring will prevent any biaryl bond rotation at this stage.

5.3. Final Conclusions on the Synthesis of Convolutamydine E

The synthesis of convolutamydine E was undertaken in support of the Cook group's primary research area of environmentally benign allylation methodologies. Using indium metal and a simple, amino-acid derived chiral ligand, the allylation of 4,6-dibromoisatin was successful with a high enantioselectivity and nearly quantitative yield. Final transformations towards convolutamydines A and E were also successful, with convolutamydine A being unstable to isolation. Convolutamydine E was isolated and fully characterized with excellent comparisons to the literature. This chemistry has shown that simple, effective methods for forming new C-C bonds can be achieved in high yields and enantioselectivities using environmentally friendly indium, with wide functional group tolerance. The prerequisite synthesis of 4,6-dibromoisatin was also achieved in yields far exceeding previously reported routes, making the complete synthesis very attractive. The chemistry has been expanded to linear α -ketoamides, and the nucleophilic diversity has been increased to include crotylations and cyclohexenylations. Identification of new total synthesis targets with substitution patterns on the allyl chain will open up new possibilities for showcasing this important chemistry.

5.4. References

- ¹ Fujita, K-i., Komatsubara, A., Yamaguchi, R.; *Tetrahedron*, **2009**, *65*, 3624-3628.
- ² Fleming, I., Dunogués, J., Smithers, R.; *Organic Reactions*, **2004**, The Electrophilic Substitution of Allylsilanes and Vinylsilanes. *Organic Reactions*. 57-575.
- ³ Ankner, T., Hilmersson, G.; *Org. Lett.*, **2009**, *11*, 503-506.
- ⁴ Nayak, S.; *Synthesis*, **2000**, *11*, 1575-1578.
- ⁵ Urata, H., Suzuki, H., Moro-Oka, Y., Ikawa, T.; *Bull. Chem. Soc. Jpn.*, **1984**, *57*, 607-608.
- ⁶ Wender, P., Haustedt, L., Lim, J., Love, J., Williams, T., Yoon, J-Y.; *J. Am. Chem. Soc.*, **2006**, *128*, 6302-6303.
- ⁷ Lin, M., Kang, G-U., Guo, Y-A., Yu, Z-X.; *J. Am. Chem. Soc.*, **2012**, *134*, 398-405.
- ⁸ Shibata, T., Fujiwara, D., Endo, K.; *Org. Biomol. Chem.*, **2008**, *6*, 464-467.
- ⁹ Šebesta, R., Pizzuti, M., Boersma, A., Minnaard, A., Feringa, B.; *Chem. Commun.*, **2005**, 1711-1713.
- ¹⁰ Wang, X., Turunen, B., Leighty, M., Georg, G.; *Tetrahedron Lett.*, **2007**, *48*, 8811-8814.
- ¹¹ Mal, D., Pahari, P., Senapati, B.; *Tetrahedron Lett.*, **2005**, *46*, 2097-2100.
- ¹² Baudoin, O.; *Eur. J. Org. Chem.*, **2005**, 4223-4229.
- ¹³ Heravi, M., Hashemi, E.; *Tetrahedron*, **2012**, *68*, 9145-9178.
- ¹⁴ Buchwald, S., Huang, X., Zim, D; *US Patent No. 0171833*, **2004**.
- ¹⁵ Quideau, S., Lyvinec, G., Marguerit, M., Bathany, K., Ozanne-Beudenon, A., Buffeteau, T., Cavagnat, D., Chénéde, A.; *Angew. Chem. Int. Ed.*, **2009**, *48*, 4605-4609.